IMPACT OF PWR SPENT FUEL VARIATIONS ON TRU-FUELED VHTRs

A Thesis

by

AYODEJI B. ALAJO

Submitted to the Office of Graduate Studies of
Texas A&M University
in partial fulfillment of the requirements for the degree of

MASTER OF SCIENCE

December 2007

Major Subject: Nuclear Engineering

IMPACT OF PWR SPENT FUEL VARIATIONS ON TRU-FUELED VHTRs

A Thesis

by

AYODEJI B. ALAJO

Submitted to the Office of Graduate Studies of
Texas A&M University
in partial fulfillment of the requirements for the degree of

MASTER OF SCIENCE

Approved by:

Chair of Committee,	Pavel V. Tsvetkov
Committee Members,	Yassin A. Hassan
	William S. Charlton
	Joe Pasciak
Head of Department,	Raymond J. Juzaitis

December 2007

Major Subject: Nuclear Engineering

ABSTRACT

Impact of PWR Spent Fuel Variations on TRU-Fueled VHTRs. (December 2007)

Ayodeji B. Alajo, B.Sc., University of Ibadan

Chair of Advisory Committee: Dr. Pavel Tsvetkov

Several alternative strategies are being considered as spent nuclear fuel (SNF) management options. Transuranic nuclides (TRU) are responsible for the SNF long-term radiotoxicity beyond the first 500 years. One of the most viable approaches suggests creating new transmutation fuels containing TRUs for use in thermal and fast nuclear reactors. Irradiation of TRUs results in their transmutation and ultimate incineration by fission.

The objective of this thesis is to analyze the impact of conventional PWR spent fuel variations on TRU-fueled Very High Temperature Reactor (VHTR) systems. This effort was focused on the prismatic core configuration. The 3D core models were created for use in calculations with the SCALE 5.1 code system. As part of the research effort, basic nuclear characteristics of TRUs were taken into consideration. The potential variations of PWR spent fuel compositions were modeled with the International Atomic Energy Agency (IAEA) Nuclear Fuel Cycle Simulation System, VISTA.

The VHTR configurations with varying TRU compositions were analyzed assuming a single-batch core operation. Their performance was compared to the VHTR cases with low enriched uranium (LEU). The analysis shows that TRUs can be effectively utilized in the VHTR systems. The TRU-fueled VHTRs exhibit favorable performance characteristics.

ACKNOWLEDGMENTS

I would like to offer my sincere gratitude to my adviser Dr. Pavel Tsvetkov for his guidance and support in the completion of this thesis. His dedication and help guided me throughout the duration of the project.

My appreciation also goes to Dr. Yassin Hassan and Dr. William Charlton from the department of nuclear engineering, and Dr. Joe Pasciak from the department of mathematics for serving on my graduate committee.

A heart-felt thanks goes to my friends: The H19 boys; GCI, UI and UCH crews; friends from Andersen, KPMG, Chicago, College station and Houston. Thanks for standing by me through the nice and hard times.

The acknowledgment is not complete without honoring my family. To my parents Amos and Victoria Alajo, my brothers, the Akinyedes and the Abikoyes, I appreciate your prayers and encouragement in completing this thesis.

Above all, I give all glory and praise to the Wise & Holy One. His words have kept me over the years and the Word works.

This thesis is based upon work supported by the U.S. DOE under Award Number DE-FC07-05ID14655 (05-094).

TABLE OF CONTENTS

Page

ABSTRACT……... iii

ACKNOWLEDGMENTS……..… iv

TABLE OF CONTENTS……... v

LIST OF FIGURES…….…… viii

LIST OF TABLES……. x

CHAPTER

I INTRODUCTION……..……. 1

I.A Background…….……..…. 1

I.A.1 Nuclear Wastes and Waste Management Options..... 1

I.A.2 Advanced Fuel Cycle Initiative (AFCI)…..……..…... 2

I.A.3 Global Nuclear Energy Partnership (GNEP)……. 3

I.A.4 Generation VI Energy Systems Initiative (GEN-IV)…..……... 3

I.A.5 General Atomics (GA) Deep-Burn Concept ……..... 4

I.A.6 Very High Temperature Reactor (VHTR) Systems 5

I.B Research Objectives and Approach ……..……..... 6

II NUCLEAR CHARACTERISTICS OF TRUs …….. 8

II.A Analysis Tools ……..... 8

II.A.1 Java-based Nuclear Information Software (JANIS)..... 8

II.A.2 Equilibrium TRU Neutron Balance Model…..…….... 9

II.A.2.1 Equilibrium Cycle Model ……... 10

II.A.2.2 Neutron Balance Calculation: D-Method…… 11

II.B Analysis of Energy Dependent Characteristics of TRU Nuclides…… 12

II.B.1 TRU Composition..... 13

II.B.2 Nuclear Data Libraries..... 14

II.B.3 Basic Nuclear Characteristics of TRUs..... 15

II.B.4 Neutron Balance in Thermal and Fast Spectra……. 19

II.C Assessment of Existing Uncertainties in Nuclear Data……. 24

II.D Impact of TRU Nuclear Characteristics on Transmutation Strategies... 28

CHAPTER Page

III PWR SPENT FUEL VARIATIONS 29
III.A VISTA Fuel Cycle Analysis 29
III.A.1 Material Flow in VISTA 29
III.A.2 VISTA Reactor Model (In-core Fuel Cycle) 31
III.A.3 VISTA Input and Output Parameters 33
III.A.4 Limitations of VISTA 35
III.B PWR Spent Fuel Analysis 36
III.B.1 Pressurized Water Reactor (PWR) 36
III.B.2 PWR Parameters in VISTA 36
III.B.3 Sensitivity Analysis 39
III.C Spent Fuel Vectors 40
III.C.1 Presentation of Spent Fuel Composition in VISTA 40
III.C.2 Spent Fuel Vector from Default VISTA Parameters 42
III.C.3 Fluctuations of Spent Fuel Vectors 43
III.D TRU Vectors from Legacy Spent Fuels 50
III.E Reference TRU Vectors for TRU-bearing Compositions for Use in VHTRs 51

IV BEHAVIOR OF TRU-FUELED VHTRs 53
IV.A VHTR Model 53
IV.A.1 The Fuel Block 55
IV.A.2 The Replaceable Reflector Blocks 60
IV.A.3 The Control Rod Block 62
IV.A.4 The 3-D Whole Core VHTR Model 64
IV.B VHTR Modeling with the SCALE 5.1 Code System 66
IV.B.1 The Criticality Safety Analysis Sequence (CSAS) 66
IV.B.2 The TRITON Depletion Sequence 70
IV.B.3 Limitations of SCALE 72
IV.C Metrics Employed in Analysis 73
IV.C.1 Fuel Utilization Metrics 74
IV.C.2 Nuclear Waste Generation Metrics 76
IV.D Performance Characteristics of VHTRs with TRU 78
IV.D.1 Neutron Distributions in VHTR Cores with LEU and TRU 79
IV.D.1.1 Equilibrium Neutron Balance 85

CHAPTER Page

IV.D.1.2 Beginning-Of-Life (BOL) Analysis…..……... 86
IV.D.1.3 Core Lifetime …….. 90
IV.D.1.4 Fuel Utilization ……... 92
IV.D.2 Out-of-Core Fuel Cycle Analysis..... 94

V CONCLUSIONS ……...……..…… 98

REFERENCES……..... 101

APPENDIX A ……..... 108

APPENDIX B ……..... 139

APPENDIX C ……... 141

VITA……..... 145

LIST OF FIGURES

FIGURE		Page
1	Fission cross-sections of MAs in ENDF/B6.8	15
2	Capture cross-sections of MAs in ENDF/B6.8	16
3	Neutron yield per fission of MAs in ENDF/B6.8	17
4	Neutron production per neutron absorbed based on ENDF/B6.8 and JENDL3.3	18
5	Capture-to-fission rate ratio based on ENDF/B6.8	19
6	U-TRU transformation scheme in thermal spectrum	20
7	U-TRU transformation scheme in fast spectrum	20
8	Flux dependent equilibrium neutron balance in thermal spectrum	22
9	Flux dependent equilibrium neutron balance in fast spectrum	23
10	Fission cross sections of ^{237}Np, ^{243}Am and ^{242}Cm	25
11	VISTA once-through fuel cycle model	30
12	VISTA uranium and plutonium recycling model	30
13	Transformation chain of TRU nuclides in CAIN	32
14	VISTA input and output parameters	35
15	TRU vectors from O-T cycle and U-Pu recycling option	43
16	Normalized TRU content of PWR spent fuel as a function of fuel burnup	47
17	Sensitivity factor of TRU vectors from spent fuel with respect to burnup	49
18	Comparison of selected TRU vectors	52
19	Fuel assembly block	55
20	Fuel assembly block dimensions	56

FIGURE Page

21 TRISO fuel structure…….. 58

22 TRISO particle approximation in the VTHR model…….. 59

23 Reflector blocks…….. 61

24 Control rod block dimensions……. 63

25 3-D whole-core VHTR model with horizontal cross-section view…… 65

26 Flow chart of the CSAS25 sequence……. 67

27 Flow chart of the TRITON sequence…… 71

28 Active core map…….. 80

29 Neutron distributions in compacts as a function of their location in the core…….. 81

30 Neutron distribution in the fuel zones…… 82

31 Neutron distributions in VHTRs with LEU and TRUs…….. 84

32 Flux dependent equilibrium neutron balance at thermal and fast energies… 85

33 Multiplication factor as a function of moderator-to-fuel ratio…… 87

34 Temperature coefficients of reactivity…… 88

35 Time dependent multiplication factor……. 92

36 Fissile fuel utilization……. 93

37 Transmutation efficiency…… 95

38 TRU, MA and Plutonium destruction rates…… 96

39 TRU and MA materials to be disposed……... 97

LIST OF TABLES

TABLE		Page
I	Reactions with R_r^k and P_r^k values ……	12
II	Average PWR spent fuel composition…..……...	13
III	Nuclear characteristics available on nuclear data libraries …..……	24
IV	Ranking of data magnitude for MA characteristics.……	27
V	VISTA input parameters..……	34
VI	VISTA output parameters ……	34
VII	Reference PWR design ……	37
VIII	Default VISTA PWR design parameters …….	38
IX	Perturbed parameters in VISTA calculations ……...	38
X	VISTA output for the reference PWR configuration……	41
XI	Normalized contents of discharged fuel……	42
XII	PWR spent fuel vectors as a function of load factor variations……	44
XIII	PWR spent fuel vectors as a function of fuel Burnup variations……..	45
XIV	MA content of PWR spent fuel……	46
XV	TRU vector from average PWR spent fuel……	50
XVI	Selected TRU vectors from PWR spent nuclear fuel for VHTR analysis…	51
XVII	VHTR core specifications……	54
XVIII	Fuel assembly block specifications……...	57
XIX	Fuel element specifications……...	58
XX	TRISO particle specifications……...	59

TABLE Page

XXI Burnable poison rod specifications……... 60

XXII The specification of replaceable reflector block with coolant channels…... 60

XXIII Solid reflector blocks specifications…….. 62

XXIV Control rod block specification…… 62

XXV Quantitative metrics for the TRU-fueled VHTR analysis…… 73

XXVI Beginning-of-life multiplication factors……..…….. 79

XXVII Moderator-to-fuel ratio in fuel compact…… 86

XXVIII Temperature coefficients of reactivity…….. 89

XXIX Helium reactivity worth……. 89

XXX Boron reactivity worth…….. 89

XXXI Cycle lengths and fast fluence with various fuels……. 91

XXXII Cycle lengths and fraction of fissile fuel utilized…….. 93

XXXIII Fraction of initial TRU material going to waste stream……..... 94

CHAPTER I

INTRODUCTION

I.A BACKGROUND

This chapter discusses nuclear wastes, nuclear waste management options and the current approach in waste management technologies. These topics established a basis for the work described in this thesis. The work performed was inspired by international and United States of America programs such as the Advanced Fuel Cycle Initiative (AFCI), Global Nuclear Energy Partnership (GNEP) and Generation IV Energy Systems Initiative (Gen-IV).

I.A.1 NUCLEAR WASTES AND WASTE MANAGEMENT OPTIONS

Current nuclear fuels are uranium base, usually UO_2. The fuel designs have utilized low enriched uranium (LEU) as well as mixed oxide (MOx) fuel. Once irradiated, High Level Wastes (HLW) pose a challenge for their safe disposal. The long-lived fission products and minor actinides (MAs) constitute the most undesirable long-term radiotoxicity.

The concerns cover a variety of aspects such as environmental impact, health concerns of local communities, safety issues, and proliferation risks. The environmental impact and health concerns are related to heat load as well as long-term radiotoxicity in geological repositories and storage locations. The absence of the HLW in spent fuel will reduce the storage time to about 1000 years for the fuel waste to attain the emission level of natural uranium [1].

This thesis follows the style of *Nuclear Science and Engineering*.

New approaches to spent fuel recycling are being developed. They involve recovery and reuse of spent fuel to reduce the amount of wastes requiring permanent geological disposal. The closed fuel cycle with partitioning and transmutation (P&T) is the most comprehensive approach [1]. Current research efforts explored TRU-bearing fuels for use in next generation nuclear systems.

I.A.2 ADVANCED FUEL CYCLE INITIATIVE (AFCI)

The Advanced Fuel Cycle Initiative (AFCI) program was designed to identify the most effective technologies leading to reduced HLW volume from spent fuel and recovery of energy contained in the highly toxic spent fuel elements that present the most difficult disposition challenge while providing for their destruction [2]. Subsequent to the United State government's announcement of the Global Nuclear Energy Partnership (GNEP) program, AFCI was refocused to support the new program.

The AFCI program sought to develop advanced technologies for various fuels and fuel cycles that are significantly different from those used by existing U.S. reactors. The AFCI program considers the following classes of fuel cycles:

- Fuel cycles with partial plutonium recycle.
- Fuel cycles with full plutonium recycle.
- Closed fuel cycles (with full recycle of transuranics).

Implementation of technologies developed under AFCI program requires successful deployment of Generation IV nuclear energy systems [2].

I.A.3 GLOBAL NUCLEAR ENERGY PARTNERSHIP (GNEP)

Countries such as the United States of America, Russia, United Kingdom, Japan, Switzerland and France have developed advanced nuclear capabilities. Other countries are at significantly earlier stages in developing nuclear power technologies. There are proliferation risks and global security concerns associated with the potential spread of nuclear technologies. Since nuclear technology is a sensitive issue, an international program that will encourage deployment of nuclear technology for peaceful purposes while protecting global security is imperative.

The Global Nuclear Energy Partnership (GNEP) is a United States Department of Energy (DOE) initiative aimed at increasing U.S. and global energy security, while reducing nuclear proliferation risks. Under GNEP, nations seeking nuclear technology for power generation (users) would operate a once-through fuel cycle. Nations with advanced nuclear capabilities (suppliers) would be responsible for the users' fresh fuel supply and spent fuel management [3]. The GNEP envisions closed fuel cycle development by the suppliers. The closed fuel cycle technology development and deployment would enable recycling and consumption of TRU employing new proliferation-resistant technologies. The research and development efforts in this regard are built on DOE's Advanced Fuel Cycle Initiative (AFCI) program.

I.A.4 GENERATION VI ENERGY SYSTEMS INITIATIVE (GEN-IV)

The Generation IV program is an international collaborative effort established by the US Department of Energy (DOE) to develop the next generation nuclear energy systems that will broaden the opportunities for the use of nuclear energy. Based on the

requirements of the Generation IV roadmap, six reactor designs were selected as the Generation IV system. These are [4]:

- Gas-Cooled Fast Reactor (GFR).
- Lead-Cooled Fast Reactor (LFR).
- Molten Salt Reactor (MSR).
- Sodium-Cooled Fast Reactor (SFR).
- Supercritical Water-Cooled Reactor (SCWR).
- Very High Temperature Reactor (VHTR).

I.A.5 GENERAL ATOMICS (GA) DEEP-BURN CONCEPT

The present analysis is focused on the TRU-fueled VHTRs and their performance characteristics during operation in a single-batch mode without refueling. Incineration of TRUs in the considered systems is also evaluated.

The alternative approach for potential use of TRUs in High Temperature Gas Reactors (HTGRs) is represented by “deep-burn” transmutation concept originally proposed by General Atomics (GA). The deep-burn concept is based on utilization of thermal neutrons and high burn-up fuels in modular helium reactor (MHR) systems. The concept is focused on TRU s from LWR spent fuels. An essential factor in this approach is the use of ceramic-coated fuels to achieve high TRU destruction levels [5,6]. Deep-burn concept takes advantage of the multi-batch reloading and recycling.

I.A.6 VERY HIGH TEMPERATURE REACTOR (VHTR) SYSTEMS

The VHTR is a graphite moderated helium-cooled reactor that supplies heat with core outlet temperatures equal to or greater than 850 degree Celsius. Its basic technology has been well established in High Temperature Gas Reactors (HTGR), such as the German AVR and THTR prototypes, and the U.S. Fort Saint Vrain and Peach Bottom prototypes. The VHTR extends the capabilities of HTGRs to achieve further improvements in thermal efficiency and open up additional high-temperature applications [7]. The VHTR reactor core can be a prismatic block core such as the High Temperature Test Reactor (HTTR) operating in Japan, or a pebble bed core such as the Chinese High Temperature Test Module (HTR-10). [8,9]

The fuel design is characterized by the use of TRISO (TRIstructual ISOtropic) coated fuel particles. The TRISO coating provides self-containment for each fuel particle. A strong and highly irradiation resistant layer of coating allows complete retention of fission products at high temperatures, representing an attractive spent fuel form.

The prismatic core configuration features annular fuel compacts composed of TRISO coated fuel particles that are embedded in graphite matrix. The fuel compacts are stacked together forming the fuel element. The fuel block is a hexagonal graphite block with borings for the fuel elements. The core is formed by arranging fuel blocks, reflector blocks and control rod blocks in an annual layout. The details of the prismatic core is discussed in section IV.A.

The VHTR is the candidate for the Next Generation Nuclear Plant (NGNP). The high outlet temperature enables applications such as hydrogen production, sea water desalination, or heat supply for petrochemical industry. It is designed for high efficiency

operation due to its high coolant temperature, and for passive safety due to the ceramic properties of coated fuel particles and graphite moderator. The passive safety feature is enhanced in the annular core layout due to improved passive decay heat removal [6].

I.B RESEARCH OBJECTIVES AND APPROACH

The objective of this thesis is to analyze the impact of conventional PWR spent fuel variations on TRU-fueled Very High Temperature Reactor (VHTR) systems. The effort is focused on prismatic core configurations. In order to achieve this objective, the following studies were completed:

1. Analysis of basic nuclear characteristics of TRU nuclides. This effort covered analysis of energy dependent nuclear characteristics of TRU nuclides and evaluation of their expected behavior as fuel components.
2. Assessment of TRU nuclear data reliability. Existing nuclear data for TRU nuclides, particularly MA are not complete and consistent over various nuclear data libraries. The evaluation of uncertainties associated with the data was performed. Such uncertainties and their impact on system performance are important factors in conclusions regarding TRU transmutation options.
3. Determination of potential PWR spent fuel variations. This study involved determination of various TRU vectors representing PWR spent fuel compositions.

4. Analysis of TRU-fueled VHTR systems. The study focused on the effects of variations in fresh TRU-based fuel compositions on VHTR performance characteristics.

To complete the first and second studies, 3 nuclear data files were reviewed: ENDF/B6.8 (U.S.A), JENDL3.3 (Japan) and JEF2.2 (Europe). Neutron reaction cross-sections, neutron yields and reaction rates were analyzed. Discrepancies among the nuclear data files were evaluated. The neutron balances at equilibrium concentrations were evaluated. These studies are presented in Chapter II.

Potential PWR spent fuel compositions were determined using the IAEA's nuclear fuel cycle simulation system (VISTA code system). In the present analysis, fuel burnup and load factor values were perturbed to achieve variations in discharged fuel compositions. Four different PWR spent fuel compositions were selected from VISTA simulations. An addition composition was determined from the analysis of legacy spent fuel that is given in the Yucca Mountain Safety Assessment Report. Chapter III discusses the details of the study.

The concluding study was accomplished through the use of ORNL SCALE5.1 code system. The detailed whole-core 3-D models were developed and implemented. The reactor fuel loadings were based on the PWR spent fuel vectors identified in the preceding study. To establish a reference reactor system, calculations for 15% LEU-fueled VHTR were performed and the results were used as the basis for comparative studies of the TRU-fueled systems. This study is discussed in Chapter IV.

CHAPTER II

NUCLEAR CHARACTERISTICS OF TRUs

This chapter presents the analysis of nuclear characteristics for selected nuclides and their implications on advanced fuel performance characteristics. Neutron reaction cross-sections, neutron yields and reaction rates were analyzed. Neutron balance evaluations were also performed. The nuclear characteristics of ^{235}U and ^{238}U were selected as references since the uranium isotopes are the main constituents of conventional fresh fuel loadings. The analysis is based on nuclear data from ENDFB 6.8, JEF 2.2 and JENDL 3.3. JANIS version 2.2 (discussed in section II.A) was used for basic nuclear property analysis. Section II.B considers various energy-dependent nuclear characteristics of TRUs and assesses their implications. Section II.C assesses existing uncertainties in nuclear data.

II.A ANALYSIS TOOLS

II.A.1 JAVA-BASED NUCLEAR INFORMATION SOFTWARE (JANIS)

Java-based nuclear information software (JANIS) is a program designed to facilitate the visualization and analysis of nuclear data. It allows the user to access and analyze nuclear data [10]. The program is a stand-alone application with direct access to large databases of nuclear data files.

JANIS is capable of computing basic reaction rate ratios such as capture-to-fission rate ratios, delayed neutron fractions and number of neutrons released per neutron absorbed. Cross-sections are viewable as point-wise data. Fission yield data and

spontaneous fission yields are provided. The yield data include thermal neutron-induced, fast neutron-induced and high-energy neutron-induced fission. The radioactive decay data set provides nuclide mass, half-life, excitation energy, spin and parity, mean decay energies and decay modes. The Q value, branching ratio and daughter nuclide are provided for each decay mode [11].

JANIS provides particle interaction data from a number of nuclear data libraries. The libraries are ENDF (U.S), JEF (Europe), JENDL (Japan), BROND (Russia), CENDL (China) EXFOR (experimental data library) and others. Bibliographic information is retrievable from CINDA (computer index of neutron data). The application's capability and access to various data libraries made it suitable for nuclear data analysis.

II.A.2 EQUILIBRIUM TRU NEUTRON BALANCE MODEL

The possibility of transmuting TRU nuclides depend on the neutron balance in the transmutation system. The only way to dispose actinides is to induce their fission. Fission is accompanied by neutron production. However, several neutron captures may occur before a fission event. Therefore, the net number of neutrons necessary for TRU transmutation should be:

$$\alpha + (1 - \nu_f) \tag{1}$$

where α is the number of captures before a fission event, which can be represented by the capture to fission rate ratio. ν_f is the number of neutrons released per fission, and $(1-\nu_f)$, a negative number is the surplus neutrons following fission. Thus a negative result of equation (1) implies excess neutron production in transmutation scenario, while a positive number indicates neutron deficit. The negative result is

indicative of effective TRU incineration since excess neutrons can only be sustained with increased fission rate. This translates to improved neutron economy since the consumption of one neutron produces more than one neutron in return.

Equation (1) offers a simplified form of the neutron balance in a system. A more rigorous approach uses the nuclide number densities, reaction rates and spatial flux magnitude to determine the system neutron balance. The time dependence of the input parameters was circumvented by calculating the neutron balance for equilibrium TRU vector.

II.A.2.1 EQUILIBRIUM CYCLE MODEL

The Bateman equation for nuclide production-destruction rate can be written as:

$$\frac{dN_i}{dt} = \sum_{\substack{j=1 \\ j\neq i}}^{n} \left[\lambda_{ji} + \overline{\sigma_{ji}\phi} \; N_j - \lambda_{ij} + \overline{\sigma_{ij}\phi} \; N_i \right]; \tag{2}$$

where N_i is the concentration of nuclide i, λ_{ji} is the decay constant of nuclide j creating nuclide i, $\overline{\sigma_{ji}\phi}$ is the average transmutation rate of nuclide j producing nuclide i, and n is the total number of nuclides in the transmutation chain of nuclide i.

Equation (2) can be written in vector form:

$$\frac{d}{dt}\vec{N} = M.\vec{N}; \tag{3}$$

where $\vec{N}$ is a column vector of n nuclide concentrations. M is an $n \times n$ matrix. A problem of this form has an exponential solution.

A periodic feed $\vec{F}$ of nuclides to a reactor system modifies equation (2) to the form:

$$\frac{d}{dt}\vec{N} = M.\vec{N} + \vec{F} \tag{4}$$

As time $t \to \infty$, the asymptotic solution to equation (4) corresponds to $d\vec{N}/dt = 0$, at which point the equilibrium cycle is reached. The solution vector $\vec{N}$ is the equilibrium concentration of nuclides in the system. Thus the solution to equation (4) is:

$$\vec{N} = -M^{-1}.\vec{F} \tag{5}$$

The linear character of the equation (5) allows evaluation of the concentration of each vector nuclide independently, with a "unit" source for the corresponding feed $F_i = 1$. The feed vector is defined by $\vec{F} = \begin{bmatrix} 0...0 & F_i & 0...0 \end{bmatrix}^T$, a column vector of n nuclides [12].

Thus the solution to equation (5), which is the equilibrium cycle model, gives the equilibrium nuclide concentrations resulting from transformation of nuclide i. For each selected TRU nuclide, a corresponding equilibrium cycle model was developed. The solution is retained in terms of system flux ϕ.

II.A.2.2 NEUTRON BALANCE CALCULATION: D-METHOD

The neutron balance in a system composed of equilibrium concentrations of TRU nuclides is represented as D_{eq}^{TRU}. The equilibrium neutron balance D_i for a unit feed of nuclide i is given as [12]:

$$D_i = \sum_k \sum_r R_r^k P_r^k \bar{N}_{k,i} \tag{6}$$

where $\bar{N}_{k,i}$ is the concentration of nuclide k in the equilibrium composition resulting from nuclide i's transformation, P_r^k is the reduced transmutation rate for

reaction r and nuclide k i.e. $P_r^k = \sigma_r^k \phi$, and R_r^k is the neutron consumption factor for reaction r and nuclide k. Table I shows R_r^k and P_r^k for the main reactions.

Table I. Reactions with R_r^k and P_r^k values.

Reaction, *r*	$\boldsymbol{P^k_r}$	$\boldsymbol{R^k_r}$
Radiative capture	$\sigma_c\phi$	1
fission	$\sigma_f\phi$	$1-\nu_f$
decay	λ	0

For a TRU feed to a system, the equilibrium neutron balance for the TRU vector would be given as [12]:

$$D_{eq}^{TRU} = \sum_i w_i D_i \tag{7}$$

where w_i is the fraction of nuclide i in the TRU vector.

The solution to equation 7 gives D_{eq}^{TRU} as a function of system flux. The solutions for thermal and fast systems were evaluated between fluxes of 10^{12} n/cm^{2}s and 10^{18} n/cm^{2}s.

II.B ANALYSIS OF ENERGY DEPENDENT CHARACTERISTICS OF TRU NUCLIDES

The TRU elements (neptunium, plutonium, americium, and curium) are important in the study of spent nuclear fuel because of their contribution to long-term radiotoxicity in high-level wastes. At discharge, spent fuel radiotoxicity is dominated by short-lived fission products. After a few decades of decay and cooling, the decay of TRU nuclides becomes the main source of heat load at spent fuel storage locations or geological repositories [13].

II.B.1 TRU COMPOSITION

The purpose of this study is to assess the expected behavior of TRU nuclides as fuel components and reliability of TRU nuclear data with regards to conclusions on transmutation options. Uranium and TRU compositions of a typical spent fuel are provided in Table II. The uranium content is 98.7 percent of the total composition. Excluding ^{236}U, the spent fuel uranium vector is comparable to natural uranium. The long-term issues associated with spent fuel are significantly reduced once TRU are extracted for utilization with advanced fuel cycle options.

Table II. Average PWR spent fuel composition.*
Burnup = 41.2 GWd/MTHM, enrichment = 3.75 %, decay time = 23 years.

Element	Nuclide	Decay Heat (W/g)	TRU Composition (atom %)
U	^{234}U	-	0.0248
	^{235}U	-	0.8756
	^{236}U	-	0.5099
	^{238}U	-	97.2846
Np	^{237}Np	0.00002	0.0799
Pu	^{238}Pu	0.56000	0.0259
	^{239}Pu	0.00200	0.6750
	^{240}Pu	0.00700	0.2858
	^{241}Pu	0.00400	0.0536
	^{242}Pu	0.00010	0.0581
Am	^{241}Am	0.11000	0.1077
	^{242m}Am	-	0.0003
	^{243}Am	0.00700	0.0160
Cm	^{244}Cm	2.80000	0.0025
	^{245}Cm	-	0.0003
			100.0000

Utilization of TRU, particularly MA in next generation nuclear reactors offers improvement in backend management of the current once-through fuel cycle. Transmutation of MA is dependent on the nuclear characteristics of the nuclides. The

*Values are based on Inventory and Characteristics of Spent Nuclear Fuel from [14]

characteristics affect MA performance as nuclear fuel. Utilizing the nuclides in fuel design requires understanding of their nuclear characteristics in different neutron spectra.

II.B.2 NUCLEAR DATA LIBRARIES

The ENDF, JEF and JENDL libraries were used in the analysis of nuclear characteristics. Data from ENDF/B6.8, JEF2.2 and JENDL3.3 were compared with regards to variations in nuclear data across libraries. ENDF/B6.8 data file was employed for the analysis of MA characteristics. The ENDF/B6.8 file was used since it is widely employed in several neutron transport codes. Moreover, the SCALE code system used in later analyses employee ENDF/B6.8 cross-sections for its calculations.

Preliminary assessment of the data files showed that some files in different libraries shared data with common source. This may be due to collaboration amongst scientists who maintain such data. The instances identified were:

- ENDF/B6.8 and JEF2.2: ^{237}Np evaluated data below 8keV were from evaluations by Derrien et al
- ENDF/B6.8 and JENDL3.3: ^{243}Cm and ^{245}Cm data were based on evaluations by V. Maslov et al.

There are more recent versions of evaluated data files from ENDF and JEF libraries; these are ENDF/B7.0 and JEFF3.,1 respectively. The more recent versions were not employed in this analysis for the following reasons:

- Most existing neutron transport codes at the time of analysis support ENDF/B6.8 data file.

- For all nuclides of interest except ^{238}U, JEFF3.1 data were from JEF2.2, ENDF library, JENDL library or a combination of any of these libraries.

II.B.3 BASIC NUCLEAR CHARACTERISTICS OF TRUs

Figure 1 showed the microscopic fission cross-section for selected TRU nuclides. It can be noted (see Fig. 1) that ^{242m}Am and ^{245}Cm have higher fission cross-section compared to ^{235}U in the thermal region up till neutron energy of about 0.2 eV. All TRUs have higher fission cross-section than ^{238}U at thermal energies and above 100 keV. The fission cross-section of all selected nuclides tended towards the same order of magnitude at fast neutron energy range. The cross-sections were between 2 and 3 barns. This suggests that TRU nuclides have similar probability of fission events in fast neutron spectrum.

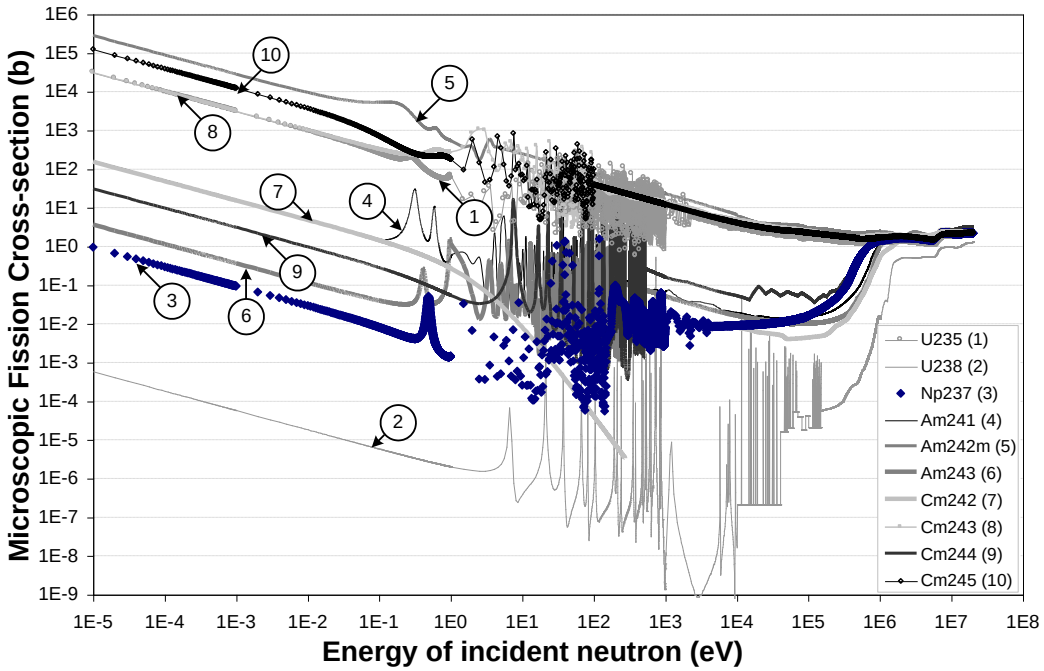

Figure 1. Fission cross-sections of MAs in ENDF/B6.8.

Figure 2 presents the microscopic capture cross-sections for selected TRU nuclides. The plots showed that ^{237}Np, ^{241}Am, ^{242m}Am and ^{245}Cm have higher capture cross-sections compared to ^{235}U in the thermal region up till neutron energies of about 0.1eV. All MAs generally have higher capture cross-section than ^{238}U at thermal energies. This indicated higher probability of transmutation through radiative capture in thermal spectrum. Above 0.5 keV, capture cross-sections of all selected nuclides are below 1 barn.

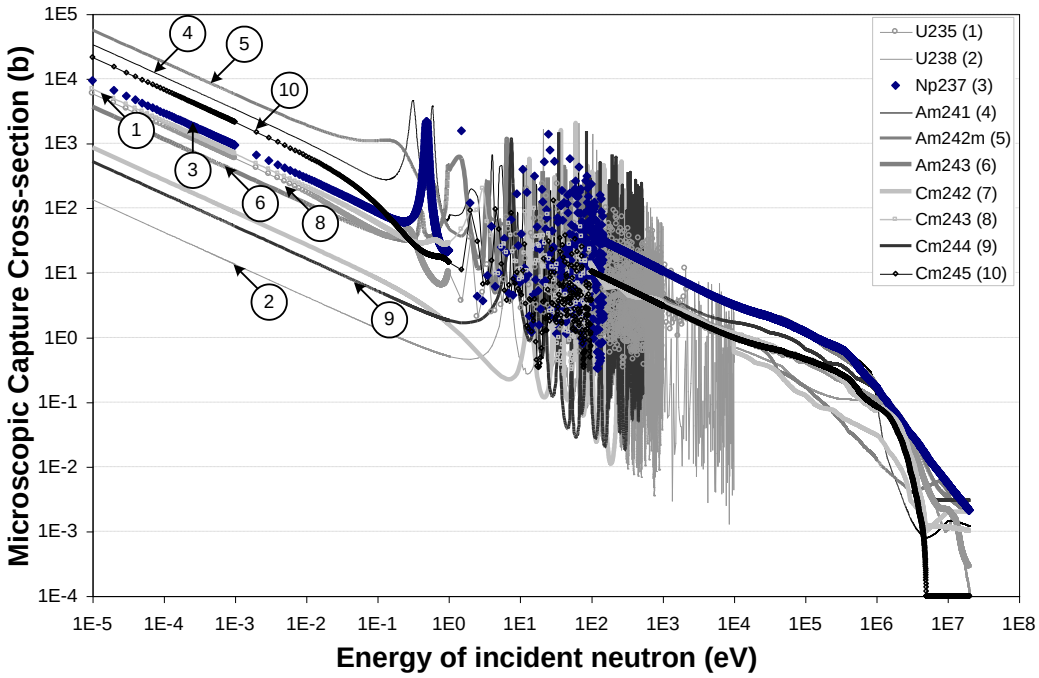

Figure 2. Capture cross-sections of MAs in ENDF/B6.8

Neutron yield per fission plots are shown in Figure 3. TRU nuclides have higher rates of neutron production than the uranium isotopes. Neutron yield per fission event for each nuclide showed negligible variations between thermal and epithermal energies. Beyond these energies, the relationship between neutron energies and neutron yield per

fission was linear. Based on the increasing neutron production at fast energies, fission of TRU nuclide may be more likely at these energies.

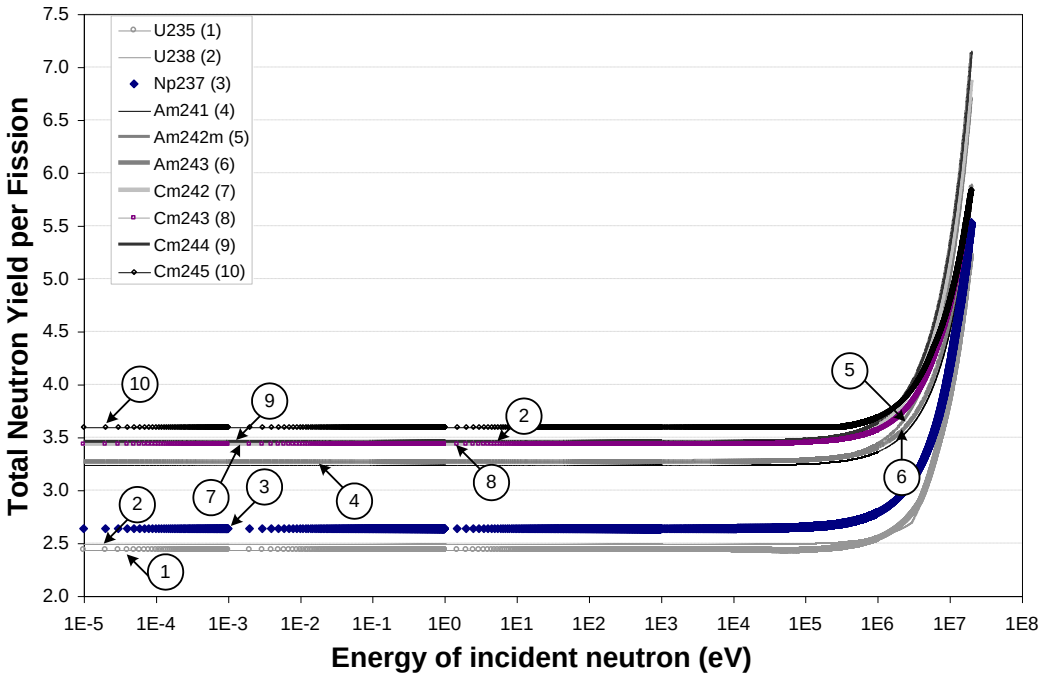

Figure 3. Neutron yield per fission of MAs in ENDF/B6.8

Figure 4(a) showed the neutron production per absorption, $\eta^X(E)$* computed using ENDF data. It can be seen that ^{242m}Am, ^{243}Cm and ^{245}Cm have higher $\eta^X(E)$ values than ^{235}U for neutron energies up to 1.0 eV. ^{238}U has the least value of $\eta^X(E)$ within this range. For nuclides with low $\eta^X(E)$, there is the probability of transmutation to nuclides with higher values of $\eta^X(E)$ through combinations of radiative capture and radioactive decay events.

* The superscript 'x' refers to nuclides of interest

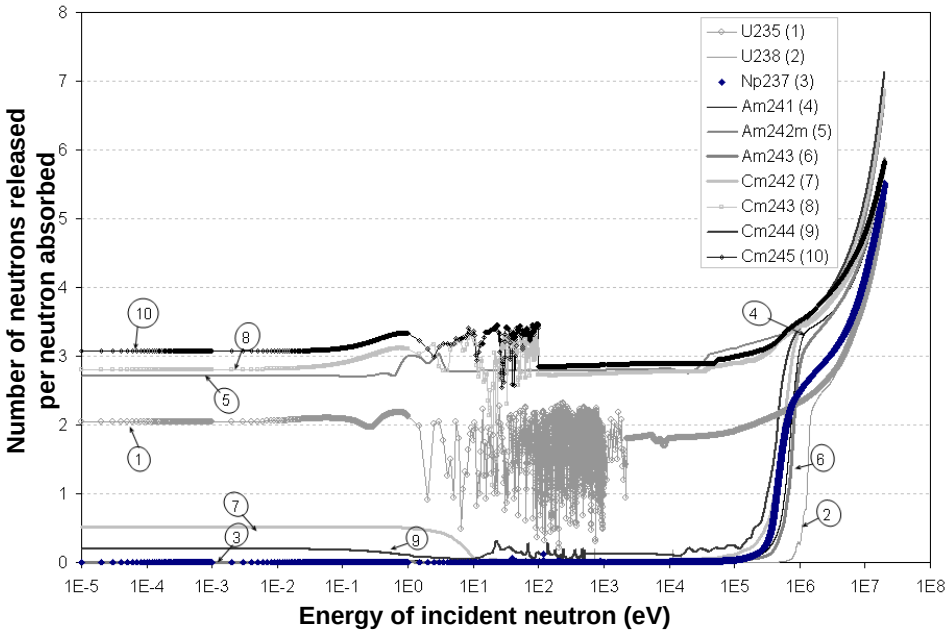

(a) ENDF/B6.8

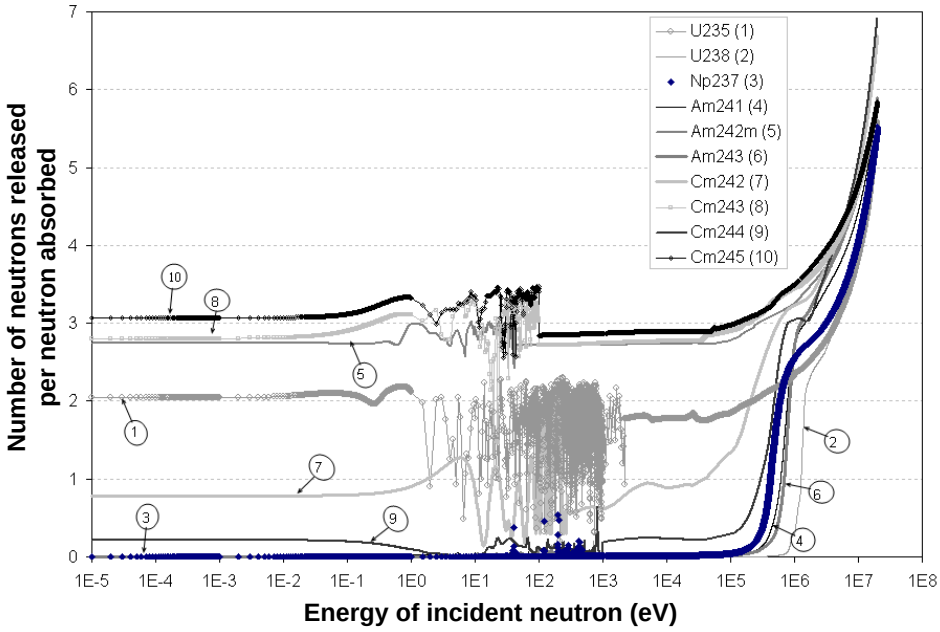

(b) JENDL3.3

Figure 4. Neutron production per neutron absorbed based on ENDF/B6.8 and JENDL3.3.

The capture-to-fission rate ratio, $\alpha^X(E)$ is shown in Figure 5. All MAs except ^{245}Cm have higher values of $\alpha^X(E)$ than ^{235}U at energies below 1.0 eV. Within the same

energy range, ^{238}U has the largest values of $\alpha^X(E)$. In the fast neutron energy range, $\alpha^X(E)$ is low for each nuclide. Hence, MAs have higher probability of fission in fast neutron spectrum.

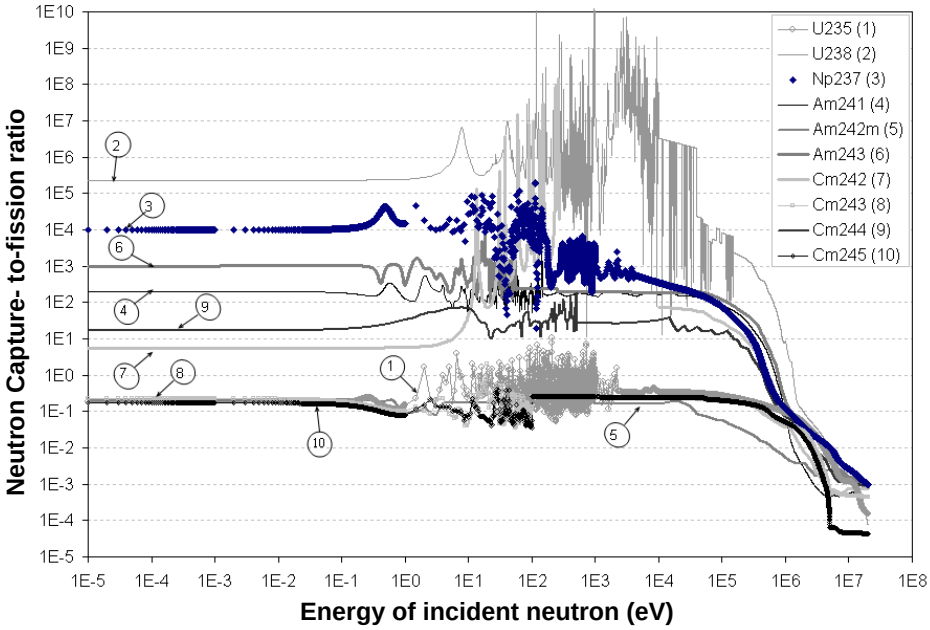

Figure 5. Capture-to-fission rate ratio based on ENDF/B6.8

II.B.4 NEUTRON BALANCE IN THERMAL AND FAST SPECTRA

Figures 6 and 7 showed transformation schemes for TRU nuclides in thermal spectrum and fast spectrum, respectively. Based on the transformation schemes, transformation chains were developed for each major TRU nuclides from typical spent PWR fuel. For each of the selected TRU nuclides, a corresponding equilibrium cycle model was developed from the nuclide production-destruction equation. Average thermal neutron cross-sections was used for equilibrium neutron balance calculation in thermal

spectrum. Neutron cross-sections at 0.5 MeV was used in the fast spectrum calculations. All nuclear data were from ENDF/B6.8 nuclear data library.

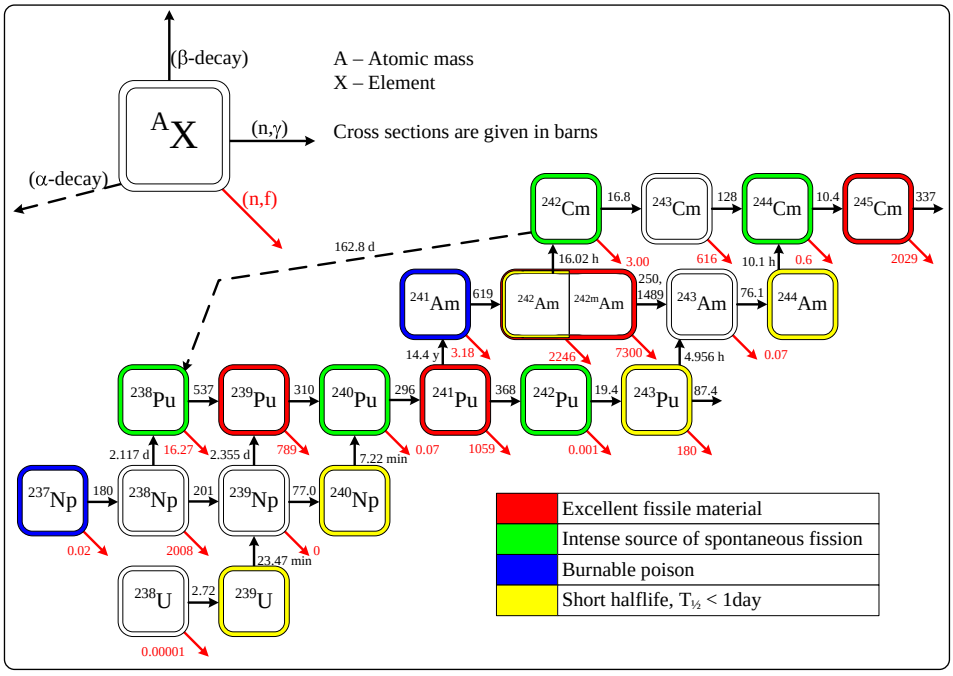

Figure 6. U-TRU transformation scheme in thermal spectrum.

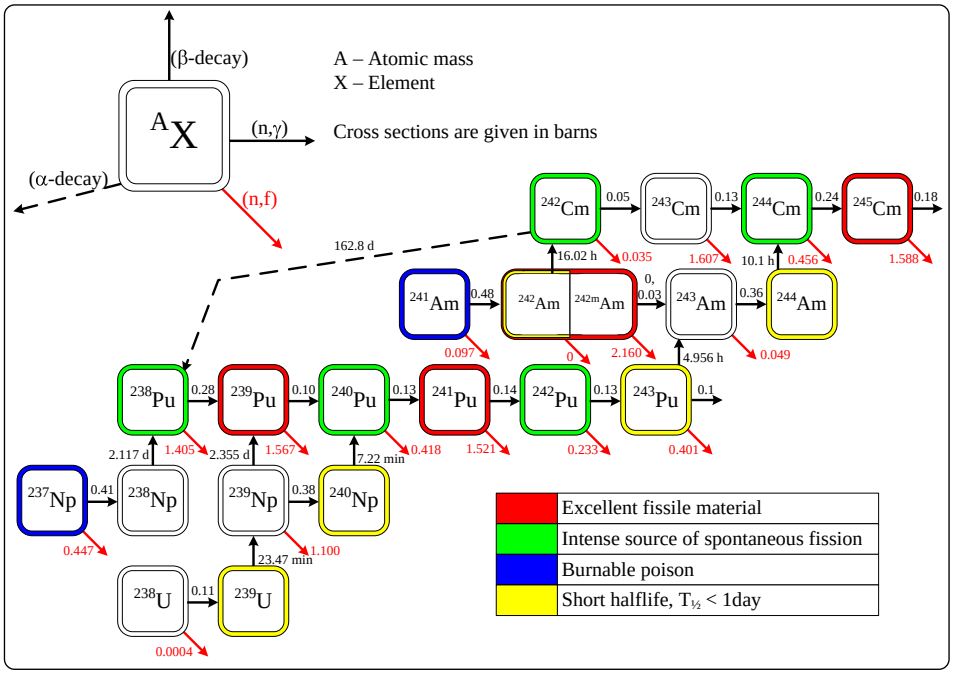

Figure 7. U-TRU transformation scheme in fast spectrum.

Figures 8 and 9 provided the flux dependent equilibrium neutron balance in thermal spectrum and fast spectrum respectively. Negative values of neutron balance indicate excess neutrons, while positive values implied neutron deficit. The neutron balance for the selected nuclides varied between excess and deficit values in thermal spectrum. The nuclides ^{237}Np and ^{241}Am showed transitions from neutron deficit to excess neutron as thermal flux increased, indicating improved incineration rate with flux increase. ^{242}Pu exhibited a neutron deficit over the flux range considered confirming the nuclide as a parasitic absorber. However, the transmutation of ^{242}Pu could create ^{244}Cm, a nuclide with balance of excess neutrons. ^{242m}Am and ^{243}Cm would readily fission in thermal spectrum. Other nuclides indicated excess neutrons, which were mostly below 1.2 neutrons. Only ^{242m}Am and ^{243}Cm had balances of excess neutrons greater than 1.5 neutrons in thermal spectrum, indicating that both nuclides can be effectively incinerated in thermal spectrum. All nuclides exhibited maximum attainable neutron balance as flux continued to increase. The overall neutron economy in thermal spectrum would be improved with higher system flux.

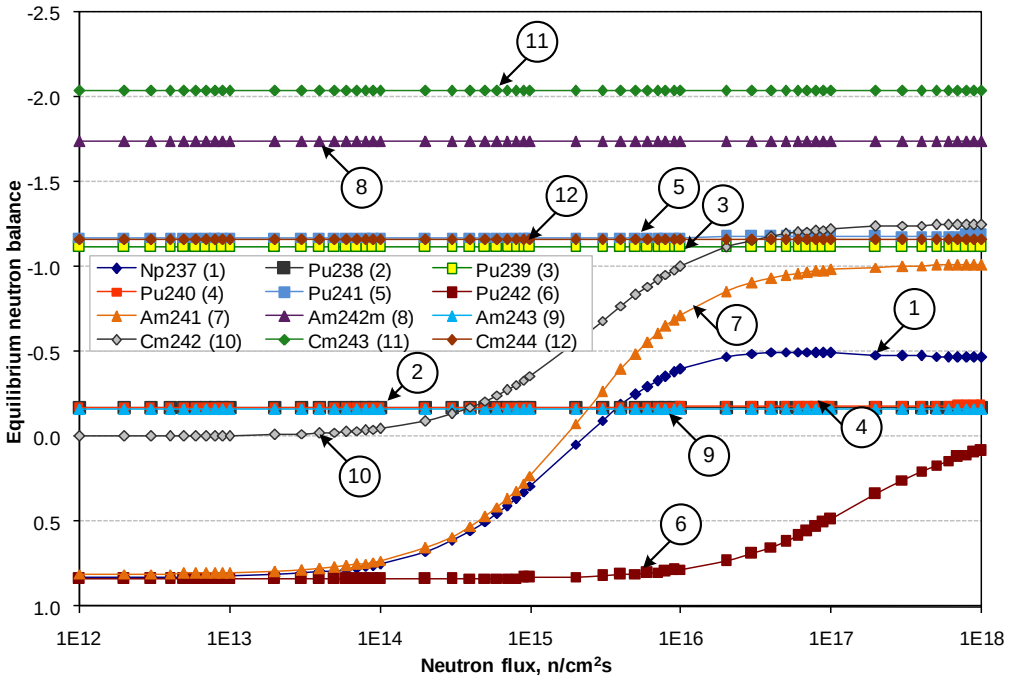

Figure 8. Flux dependent equilibrium neutron balance in thermal spectrum.

In the fast spectrum, all nuclides have excess neutrons. ^{241}Am and ^{242}Cm exhibited the potential for increasing negative neutron balance as flux increases. All other nuclides appeared to have a constant neutron balance over the flux range. All nuclides indicated excess neutrons greater than 1.2 neutron within the flux levels considered, with the exception of ^{241}Am and ^{242}Cm. These fast spectrum observations confirm that fast spectrum systems are better at TRU incineration. The excess neutrons would provide better neutron economy in fast spectrum than in thermal spectrum

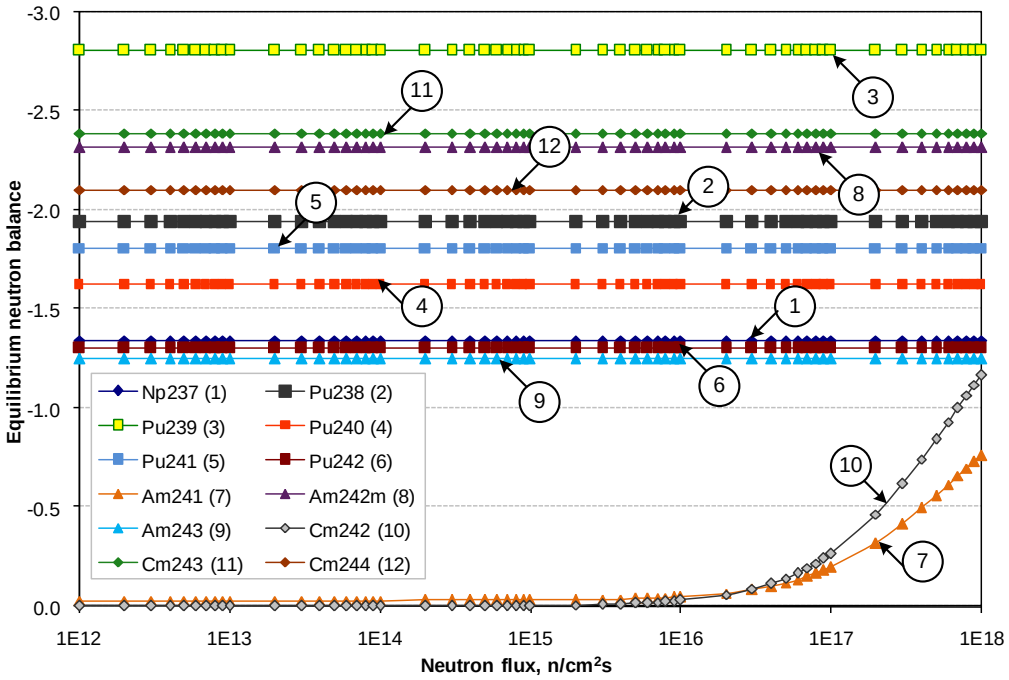

Figure 9. Flux dependent equilibrium neutron balance in fast spectrum.

II.C ASSESSMENT OF EXISTING UNCERTAINTIES IN NUCLEAR DATA

A review of the different libraries showed which properties were available in the nuclear data files. Table III provides a table of nuclides and nuclear data files. Cells marked with 'x' indicated available data. Fission cross-section and radiative capture data were available in all libraries. JENDL3.3 represented the most comprehensive library. Delayed neutron data for ^{244}Cm was not available in ENDF/B6.8. Neutron yield data sets were not available in JEF2.2 for most minor actinides.

Table III. Nuclear characteristics available on nuclear data libraries.

Cross sections	U 235	U 238	Np 237	Pu 238	Pu 239	Pu 240	Pu 241	Pu 242	Am 241	Am 242m	Am 243	Cm 242	Cm 243	Cm 244	Cm 245	Cm 246
ENDFB 6.8																
Fission- σ_f	x	x	x	x	x	x	x	x	x	x	x	x	x	x	x	x
Radiative capture- σ_c	x	x	x	x	x	x	x	x	x	x	x	x	x	x	x	x
Neutron (N) per fission- ν_f	x	x	x	x	x	x	x	x	x	x	x	x	x	x	x	x
Delayed N per fission- ν_d	x	x	x	x	x	x	x	x	x	x	x	x	x		x	x
JENDL 3.3																
Fission- σ_f	x	x	x	x	x	x	x	x	x	x	x	x	x	x	x	x
Radiative capture- σ_c	x	x	x	x	x	x	x	x	x	x	x	x	x	x	x	x
Neutron (N) per fission- ν_f	x	x	x	x	x	x	x	x	x	x	x	x	x	x	x	x
Delayed N per fission- ν_d	x	x	x	x	x	x	x	x	x	x	x	x	x	x	x	x
JEF 2.2																
Fission- σ_f	x	x	x	x	x	x	x	x	x	x	x	x	x	x	x	x
Radiative capture- σ_c	x	x	x	x	x	x	x	x	x	x	x	x	x	x	x	x
Neutron (N) per fission- ν_f	x	x	x	x	x	x	x	x	x		x					x
Delayed N per fission- ν_d	x	x	x		x	x	x									

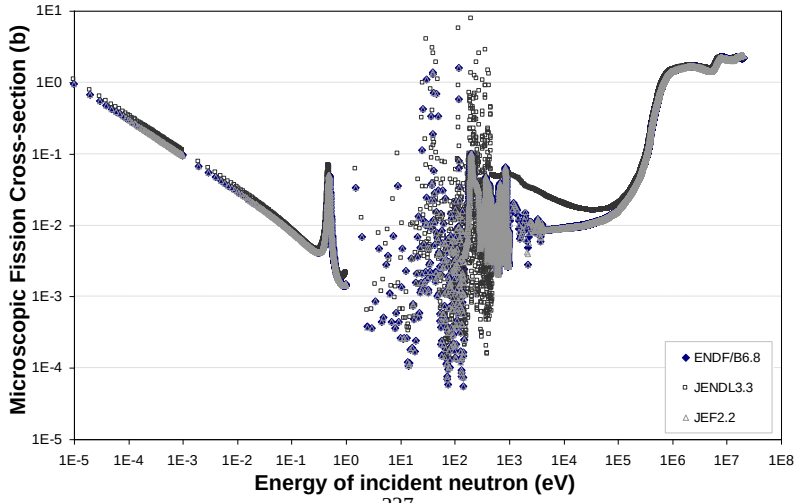

(a) ^{237}Np

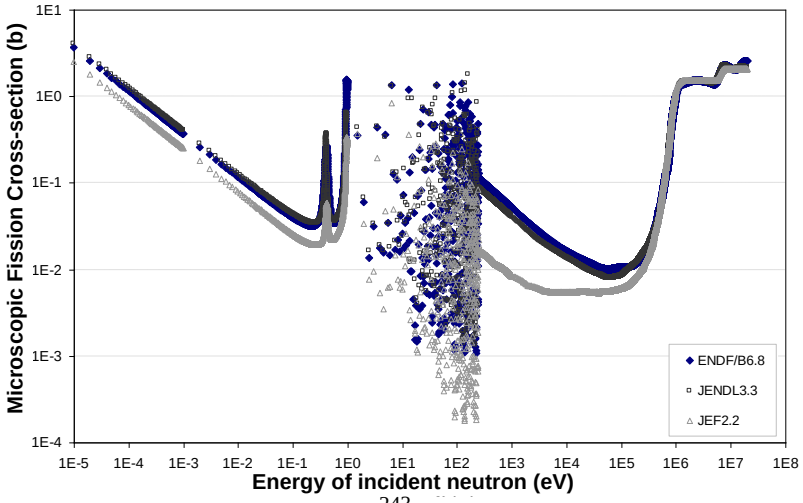

(b) ^{243}Am

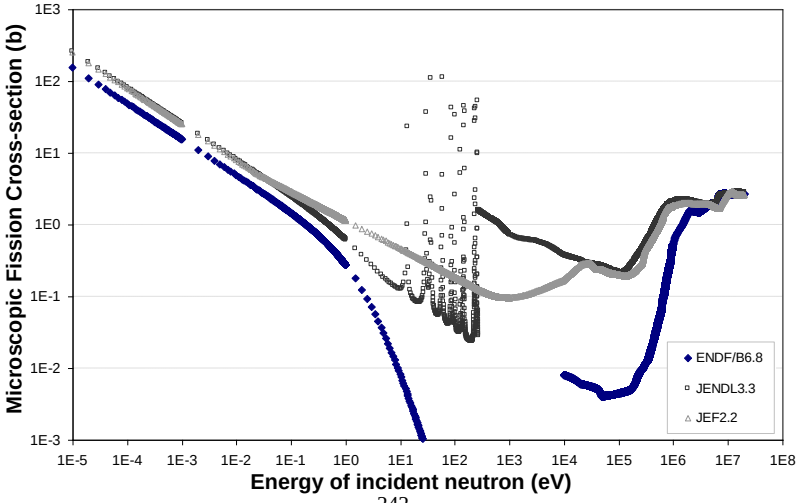

(c) ^{242}Cm

Figure 10. Fission cross sections of ^{237}Np, ^{243}Am and ^{242}Cm.

There were significant discrepancies found among ENDF/B6.8, JENDL3.3 and JEF2.2 with respect to the nuclear data for MAs. Figure 10 provided examples of differences in the evaluated nuclear data. The microscopic fission cross-sections of ^{237}Np, ^{243}Am, and ^{242}Cm were provided in Figure 10. For each nuclide, available fission cross-section data varied with library. The evaluated fission cross-section data for ^{242}Cm is shown in Fig. 10(c). The cross-section data in ENDF/B6.8 were discontinuous between 275 eV and 1.0E+4 eV. The discontinuity represented 0 barns fission cross-section since zero values are impossible to display on log scale. The discontinuity may be exclusion of cross-section data due to inadequate resonance measurement for ^{242}Cm cross-section evaluation. The fission cross-section data of ^{242}Cm in JEF 2.2 appeared continuous at all energies. Conversely, the fission cross-section data of ^{242}Cm in JENDL3.3 have a defined resonance structure between 275 eV and 1.0E+4 eV. The nuclear data from ENDF/B6.8 were significantly different in comparison with other libraries. JENDL3.3 and JEF2.2 had similar values outside the resonance band. These discrepancies are expected to cause differences in reactor physics analysis since the nuclear data are input parameters in neutron transport calculations.

Nuclear characteristics of MA displayed notable trend at thermal energies. A rank based analysis method was developed for the trend. The method assigned ranks to nuclides based on the magnitudes of their values. For example, the ranking of $\eta^X(E)$ from ENDF/B6.8 and JENDL3.3 (see Table IV(a)) were based on $\eta^X(E)$ profile in Fig. 4. ^{245}Cm had the highest value of $\eta^X(E)$ at thermal energy. The nuclide was ranked 1 because of its magnitude. ^{238}U was ranked 10 since it had the least $\eta^X(E)$ value. The ranking system provided a basis of comparison between data from different libraries.

Table IV. Ranking* of data magnitude for MA characteristics.

(a) Ranking of the number of neutrons released per neutron absorbed, η at thermal neutron energies

File	^{235}U	^{238}U	^{237}Np	^{241}Am	^{242m}Am	^{243}Am	^{242}Cm	^{243}Cm	^{244}Cm	^{245}Cm
ENDF/B-6.8	4	10	9	7	3	8	5	2	6	1
JENDL-3.3	4	10	9	7	3	8	5	2	6	1
JEF-2.2	1	4	3	-	-	2	-	-	-	-

(b) Ranking of the capture-to-fission rate ratio, α at thermal neutron energies

File	^{235}U	^{238}U	^{237}Np	^{241}Am	^{242m}Am	^{243}Am	^{242}Cm	^{243}Cm	^{244}Cm	^{245}Cm
ENDF/B-6.8	9	1	2	4	8	3	6	7	5	10
JENDL-3.3	9	1	2	4	8	3	6	7	5	10
JEF-2.2	9	1	2	4	8	3	6	7	5	10

(c) Ranking of the microscopic fission cross-sections below 0.2 eV

File	^{235}U	^{238}U	^{237}Np	^{241}Am	^{242m}Am	^{243}Am	^{242}Cm	^{243}Cm	^{244}Cm	^{245}Cm
ENDF/B-6.8	3	10	9	6	1	8	5	4	7	2
JENDL-3.3	3	10	9	6	1	8	5	4	7	2
JEF-2.2	3	10	9	6	1	8	5	4	7	2

(d) Ranking of the microscopic capture cross-sections below 0.1 eV

File	^{235}U	^{238}U	^{237}Np	^{241}Am	^{242m}Am	^{243}Am	^{242}Cm	^{243}Cm	^{244}Cm	^{245}Cm
ENDF/B-6.8	6	10	4	2	1	7	8	5	9	3
JENDL-3.3	6	10	4	2	1	7	8	5	9	3
JEF-2.2	6	10	4	2	1	7	8	5	9	3

(e) Ranking of the total neutron yields per fission below 1.0E+5 eV

File	^{235}U	^{238}U	^{237}Np	^{241}Am	^{242m}Am	^{243}Am	^{242}Cm	^{243}Cm	^{244}Cm	^{245}Cm
ENDF/B-6.8	10	9	8	7	6	5	3	4	2	1
JENDL-3.3	10	9	8	7	3	6	4	2	5	1
JEF-2.2	4	3	1	-	-	2	-	-	-	-

(f) Ranking Comparison of the Elementary Reaction Rate Ratios

File		^{245}Cm	^{243}Cm	^{242m}Am	^{235}U	^{242}Cm	^{244}Cm	^{241}Am	^{243}Am	^{237}Np	^{238}U
ENDF/B-6.8	η	1	2	3	4	5	6	7	8	9	10
	α	10	7	8	9	6	5	4	3	2	1
JENDL-3.3	η	1	2	3	4	5	6	7	8	9	10
	α	10	7	8	9	6	5	4	3	2	1
JEF-2.2	η	-	-	-	1	-	-	-	2	3	4
	α	10	7	8	9	6	5	4	3	2	1

*Ranking basis: 1 – highest cross section value, 10 – smallest cross section value

Table IV provided comparison of MA characteristics based on different data libraries. The rankings showed consistency in sequences of the magnitudes for $\eta^X(E)$, $\alpha^X(E)$, fission cross-sections and radiative capture cross-sections (see Table IV (a)-(d)). The inconsistency in ranking sequences of total neutron yields per fission further demonstrated discrepancies in nuclear data from different libraries (see Table IV(e)). Rankings of americium and curium nuclides confirmed disagreement in MA neutron yield evaluations from different libraries.

A reverse trend was noted between the sequences of magnitudes for $\eta^X(E)$ and $\alpha^X(E)$ (see Table IV(f)). The higher a nuclide ranked on the $\eta^X(E)$-scale, the lower it ranked on the $\alpha^X(E)$-scale. The trend applied to all MAs with the exception of ^{243}Cm and ^{235}U. This confirms that reduced capture-to-fission ratio improves neutron yield per neutron absorbed in fuel materials.

II.D IMPACT OF TRU NUCLEAR CHARACTERISTICS ON TRANSMUTATION STRATEGIES

The ranking assessment showed that energy dependent characteristics of MAs from different libraries have similar profiles (see Figures 4 and 10 for ENDF/B6.8 and JENDL3.3 plots as examples). Hence, conclusions on transmutation strategies involving TRUs are independent of nuclear data source library. However, evaluated data for the characteristics are different from one library to another. Discrepancies indicate inherent uncertainties in nuclear data. Consequently, results of reactor physics calculations would depend on the nuclear data sets used.

CHAPTER III

PWR SPENT FUEL VARIATIONS

This chapter discusses the variation of TRU compositions in PWR spent fuel. A description of the spent fuel analysis method is presented. Section III.A describes the applied code system. The study resulted in the selection of TRU vectors for use in TRU-fueled VHTR.

III.A VISTA FUEL CYCLE ANALYSIS

Nuclear Fuel Cycle Simulation System (VISTA) is a computer code system which estimates nuclear fuel cycle service and material requirements including material flows. It was developed by the International Atomic Energy Agency (IAEA). VISTA estimates long-term fuel cycle requirements for both open and closed fuel cycle strategies. A variation in any input parameter results in recalculation of the whole fuel cycle [15]. VISTA was selected for this analysis because its inputs represent typical reactor types and fuel cycle options.

III A.1 MATERIAL FLOW IN VISTA

Material mass flows in VISTA represent the entire nuclear fuel cycle. It starts from mining processes and ends with spent fuel storage or HLW storage. Nuclear materials are tracked in each process of the fuel cycle. The material mass flow model is adapted to the two present options for nuclear fuel backend strategies: direct disposal

(open fuel cycle) and reprocessing & recycling (closed fuel cycle with uranium and plutonium management).

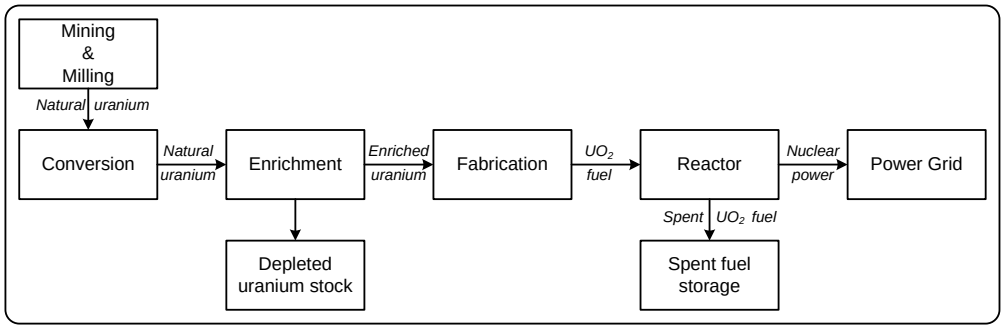

Figure 11. VISTA once-through fuel cycle model.

The direct disposal strategy is the once-through (O-T) fuel cycle option with conventional (low enriched) uranium oxide (LEU) fuels. The O-T cycle is illustrated in Figure 11. This fuel cycle option is the most widely employed option worldwide.

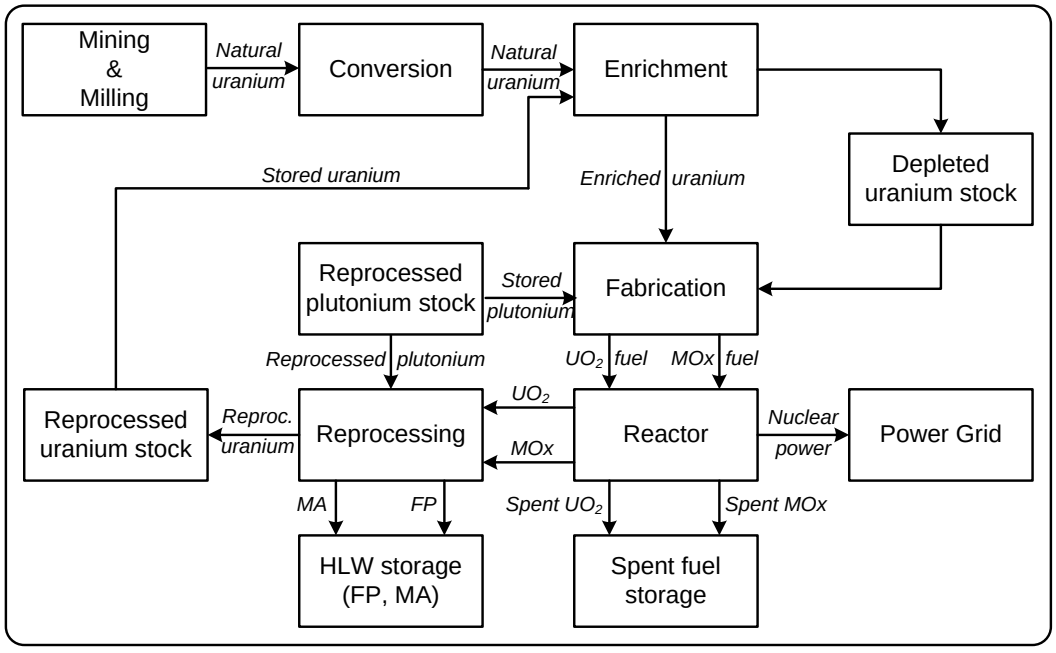

Figure 12. VISTA uranium and plutonium recycling model.

The reprocessing and recycling strategy in VISTA adopts uranium and plutonium (U-Pu) recycling option. The option is modeled in VISTA with two fuel types. The first fuel type (fuel type 1) is LEU oxide (UO_2) fuel. The second fuel type (fuel type 2) is mixed oxide (MOx) fuel. The MOx fuel is composed of uranium and plutonium oxides. The model includes reprocessing part of the spent fuels for uranium and plutonium recovery. The recovered uranium and plutonium stocks are usable materials for fuel fabrication. The spent fuels which are not reprocessed and HLWs from reprocessing are kept in storage for disposal (see Figure 12).

III.A.2 VISTA REACTOR MODEL (IN-CORE FUEL CYCLE)

The VISTA fuel burnup and depletion model is also known as the VISTA reactor module. It computes spent nuclear fuel composition characteristics. The module employed in VISTA is called CAIN (CAlculation of INventory of spent fuel). The reactor module solves Bateman's equations for a point assembly using one-group cross sections. The applied CAIN cross section library includes data for 7 reactor types:

- Pressurized Water Reactor (PWR);
- Boiling Water Reactor (BWR);
- Pressurized Heavy Water Reactor (PHWR);
- Reactor Bolshoy Moshchnosty Kanalny (RBMK);
- Advanced Gas-cooled Reactor (AGR);
- Gas Cooled Reactor (GCR);
- Vodo-Vodyanoi Energetichesky Reactor (VVER).

The library has UO_2 fuel cross sections for these reactors. It also has MOx fuel cross section data for PWR, BWR and VVER.

There are 28 neutron reaction and decay chains for irradiation phase and 14 decay chains for cooling/storage phase. The main assumptions are:

- Selected nuclides are important in radiotoxicity of the spent fuel and their nuclear characteristics.
- ^{234}U is ignored in fresh fuel composition.
- Short-lived nuclides are assumed to completely decay to the daughter nuclides instantaneously. This assumption affects nuclides with half-life less than 8 days.
- Nuclides with half-lives greater than 400 years are assumed to be stable for in-core calculations. Actual decay schemes are used during cooling periods.
- Transmutation chains are terminated for ^{238}Pu, ^{242}Cm and ^{244}Cm to simplify calculations (see "x" in Figure 13).

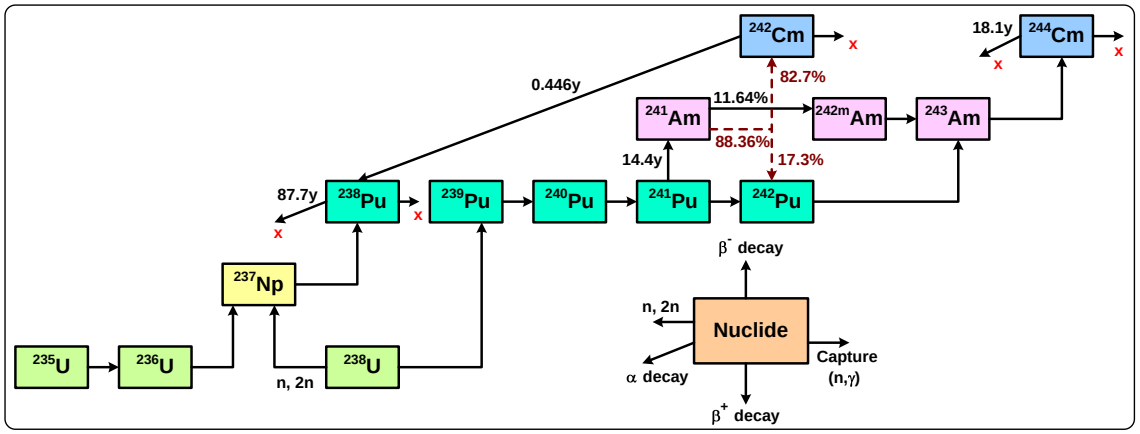

Figure 13. Transformation chain of TRU nuclides in CAIN.

Fourteen heavy nuclides are selected for CAIN depletion calculations: ^{235}U, ^{236}U, ^{237}U, ^{237}Np, ^{238}Pu, ^{239}Pu, ^{240}Pu, ^{241}Pu, ^{242}Pu, ^{241}Am, ^{242m}Am, ^{243}Am, ^{242}Cm and ^{244}Cm. The corresponding transformation chains are shown in Figure 13.

III.A.3 VISTA INPUT AND OUTPUT PARAMETERS

Calculations are done with selected input parameters in order to simplify the development and analysis of different energy scenarios. The primary input parameter is the nuclear fuel cycle option. The subsequent input data are determined by the choice of fuel cycle options. The input parameters are summarized in Table V. Historical IAEA data stored in VISTA databases are employed in the calculations. The output parameters are summarized in Table VI. Communications between VISTA/CAIN modules are illustrated in Figure 14. All outputs are presented in annual quantities.

Table V. VISTA input parameters.
Parameters with quantitative values are mark "x".

Input Parameter	**O-T cycle**	**U-Pu recycling**
Reactor Type	All seven types	PWR, BWR & VVER
Fuel Type	UO_2	UO_2 & MOx
Projected nuclear power (MWe)	x	x
Load factor (%)	x	x
Thermal efficiency (%)	x	x
Discharge burnup (GWd/t)	x	x
Initial enrichment in UO_2 (%)	x	x
Tail assay (%)	x	x
Uranium mine grade (%)	x	x
Plutonium content (%)		x
Share of Fuel Type 2 in the reactor (%)		x
Reprocessing Ratio for each fuel type (%)		x
Uranium Source for Fuel Type 2		Dep. U
Cooling time before reprocessing (yr)		x
Use of Reprocessed Uranium		Yes or No

Table VI. VISTA output parameters.

Front end output parameters
Fresh fuel requirements
Enrichment service requirements
Depleted uranium quantity
Conversion requirements
Natural uranium requirements

Back end output parameters
Discharged spent fuel quantity
Spent fuel reprocessing quantity
Spent fuel storage quantity
Reprocessed material quantity (U & Pu)
Other material quantities (MA, FP & HLW)

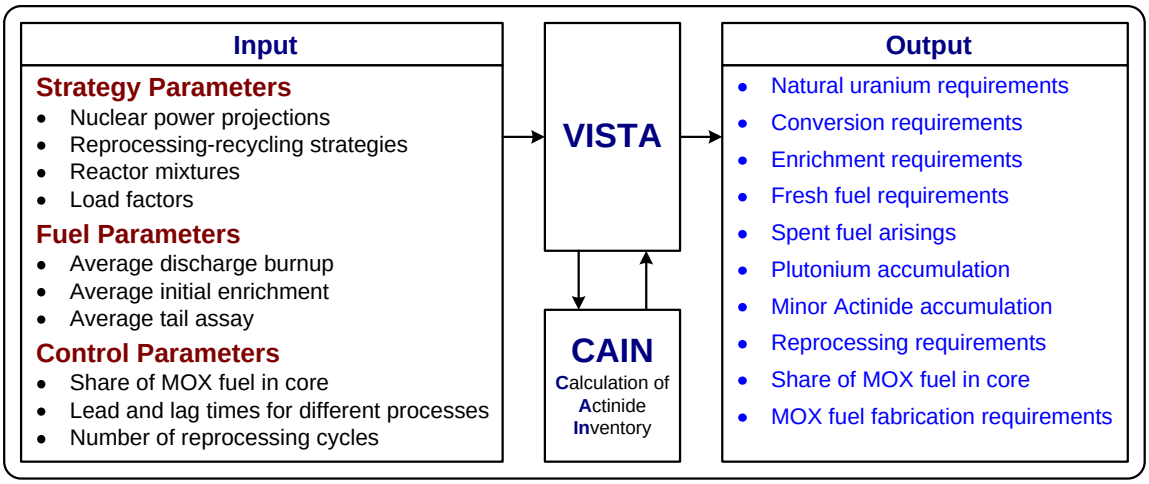

Figure 14. VISTA input and output parameters.

III.A.4 LIMITATIONS OF VISTA

- The VISTA simulation does not support calculation of time-dependent fuel isotopic compositions. The reactor model calculations are related to the equilibrium core conditions.
- Quantities such as the initial core loading and the discharged fuel at end of reactor life are not considered.
- The assumption imposed on depletion calculations simplified the fuel cycle. Hence advanced fuel types may not be reasonably simulated. Expansion of the reaction and decay chains would be required.
- User-specified sets of input and output parameters are not supported. This makes the application less adaptable for specific calculations.
- Export of the output data to file or other post processing applications is not supported.

III.B PWR SPENT FUEL ANALYSIS

The reference spent fuel isotopic compositions are based on the pressurized water reactor (PWR) spent fuel data. The selection of PWRs is based on their worldwide deployment and the fact that 69 of 104 commercial reactors licensed by the United States Nuclear Regulatory Commission (NRC) are PWRs.

III.B.1 PRESSURIZED WATER REACTOR (PWR)

The reference data for a typical PWR design are provided in Table VII [16]. The average fuel cycle length is eighteen months. A third of the core is replaced during each refueling.

III.B.2 PWR PARAMETERS IN VISTA

The PWR model in VISTA includes both O-T cycle and U-Pu recycling options. Default PWR parameters in VISTA are presented in Table VIII. The input data were broadly classified as fuel parameters and scenario parameters. Fuel types include UO_2 and MOx. Depleted uranium is assumed for MOx fuel. The selected uranium enrichment in UO_2 fuel is about 4%. The corresponding tail assays from enrichment service requirements are 0.3%. The configuration is expected to attain 45 GWd/tHM assuming operation at 1000 MWe. The reactor capacity factor is 85%.

Table VII: Reference PWR design.

Design Parameter	**Specification**
General	
Thermal Power (MW)	3400
Operating Pressure (MPa)	15.5
Inlet coolant temperature (^{o}C)	286
Outlet coolant temperature (^{o}C)	324
Coolant	Water
Moderator	Water
Core axis	Vertical
Fuel	LEU: UO_2
Enrichment (wt. %)	3 to 5
Reactor vessel	
Diameter (m)	4.83
Height (m)	13.4
wall thickness (cm)	22.4
material	Steel
Core	
Assembly type	17 x 17
Number of assemblies	193
Number of fuel elements per assembly	264
Assembly pitch (cm)	21.5
Fuel element height (m)	3.851
Active fuel height (m)	3.66
Equivalent core diameter (m)	3.37
Fuel element	
outer diameter (cm)	0.95
pellet diameter (cm)	0.82
Clad thickness (cm)	0.057
Clad material	Zircaloy-4

Table VIII. Default VISTA PWR design parameters.

Input	O-T Cycle	U & Pu Recycling	
Fuel Parameters		Type 1	Type 2
Fuel Types	UO_2	UO_2	MOx
Mine Grade (%U) -Fuel type 1	1	1	
Fuel type 2 (share %)			5
Enrichment - type 1 (%)	3.968	3.968	
Total Pu content - type 2 (%)			7.23
Burnup (GWD/t)	45	45	45
Reprocessing ratio (%)		33	0
Cooling time before reprocessing (y)		5	7
Rep U use - type 1 (Yes/No)		No	
Uranium source - type 2			Dep. U
Scenario Parameters			
Nuclear Power (MWe)	1000	1000	
Thermal Efficiency (%)	32.6	32.6	
Load Factor (%)	85	85	
Tails assay from enrichment (%)	0.3	0.3	

Fuel burnup and load factor were perturbed as provided in Table IX. These parameters were selected because of their applicability to both fuel cycle options and impact on fuel residence time in reactors.

Table IX. Perturbed parameters in VISTA calculations.

Parameter	Variations				
Load factor (%)	80	85	90	95	100

Parameter	Variations					
Burnup (GWd/t)	20	30	45	50	60	70

III.B.3 SENSITIVITY ANALYSIS

Perturbations of input fuel cycle parameters resulted in variations of spent fuel isotopic compositions. Sensitivity calculations were performed to assess effects of input parameters on spent fuel compositions.

The analysis accounts for dependencies of output data vectors on input parameters. The output data vectors and input parameters are denoted $\vec{N} \equiv (N_1,...,N_i,...,N_n)$ and p respectively. The corresponding uncertainties in p are given by δp.

Assuming the parameter p is varied m times, its values are designated as $p_1,..., p_j,..., p_m$. The input uncertainty of the j^{th} variation, δp_j is evaluated as:

$$\delta p_j = p_j - p_{j+1};\ j = 1,2,...,m-1 \tag{8}$$

The change in output vector due to p_j-variation is $\delta\vec{N}$. It was calculated for the i^{th} element of the output vector as:

$$\delta N_i = N_{i,p_j} - N_{i,p_{j+1}} \tag{9}$$

The sensitivity factor associated with the i^{th} element of the output vector due to uncertainties in the input parameter p_j is denoted as $S_{i,j}$. This factor is defined evaluated as:

$$S_{i,j} \cong \frac{\delta N_i}{N_i} \Big/ \frac{\delta p_j}{p_j} = \frac{p_j}{N_i}\frac{\delta N_i}{\delta p_j} \tag{10}$$

The sensitivity factor $S_{i,j}$ is a dimensionless measure of the responses of dependent variables to input independent parameters. A positive sensitivity factor represents increase in dependent variable as input parameter is increased. A negative sensitivity factor denotes reduction in dependent variable as input parameter increases. Higher magnitudes of sensitivity factors indicate increasing response to changes in input parameters.

III.C SPENT FUEL VECTORS

III.C.1 PRESENTATION OF SPENT FUEL COMPOSITION IN VISTA

VISTA outputs based on default parameters are provided in Table X. The Tables provide fresh fuel and stored (discharged) fuel compositions. Result table for U-Pu recycling option includes composition for reprocessed fuel. Fuel data are provided in separate columns for UO_2 and MOx fuels. All fuel contents are equilibrium compositions. Total content of fuels represent amount required for/arising from a refueling batch.

Table X. VISTA output for the reference PWR configuration.

(a) Contents of spent fuel from O-T cycle

Nuclide	Contents of O-T cycle fuel (ton)	
	Fresh Fuel	Stored Fuel
U235	0.839177	0.141172
U236	0.000000	0.110102
U238	20.309426	19.681061
Np237	0.000000	0.014515
Pu238	0.000000	0.005207
Pu239	0.000000	0.108183
Pu240	0.000000	0.055828
Pu241	0.000000	0.031977
Pu242	0.000000	0.013887
Am241	0.000000	0.001009
Am242m	0.000000	0.000023
Am243	0.000000	0.003144
Cm242	0.000000	0.000382
Cm244	0.000000	0.001048
Total HM	21.148603	20.167539
Total FP	-	0.981063
Grand Total	21.148603	21.148603

(b) Contents of spent fuel from U-Pu recycling option

Nuclide	Contents of U-Pu recycling option fuel (ton)					
	Fresh Fuel		Stored Fuel		Reprocessed Fuel	
	U Fuel	U-Pu	U Fuel	U-Pu	U Fuel	U-Pu
U235	0.797218	0.002943	0.089856	0.001435	0.044257	0.000000
U236	0.000000	0.000000	0.070080	0.000296	0.034517	0.000000
U238	19.293955	0.978035	12.526996	0.954458	6.170013	0.000000
Np237	0.000000	0.000000	0.009239	0.000141	0.004550	0.000000
Pu238	0.000000	0.001044	0.003314	0.001030	0.001632	0.000000
Pu239	0.000000	0.045952	0.068859	0.017361	0.033915	0.000000
Pu240	0.000000	0.016537	0.035535	0.015412	0.017502	0.000000
Pu241	0.000000	0.008945	0.020353	0.009499	0.010025	0.000000
Pu242	0.000000	0.003976	0.008839	0.005093	0.004354	0.000000
Am241	0.000000	0.000000	0.000642	0.000752	0.000316	0.000000
Am242m	0.000000	0.000000	0.000015	0.000020	0.000007	0.000000
Am243	0.000000	0.000000	0.002001	0.001834	0.000986	0.000000
Cm242	0.000000	0.000000	0.000243	0.000149	0.000120	0.000000
Cm244	0.000000	0.000000	0.000667	0.000895	0.000329	0.000000
Total HM	20.091172	1.057430	12.836639	1.008373	6.322524	0.000000
Total FP	-	-	0.624447	0.049057	0.307563	0.000000
Grand Total	20.091172	1.057430	13.461086	1.057430	6.630087	0.000000

III.C.2 SPENT FUEL VECTOR FROM DEFAULT VISTA PARAMETERS

The output vectors from VISTA default parameters illustrated variations in discharge fuel composition resulting from differences in fresh fuel compositions (see Table XI). Fuel compositions were presented in weight percent. Compositions for U-Pu recycling option are given as:

1. Total spent fuel (SNF): calculated as the sum of stored fuel and reprocessed fuel.
2. Net SNF from uranium based fuel: estimated as the difference between Total SNF and fresh MOx fuel load.

Table XI. Normalized contents of discharged fuel.

Nuclide	O-T cycle	U - Pu Recycling	
		Total SNF	Net SNF from U Fuel
U235	0.006675	0.006409	0.006600
U236	0.005206	0.004960	0.005221
U238	0.930608	0.929209	0.929435
Np237	0.000686	0.000659	0.000693
Pu238	0.000246	0.000283	0.000245
Pu239	0.005115	0.005681	0.003692
Pu240	0.002640	0.003237	0.002584
Pu241	0.001512	0.001886	0.001540
Pu242	0.000657	0.000865	0.000712
Am241	0.000048	0.000081	0.000085
Am242m	0.000001	0.000002	0.000002
Am243	0.000149	0.000228	0.000240
Cm242	0.000018	0.000024	0.000025
Cm244	0.000050	0.000089	0.000094
Total MA	0.000265	0.000424	0.000447
Total FP	0.046389	0.046389	0.048831
Grand Total	1.000000	1.000000	1.000000

Based on Table XI, the net TRU content from O-T and U-Pu cycle represents 1.11 wt. % and 0.94 wt. % of discharge fuel respectively. Hence, the U-Pu recycling option

with PWR led to 15 % reduction in TRU production. The reduction in TRU is largely due to net consumption of ^{239}Pu (see Figure 15 below). Figure 15 also shows that MA production is increased in the U-Pu recycling option.

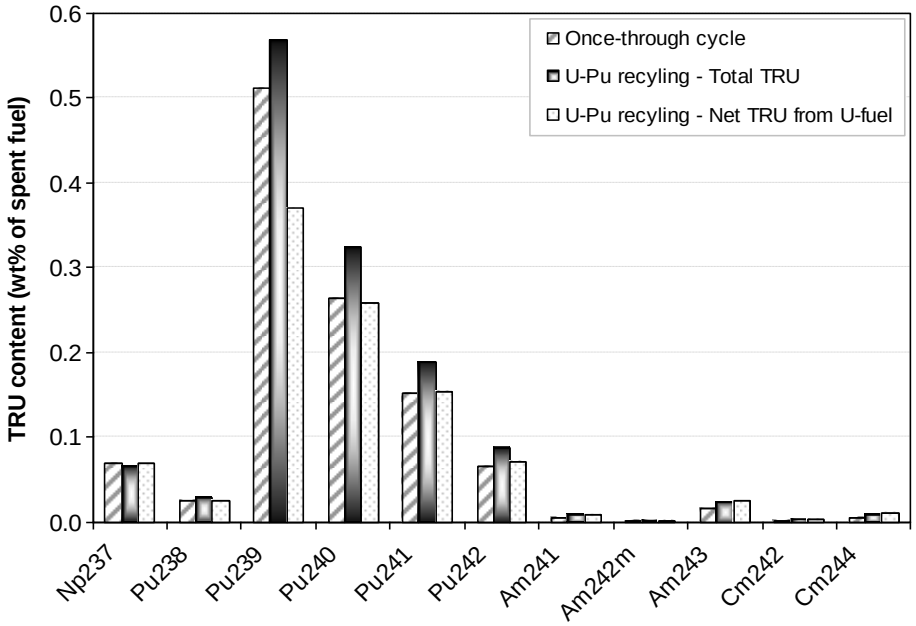

Figure 15. TRU vectors from O-T cycle and U-Pu recycling option.

III.C.3 FLUCTUATIONS OF SPENT FUEL VECTORS

The VISTA system recalculates the fuel requirements using the basic formula:

$$m_{rc} = \frac{P \times t}{B_R} \tag{11}$$

where m_{rc} is the recalculated fuel requirement, P is the reactor thermal power, t is the fuel residence time in the reactor, and B_R is the fuel burnup. Increase in load factor assuming other parameters are held constant results in increased fuel requirement. This explains the increase in discharge fuel quantities with increasing load factor (see Table XII). The linear relationship between m_{rc} and t, assuming constant burnup, results in independence of the spent fuel composition weight percentages on load factor. Thus,

the weight percents of TRU vectors resulting from load factor perturbation and default parameters provided identical results.

Table XII. PWR spent fuel vectors as a function of load factor variations.

Nuclide	**Load Factor (%)**				
	80	**85**	**90**	**95**	**100**
Once-through cycle compositions (ton)					
U235	0.132868	0.141172	0.149476	0.157780	0.166085
U236	0.103625	0.110102	0.116578	0.123055	0.129531
U238	18.523352	19.681061	20.838771	21.996480	23.154190
Np237	0.013661	0.014515	0.015369	0.016223	0.017077
Pu238	0.004901	0.005207	0.005513	0.005820	0.006126
Pu239	0.101820	0.108183	0.114547	0.120911	0.127274
Pu240	0.052544	0.055828	0.059112	0.062396	0.065680
Pu241	0.030096	0.031977	0.033858	0.035739	0.037620
Pu242	0.013071	0.013887	0.014704	0.015521	0.016338
Am241	0.000950	0.001009	0.001068	0.001128	0.001187
Am242m	0.000022	0.000023	0.000024	0.000026	0.000027
Am243	0.002959	0.003144	0.003329	0.003514	0.003699
Cm242	0.000360	0.000382	0.000405	0.000427	0.000450
Cm244	0.000986	0.001048	0.001110	0.001171	0.001233
Total FP	0.923354	0.981063	1.038773	1.096483	1.154192
Grand Total	19.904567	21.148603	22.392638	23.636673	24.880709
U-Pu recycling option compositions (ton)					
U235	0.127575	0.135548	0.143523	0.151495	0.159469
U236	0.098721	0.104893	0.111062	0.117233	0.123403
U238	18.495498	19.651467	20.807436	21.963404	23.119373
Np237	0.013110	0.013930	0.014749	0.015569	0.016387
Pu238	0.005624	0.005976	0.006327	0.006679	0.007031
Pu239	0.113068	0.120135	0.127202	0.134269	0.141336
Pu240	0.064422	0.068449	0.072475	0.076501	0.080527
Pu241	0.037531	0.039877	0.042223	0.044568	0.046914
Pu242	0.017210	0.018286	0.019362	0.020437	0.021513
Am241	0.001609	0.001710	0.001811	0.001912	0.002012
Am242m	0.000040	0.000042	0.000044	0.000046	0.000049
Am243	0.004537	0.004821	0.005105	0.005388	0.005672
Cm242	0.000482	0.000512	0.000542	0.000572	0.000602
Cm244	0.001779	0.001891	0.002001	0.002112	0.002224
Total FP	0.923358	0.981067	1.038777	1.096487	1.154197
Grand Total	19.904567	21.148603	22.392638	23.636674	24.880708

Spent fuel vectors based on load factor variations and burnup variations are provided in Tables XII and XIII. The discharged fuel quantities in U-Pu recycling option represented Total SNF as described in section III.C.2.

Table XIII. PWR spent fuel vectors as a function of fuel Burnup variations.

Nuclide	**Burnup (GWD/MTHM)**					
	20	**30**	**45**	**50**	**60**	**70**
Once-through cycle composition (ton)						
U235	0.970212	0.432213	0.141172	0.097324	0.045867	0.021367
U236	0.160486	0.139612	0.110102	0.100941	0.084080	0.069511
U238	45.162866	29.895323	19.681061	17.629895	14.544671	12.333547
Np237	0.009447	0.012024	0.014515	0.014921	0.015104	0.014588
Pu238	0.001306	0.002621	0.005207	0.006105	0.007709	0.008862
Pu239	0.212696	0.157600	0.108183	0.097224	0.080392	0.068202
Pu240	0.062616	0.064656	0.055828	0.051986	0.044665	0.038457
Pu241	0.020224	0.028932	0.031977	0.031096	0.028125	0.024776
Pu242	0.002713	0.006783	0.013887	0.015893	0.018796	0.020190
Am241	0.000339	0.000691	0.001009	0.001030	0.000978	0.000865
Am242m	0.000006	0.000014	0.000023	0.000024	0.000023	0.000021
Am243	0.000217	0.000898	0.003144	0.004142	0.006202	0.007994
Cm242	0.000058	0.000175	0.000382	0.000432	0.000483	0.000481
Cm244	0.000023	0.000163	0.001048	0.001638	0.003328	0.005584
Total FP	0.981148	0.981199	0.981063	0.981093	0.981029	0.981084
Grand Total	47.584356	31.722904	21.148603	19.033742	15.861452	13.595530
U-Pu recycling option composition (ton)						
U235	0.926784	0.413478	0.135548	0.093618	0.044341	0.020811
U236	0.152787	0.132949	0.104893	0.096180	0.080141	0.066278
U238	45.085617	29.846383	19.651467	17.604279	14.525093	12.318278
Np237	0.009098	0.011555	0.013930	0.014318	0.014494	0.014003
Pu238	0.003352	0.003908	0.005976	0.006764	0.008197	0.009224
Pu239	0.268318	0.184924	0.120135	0.106749	0.086868	0.072994
Pu240	0.100256	0.087679	0.068449	0.062486	0.052044	0.043745
Pu241	0.040468	0.042003	0.039877	0.037885	0.033173	0.028530
Pu242	0.012492	0.013463	0.018286	0.019786	0.021882	0.022656
Am241	0.001419	0.001612	0.001710	0.001664	0.001490	0.001270
Am242m	0.000026	0.000035	0.000042	0.000042	0.000039	0.000035
Am243	0.002039	0.002697	0.004821	0.005756	0.007664	0.009292
Cm242	0.000186	0.000314	0.000512	0.000555	0.000591	0.000573
Cm244	0.000366	0.000708	0.001891	0.002566	0.004399	0.006749
Total FP	0.981147	0.981198	0.981067	0.981097	0.981036	0.981090
Grand Total	47.584356	31.722903	21.148603	19.033742	15.861452	13.595531

Increase in burnup resulted in decreased discharged fuel masses (see Table XIII). The decrease can be explained by the relationship between m_{rc} and B_R (see equation (11)). Varying burnup levels impacts the equilibrium solution to the Bateman equation. Thus, burnup variations also impact the TRU vector compositions.

The plots in Figure 16 illustrate the impact of fuel burnup levels on TRU content of PWR spent fuels. The TRU nuclides have varying compositions depending on fuel burnup. Consequently, fissile content of spent fuel varies with burnup. The highest concentration of the fissile content (^{239}Pu and ^{241}Pu) was at 50GWd/tHM.

Table XIV provides the MA buildup at higher burnup. The MA content at 60 GWd/tHM was more than double the content at 45 GWd/tHM. This confirms PWRs as non-transmuters. PWR spent fuel discharged at burnups below 60 GWd/tHM should contain more fissile materials since the MA contents are reduced.

Table XIV. MA content of PWR spent fuel.

Fuel cycle	MA content (% of content at 45GWd/t)			
	45 GWd/t	50 GWd/t	60 GWd/t	70 GWd/t
O-T cycle	100	144	262	415
U-Pu recycling	100	131	211	311

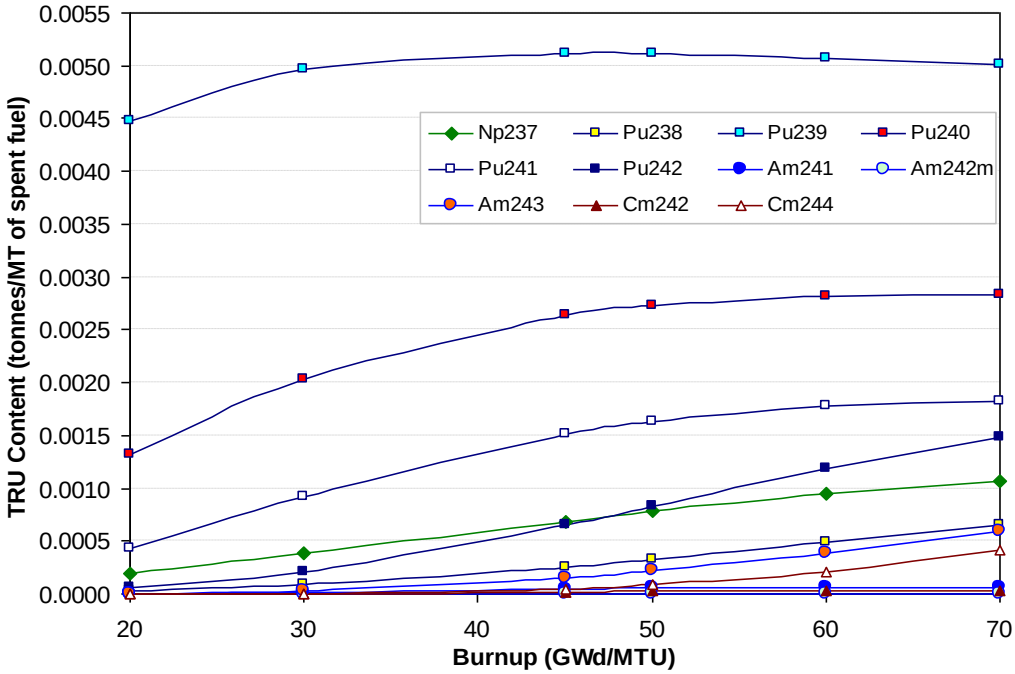

(a) TRU content of spent fuel from O-T cycle.

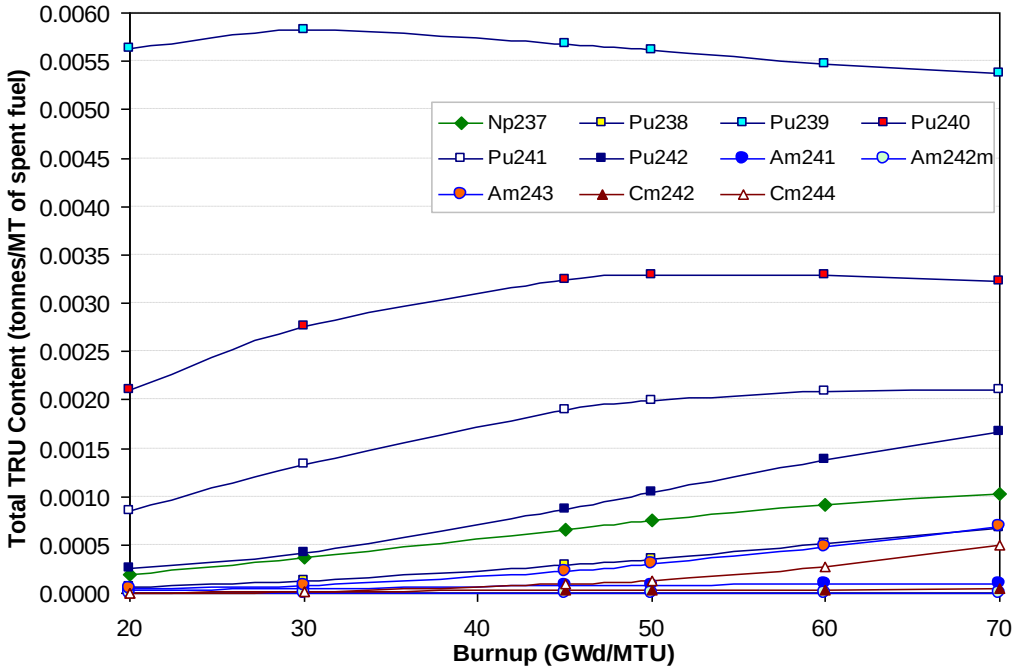

(b) TRU content of spent fuel from U-Pu recycling option.

Figure 16. Normalized TRU content of PWR spent fuel as a function of fuel burnup.

Figure 17 presents the TRU sensitivity factors with respect to fuel Burnup variations. The magnitudes of sensitivity factor of all nuclides decreased with increasing burnup in the O-T cycle scenario. An exception was noted in ^{244}Cm with a slight increase between 45 GWd/t and 50 GWd/t. The general trend in sensitivity factor indicated a rapid variation in TRU composition at lower fuel burnup. TRU vector compositions were less sensitive to burnup in the U-Pu recycling option. The low sensitivity factors at low burnup were due to initial TRU loading in MOx fuel.

The sensitivity profiles for both fuel cycle options were comparable beyond 45 GWd/t. The nuclides exhibited similar response to burnup changes between 45 GWd/tHM and 60 GWd/tHM. The sensitivity factor magnitudes were also comparable at the higher burnups. ^{244}Cm and ^{243}Am had the highest sensitivity factors. The net buildup of the nuclide with increasing burnup resulted in high sensitivity factors.

The response of TRU compositions to burnup variations reduces at burnup levels higher than 50 GWd/tHM. The trend indicates that higher fuel burnup in PWR would not significantly change the discharged TRU composition.

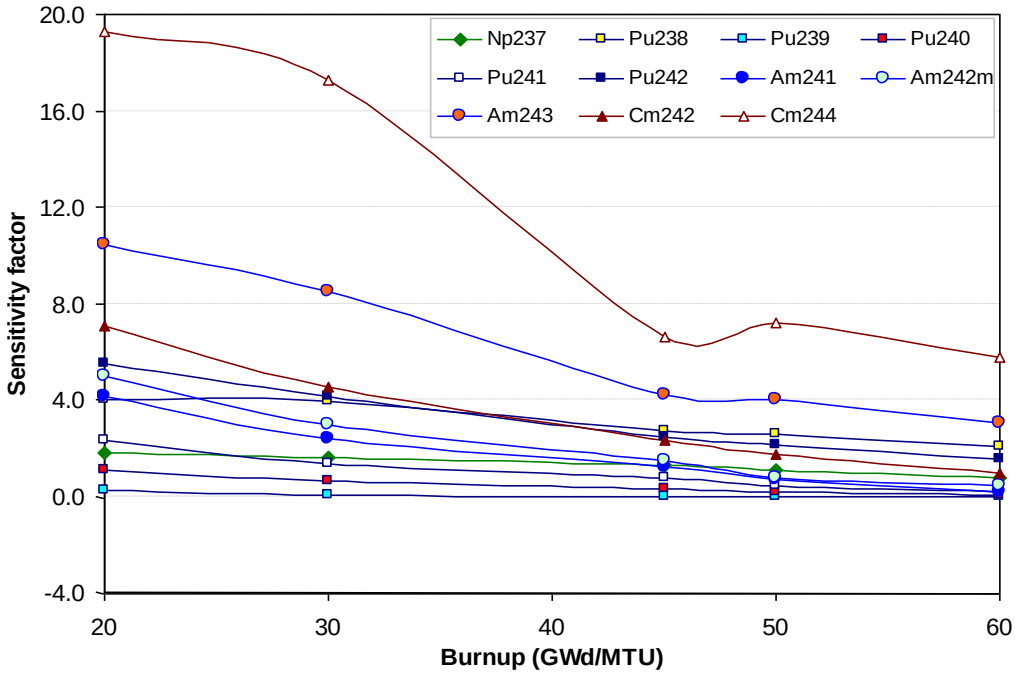

(a) Sensitivity factor of TRU from O-T cycle.

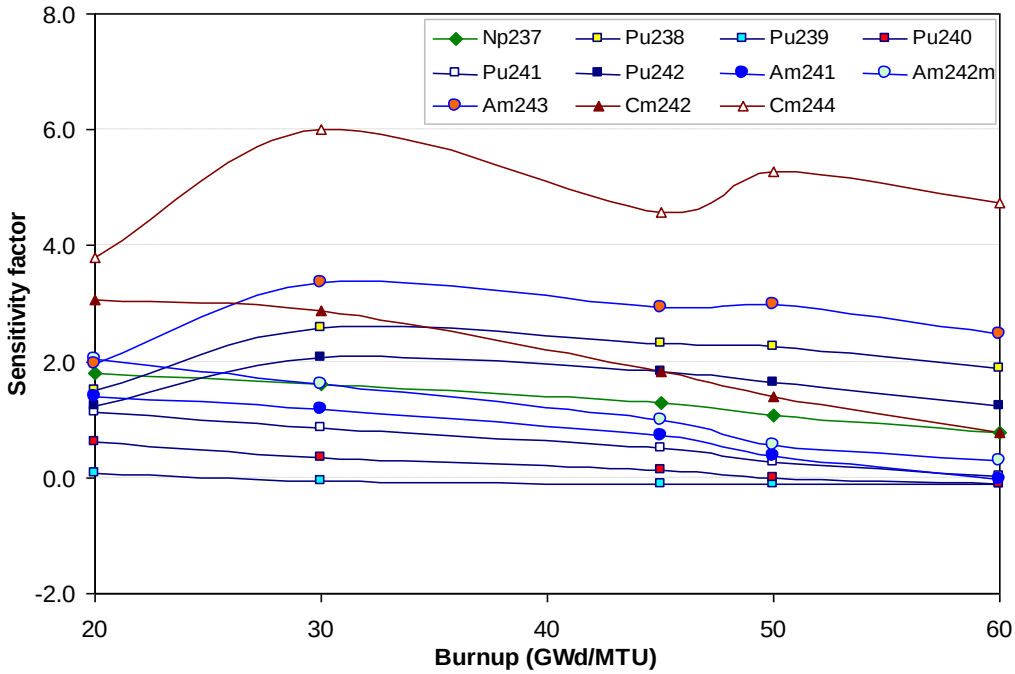

(b) Sensitivity factor of TRU from U-Pu recycling option.

Figure 17. Sensitivity factor of TRU vectors from spent fuel with respect to burnup.

III.D TRU VECTORS FROM LEGACY SPENT FUELS

A legacy spent fuel is the U.S spent nuclear fuel that is stored at four DOE locations: the Savannah River Site in South Carolina, the Hanford Site in Washington, the Idaho National Engineering and Environmental Laboratory, and Fort St. Vrain in Colorado [13,14]. DOE plans to dispose the legacy spent fuel in the proposed Yucca Mountain repository. The TRU vectors from the spent fuel are potential source of materials for advanced TRU-bearing fuel. To assure realistic quantification of the advanced fuels, the characteristics of the legacy spent fuel materials were used to derive the nuclide distributions in the fuel. Table XV summarized the derived TRU composition from the average PWR spent fuel [14].

Table XV. TRU vector from average PWR spent fuel.*
Burnup = 41.2 GWd/MTHM, enrichment = 3.75 %, decay time = 23 years.

Nuclide	TRU composition (wt %)
Np237	6.056132
Pu238	1.973126
Pu239	51.605541
Pu240	21.943351
Pu241	4.129537
Pu242	4.497216
Am241	8.301571
Am242m	0.020373
Am243	1.247513
Cm242	0.000049
Cm243	0.003342
Cm244	0.197768
Cm245	0.021760
Cm246	0.002721
Total	100.000000

*Values are based on Inventory and Characteristics of Spent Nuclear Fuel from [14]

III.E REFERENCE TRU VECTORS FOR TRU-BEARING COMPOSITIONS FOR USE IN VHTRs

Advanced TRU-bearing nuclear fuels are considered for Generation IV VHTRs. The TRU-fuels are part of the strategy to manage spent nuclear fuel and possibly close the nuclear fuel cycle. The complete closure of the fuel cycle would result in a considerable reduction of the actinide content.

Five TRU vectors were selected as possible compositions for use in VHTRs. The vectors included four compositions from VISTA calculations and the TRU composition from legacy fuel. All selected TRU vectors are presented in Table XVI. Figure 18 shows the comparison of legacy compositions and the PWR discharged compositions.

Table XVI. Selected TRU vectors from PWR spent nuclear fuel for VHTR analysis.

Nuclide	TRU Composition (wt %)				
	Vector 1	Vector 2	Vector 3	Vector 4	Vector 5
Np237	6.056132	6.171421	6.171265	6.646592	7.338986
Pu238	1.973126	2.213862	2.213832	2.719485	3.745779
Pu239	51.605541	45.995280	45.995587	43.308640	39.062219
Pu240	21.943351	23.735956	23.736092	23.157276	21.702583
Pu241	4.129537	13.595412	13.595490	13.851780	13.665849
Pu242	4.497216	5.904355	5.904261	7.079571	9.132917
Am241	8.301571	0.428967	0.428991	0.458816	0.475207
Am242m	0.020373	0.009757	0.009779	0.010691	0.011176
Am243	1.247513	1.336774	1.336718	1.845063	3.013532
Cm242	0.000049	0.162625	0.162413	0.192435	0.234688
Cm243	0.003342	0.000000	0.000000	0.000000	0.000000
Cm244	0.197768	0.445591	0.445573	0.729651	1.617065
Cm245	0.021760	0.000000	0.000000	0.000000	0.000000
Cm246	0.002721	0.000000	0.000000	0.000000	0.000000
Total	100.000000	100.000000	100.000000	100.000000	100.000000

Description of TRU vectors	
Vector 1	Legacy SNF: Average burnup of 41.2 GWd/MTHM, 23 years old
Vector 2	VISTA simulation: Burnup = 45 GWd/t; 100% load factor
Vector 3	VISTA simulation: Burnup = 45 GWd/t; 85% load factor (default)
Vector 4	VISTA simulation: Burnup = 50 GWd/t; 85% load factor
Vector 5	VISTA simulation: Burnup = 60 GWd/t; 85% load factor

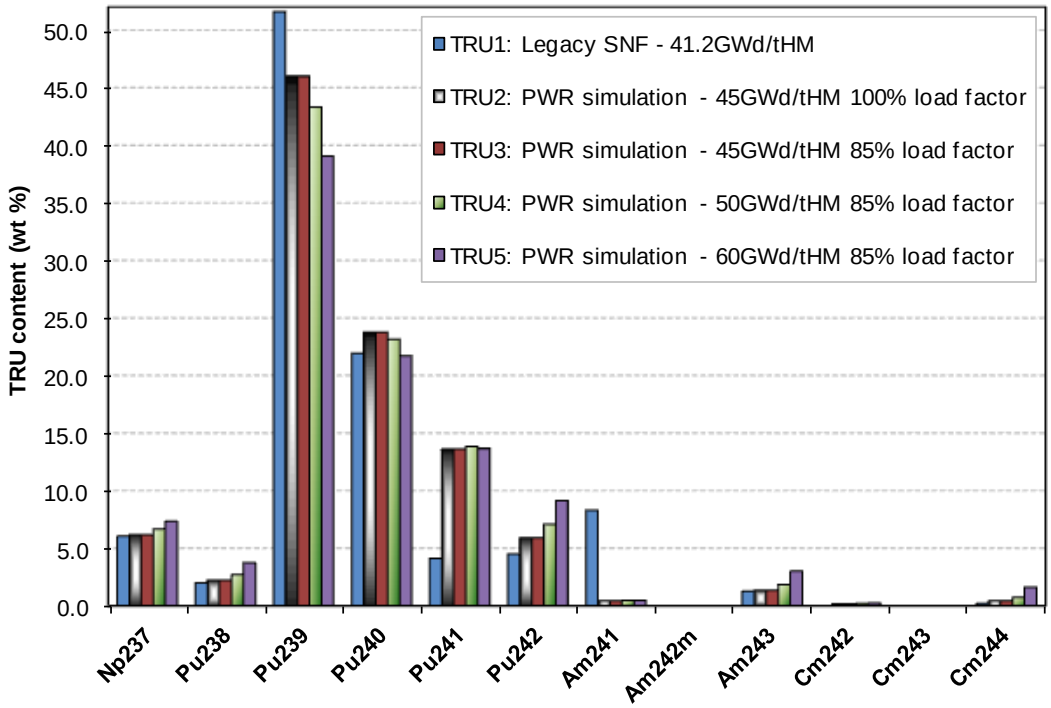

Figure 18. Comparison of selected TRU vectors.

CHAPTER IV

BEHAVIOR OF TRU-FUELED VHTRs

This chapter discusses potential performance characteristics of VHTRs with TRU-bearing fuels. A description of the VHTR and metrics developed for the analysis of TRU transmutation efficiency are presented. The chapter also describes the applied code system.

IV.A VHTR MODEL

The VHTR model was developed for use in calculations with SCALE code system. The model takes into account fuel assembly blocks, control rod blocks, replaceable reflectors and a permanent outer reflector. The fuel assembly blocks were based on HTTR fuel block configuration [31]. The HTTR fuel block was adapted into the VHTR power core model. Table XVII provides the major specification of the VHTR core.

Table XVII. VHTR core specifications.

Parameter	**Value**
Thermal Power (MW)	1480 MW
Power Density (MW/MTHM)	103
Coolant	Helium
Coolant Pressure (MPa)	4
Average Outlet Temperature (°C)	850
- Reflector material	Graphite
Core height (m)	10.44
Active core height (m)	7.54
Core diameter (m)	6.80
Core layout	
Radial arrangement	
- Fuel columns	Annular - 3 rings
- Number of Fuel Columns	66
- Center reflector	5 rings
- Outer reflector	Replaceable - 2 rings; Permanent
Axial arrangement	
- Number of fuel block layers	13
- Number of top reflector layers	2
- Number of bottom reflector layers	3
Fuel block	
- Number of fuel blocks	858
- Number of fuel elements per block	31
- Fuel element	TRISO particle in annular compact
- Fuel matrix	Graphite
- Fuel block height (cm)	58

IV.A.1 THE FUEL BLOCK

The fuel assembly block consists of fuel elements, burnable poison rod, coolant channels and hexagonal graphite block. The graphite block is 36 cm across flats. It has 31 vertical borings of diameter 4.1 cm to accommodate the fuel elements. There are 3 vertical holes representing burnable poison locations. In VHTR models utilizing burnable poison, 2 holes are loaded while the third is reserved. The block has a handling hole in the center. The coolant channels are the gaps between fuel bores and fuel elements. The fuel assembly block model is provided in Figure 19.

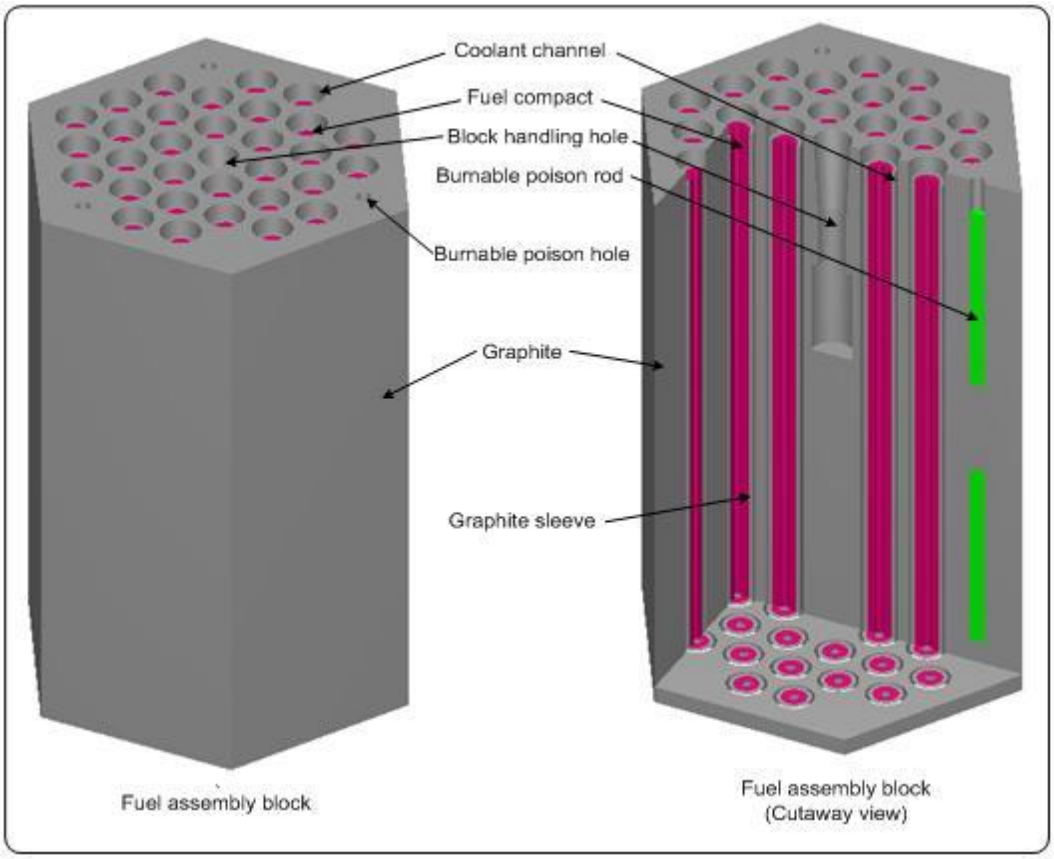

Figure 19. Fuel assembly block.

The fuel assembly block specification is provided in Table XVIII. Low concentration of natural boron was included in the fuel block model to account for impurities in graphite. Figure 20 provides the layout and dimensions of the fuel block.

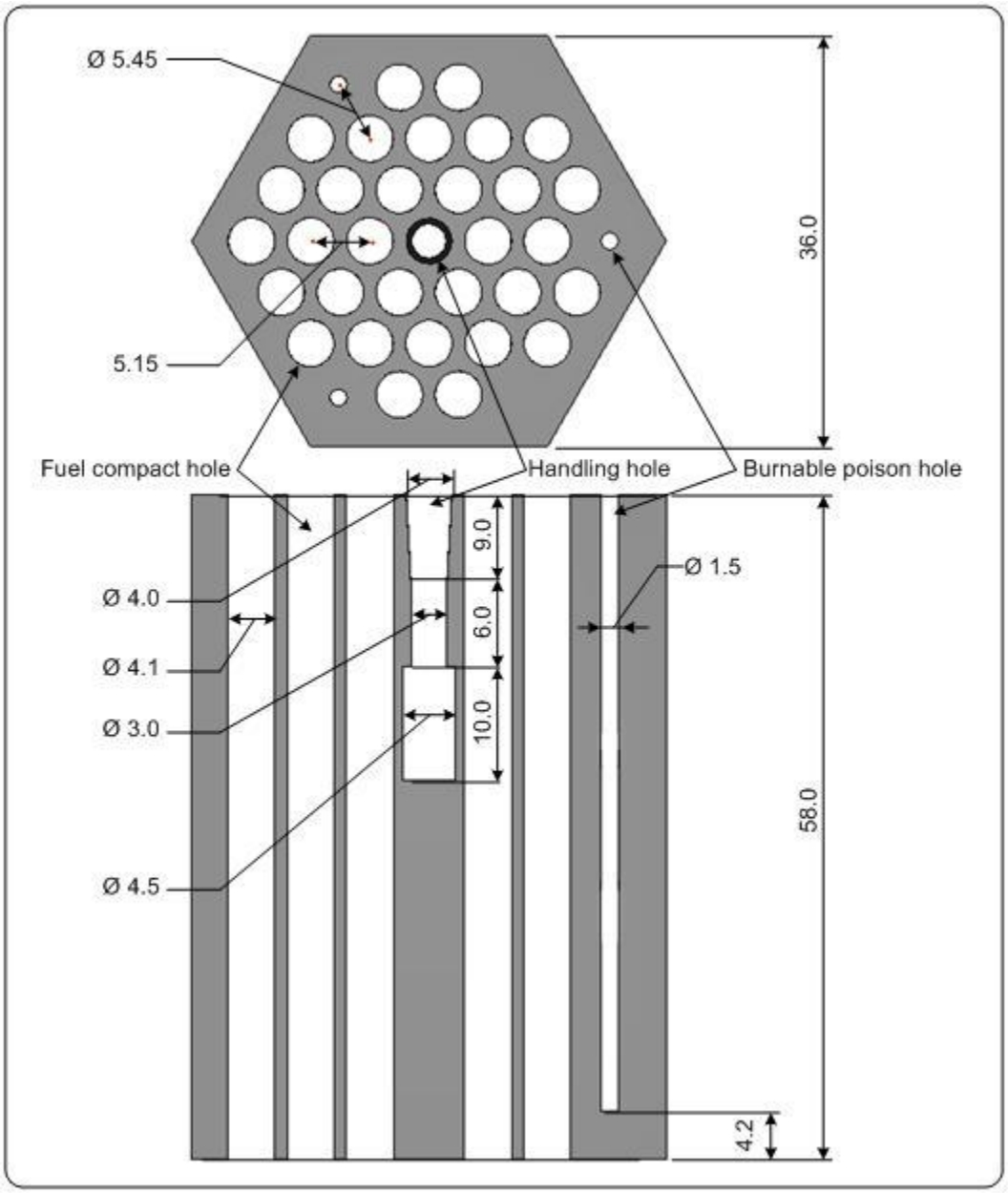

Figure 20. Fuel assembly block dimensions (all values in cm).

Table XVIII. Fuel assembly block specifications.

Parameter	Value
Assembly type	Pin-in-block
Block configuration	Hexagonal Prism
Material	Graphite
Density (g/cc)	1.770
Impurity (ppm B_{nat})	0.40
Height (cm)	58.0
Width across flats (cm)	36.0
Number of fuel holes	31
Fuel hole diameter (cm)	4.1
Fuel hole height (cm)	58.0
Number of burnable poison holes	3
Burnable poison hole diameter (cm)	1.5
Burnable poison hole height (cm)	53.8

The fuel element consists of 14 vertically stacked annular fuel compacts in graphite sleeve. The inner and outer diameters of the sleeve are 2.6 cm and 3.4 cm respectively. The graphite sleeve model included natural boron to account for impurities. The fuel compact has inner and outer diameters of 1.0 cm and 2.6 cm respectively. Each fuel compact is 3.9 cm in height. It consists of TRISO coated fuel particles at 0.2 volume fraction. The particles are embedded in graphite matrix with low concentrations of natural boron to account for impurities. Each fuel compact contains about 8,405 particles. The fuel element specifications are provided in Table XIX.

Table XIX. Fuel element specifications.

Fuel Compact	
Parameter	**Value**
Volume fraction of fuel grains	0.2
Number of fuel grains per fuel compact	8405
Number of compacts per fuel element	14
Inner diameter (cm)	1.0
Outer diameter (cm)	2.6
Compact height (cm)	3.9
Graphite matrix density (g/cc)	1.690
Matrix Impurity (ppm B_{nat})	0.82

Graphite Sleeve	
Parameter	**Value**
Material	Graphite
Density (g/cc)	1.770
Impurity (ppm B_{nat})	0.37
Inner diameter (cm)	2.6
Outer diameter (cm)	3.4
Height (cm)	54.6

The TRISO coated particles are composed of a spherical fuel kernel of diameter 0.6 mm. The kernel composition depends on the fuel type (see section IV.D). The particle structure is provided in Figure 21. The first coating is a layer of low density porous carbon. The second coating is high density pyrolytic carbon, followed by silicon carbide layer. The outermost layer is also high density pyrolytic carbon. Table XX provides the material and dimensions of the TRISO particle.

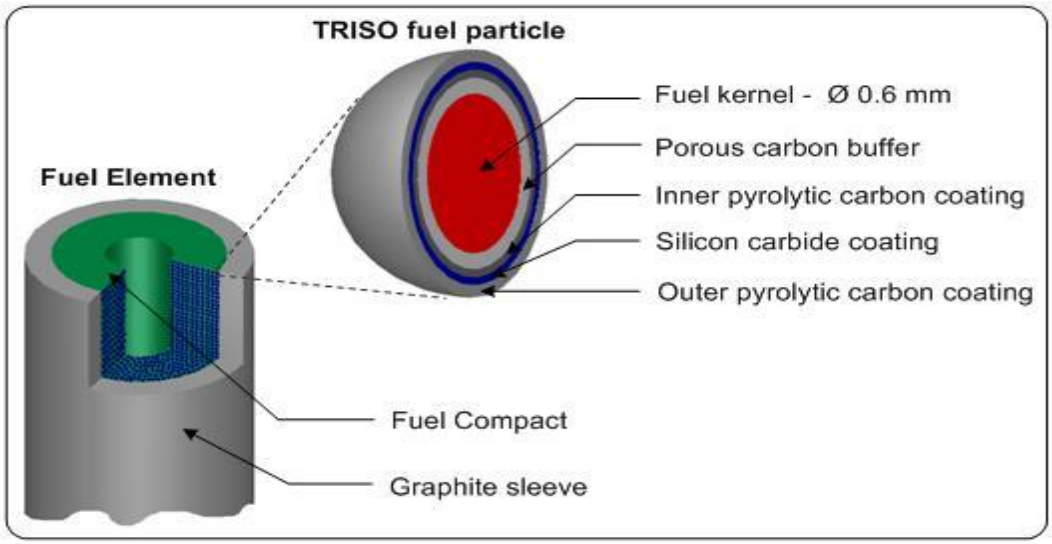

Figure 21. TRISO fuel structure.

Table XX. TRISO particle specifications.

	material	density (g/cc)	diameter (cm)
Fuel kernel	UO_2 or TRU - Carbon mix	10.41	0.0600
1st coating	Porous carbon	1.14	0.0718
2nd coating	Pyrolytic carbon	1.89	0.0780
3rd coating	Silicon carbide	3.20	0.0838
4th coating	Pyrolytic carbon	1.87	0.0930

The TRISO coatings were not explicitly described in the computational model. The 4 layers of coatings were homogenized as shown in Figure 22. The overall coating thickness of the particle was retained in the computational representation.

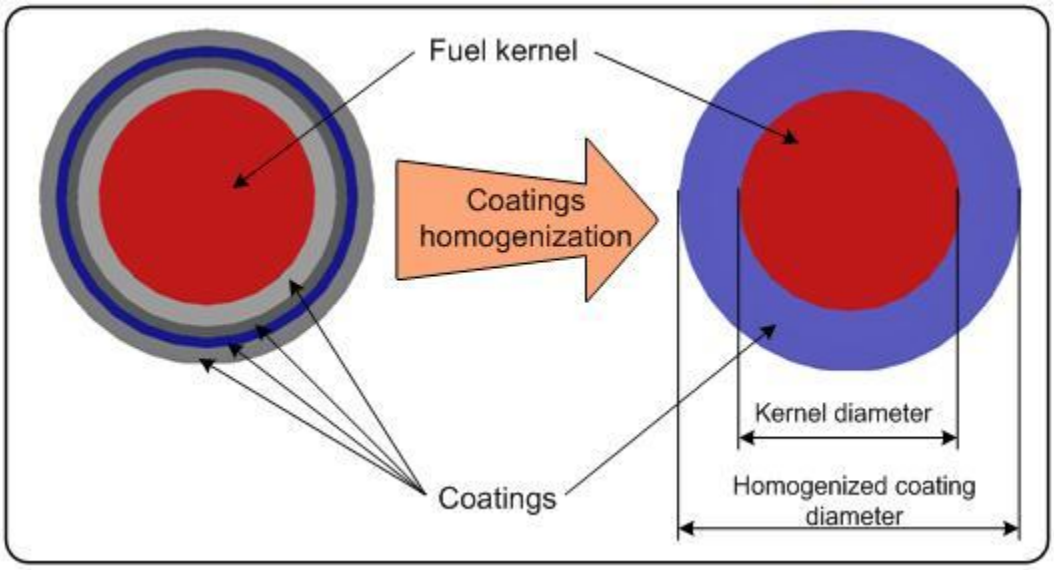

Figure 22. TRISO particle approximation in the VTHR model.

The burnable poison rod consists of 2 boron carbide/carbon sections with graphite middle section (see Fig. 19). The diameter of the rod is 1.5 cm and 50 cm height. The boron carbide/carbon sections have heights of 20 cm, while the graphite section is 10 cm. Table XXI provides the burnable poison specifications.

Table XXI. Burnable poison rod specifications.

Parameter	Value
Absorber section material	B_4C-C
Density (g/cc)	1.82
Natural boron concentration (wt.%)	2.74
Diameter (cm)	1.39
Height (cm)	20
B-10 abundance ratio (wt.%)	18.7
Graphite section - Density (g/cc)	1.77
- Diameter (cm)	1.50
- Height (cm)	10

IV.A.2 THE REPLACEABLE REFLECTOR BLOCKS

The replaceable reflector blocks are hexagonal prisms (similar to fuel block). There are two types of reflector blocks: graphite reflector blocks with coolant channels, and solid graphite blocks. Both types have handling hole in the center. Figure 23 provides images of the replaceable reflector blocks. The blocks are 36 cm across flats and 58 cm in height. Table XXII provides addition details of the blocks with coolant channels.

Table XXII. The specification of replaceable reflector block with coolant channels.

Parameter	Value
Material	Graphite
Density (g/cc)	1.760
Impurity (ppm B_{nat})	0.37
Height (cm)	58.0
Width across flats (cm)	36.0
Number of coolant holes	31
Coolant hole diameter (cm)	4.1
Coolant hole height (cm)	58.0

The blocks with coolant channels are stacked directly above and below the fuel assembly blocks. They are arranged such that the fuel columns in the core have 18 blocks: 2 top and 3 bottom layers of replaceable reflector blocks, with 13 middle layers of

fuel assembly blocks. The holes in the fuel assembly blocks and reflector blocks are aligned, creating passages for helium. The total number of in-core reflector blocks with coolant channels is 330.

The solid reflector blocks represent the central reflector column (61 block columns) and outer replaceable reflectors (102 columns). The blocks maintain the same dimensions and external form as the fuel block. The exception is the absence of holes other than the handling hole. The total number of solid reflector blocks is 2,934. Table XXIII provides addition details of the solid reflector blocks.

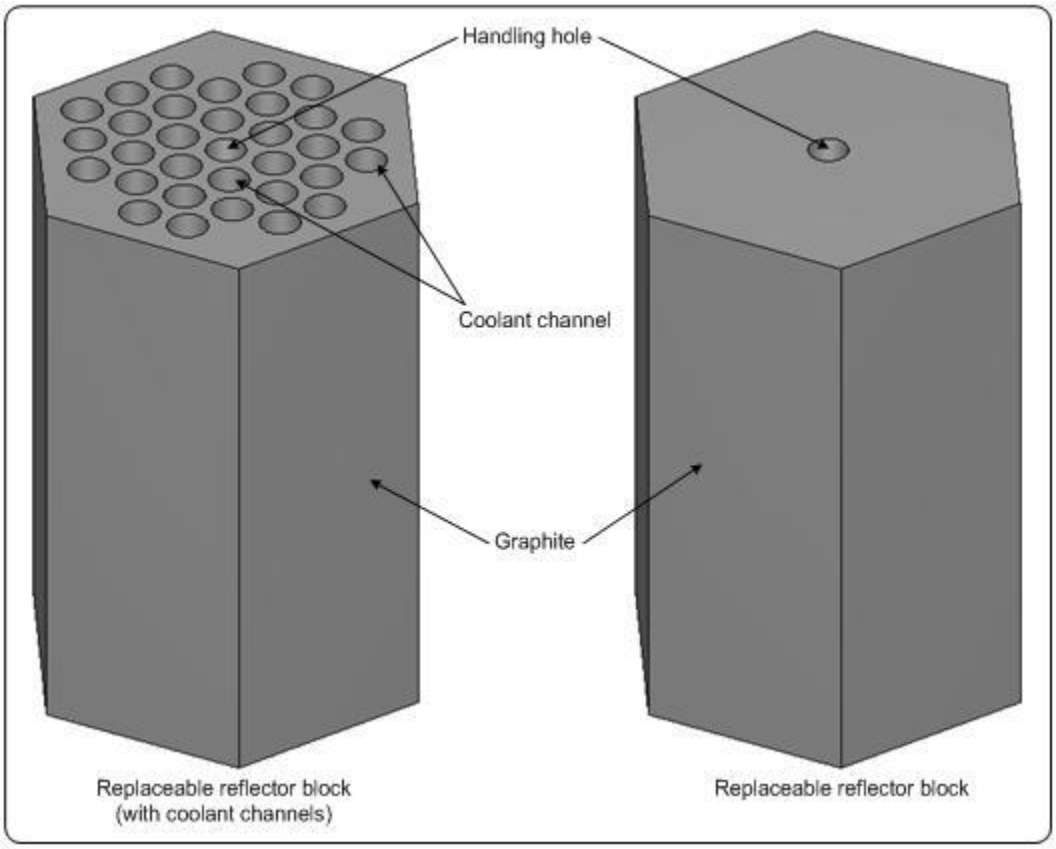

Figure 23. Reflector blocks.

Table XXIII. Solid reflector blocks specifications.

Parameter	Value
Material	Graphite
Density (g/cc)	1.760
Impurity (ppm B_{nat})	0.37
Height (cm)	58.0
Width across flats (cm)	36.0
Number of reflector columns	163
Number of blocks per column	18

IV.A.3 THE CONTROL ROD BLOCK

The control rod block consists of 3 vertical borings, each being 21.3 cm in diameter. The block is a hexagonal graphite prism with similar external form to the fuel block. It is 36 cm across flats and has a height of 58 cm. Figure 24 provides dimensions of the block. There are 36 columns of control rod blocks in the core. Each column consists of 18 blocks stacked one on another. Table XXIV provides the control rod block specification.

Table XXIV. Control rod block specification.

Parameter	Value
Material	Graphite
Density (g/cc)	1.770
Impurity (ppm B_{nat})	0.40
Height (cm)	58.0
Width across flats (cm)	36.0
Number of control rod holes in block	3
Control rod hole diameter (cm)	12.3
Control rod hole height (cm)	58.0

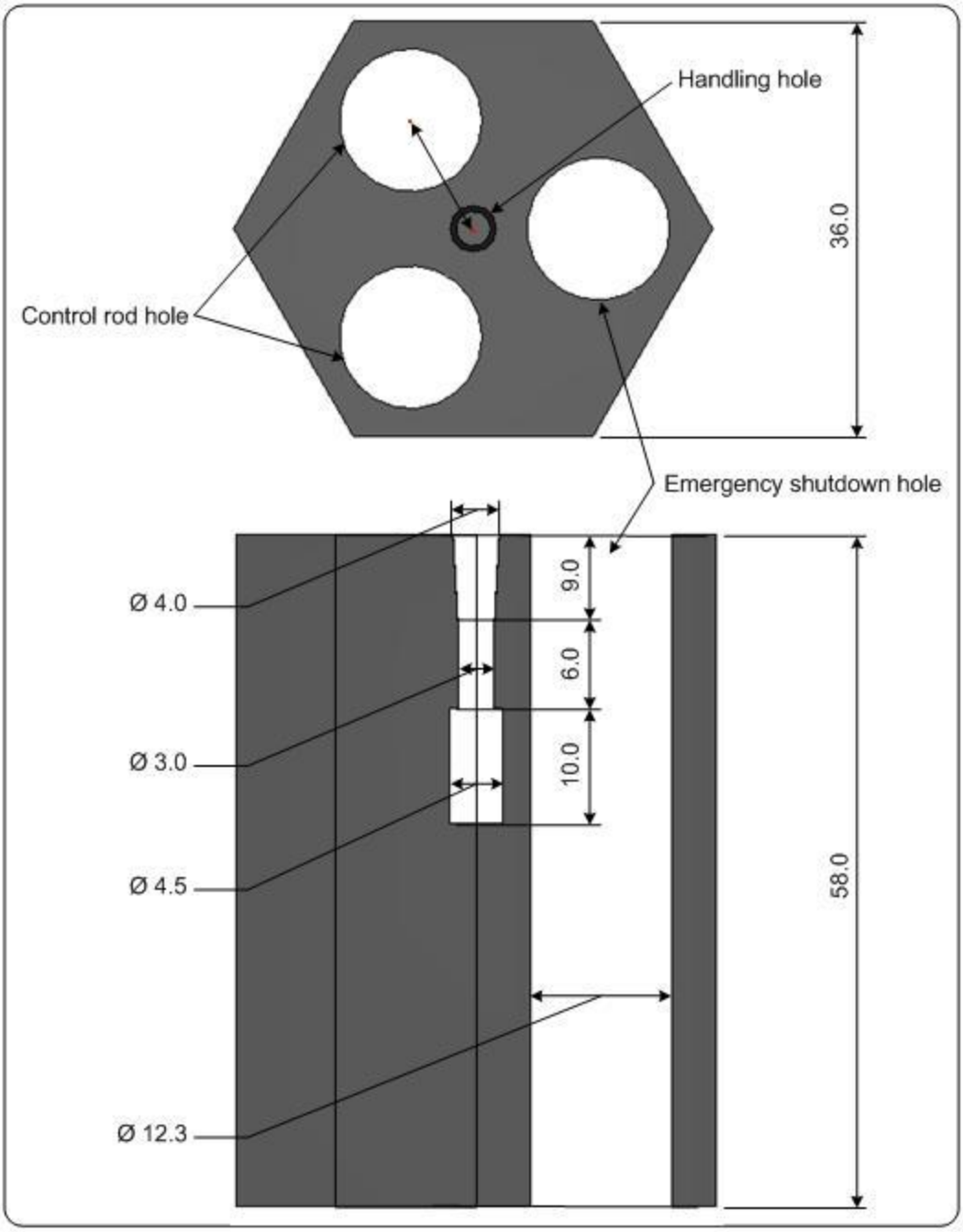

Figure 24. Control rod block dimensions (all values in cm).

IV.A.4 THE 3-D WHOLE CORE VHTR MODEL

The 3-D whole core VHTR model is provided in Figure 25. The core was built by stacking the fuel assembly blocks, replaceable reflector blocks and control rod blocks in the cavity formed by the permanent graphite reflector structures. The control rod blocks and solid replaceable reflector blocks are stacked in columns to form the core assembly. The core height is 10.44 m. It has a diameter of 6.80 m. The active core height is 7.54 m, consisting of 13 fuel assembly blocks per column. The top and bottom axial reflectors are located above and below the active core. The axial reflector assembly is similar to the active core assembly. The difference is the presence of replaceable reflector blocks with coolant channels in place of the fuel assembly block.

The solid replaceable reflectors are arranged side-to-side to form the central reflector column. There are 61 columns of solid replaceable reflectors representing the central reflector. The solid reflectors form 2 additional rings of outer radial reflector for the core. There are 102 columns in the outer reflector. The permanent graphite reflector forms a radial outer boundary for the core. A cross sectional view of the active core can be seen in Figure 25. The whole core was explicitly modeled in SCALE5.1. All calculations where performed at system temperature of 1223K, except when otherwise stated.

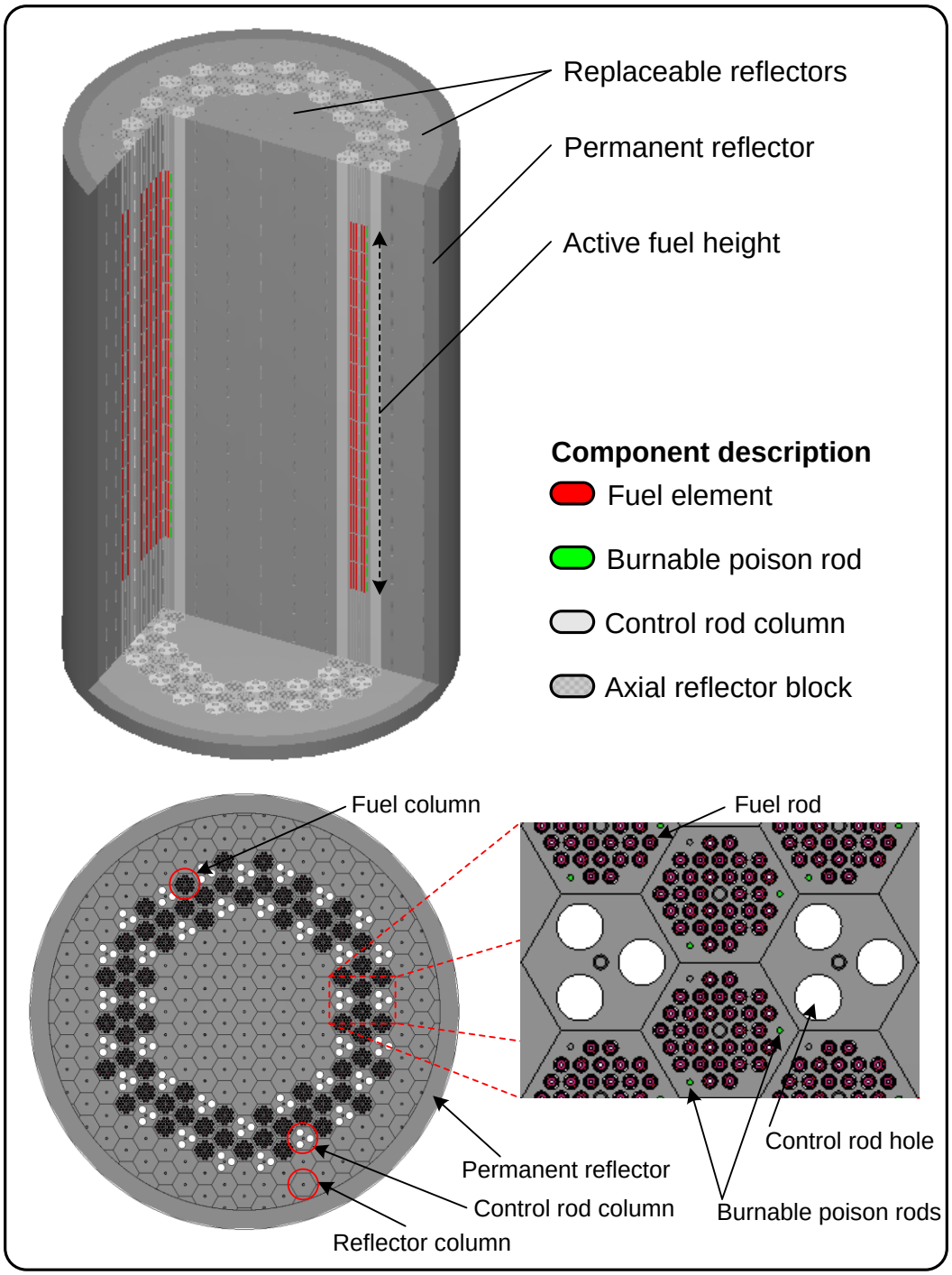

Figure 25. 3-D whole-core VHTR model with horizontal cross-section view.

IV.B VHTR MODELING WITH THE SCALE 5.1 CODE SYSTEM

The VHTR system 3-D computational model was developed for calculations with SCALE (Standardized Computer Analysis for Licensing Evaluation) version 5.1 [17]. SCALE system is a part of the Radiation Safety Information Computational Center (RSICC) code collection.

The SCALE modular code system is developed and maintained by Oak Ridge National Laboratory (ORNL) and is widely accepted around the world for a broad range of nuclear engineering modeling applications including reactor physics, fuel cycle, nuclear waste management, and criticality safety analysis. SCALE 5.1 was used in the present studies.

Two control modules of SCALE were used in the VHTR analysis. The Criticality Safety Analysis Sequence (CSAS) was called for criticality calculations. Fuel depletion calculations were performed with the Transport Rigor Implemented with Time-dependent Operation for Neutronic (TRITON) control module. The 238-Group ENDF/B-VI nuclear data library was used for all SCALE computations.

IV.B.1 THE CRITICALITY SAFETY ANALYSIS SEQUENCE (CSAS)

CSAS was developed within the SCALE code system to provide automated, problem-dependent, cross-section processing followed by calculation of the neutron multiplication factor for the system being modeled [18]. The VHTR model called CSAS No. 2 with KENO V.a (CSAS25) control module for beginning of life criticality analysis. The CSAS25 consists of the following functional modules: BONAMI, WORKER, CENTRM, PMC, CHOPS, XSDRN, CAJUN, AJAX, and KENO V.a [19-24]. Figure 26

provides the CSAS25 control module data flow diagram as it was applied in the present analysis of VHTR configurations.

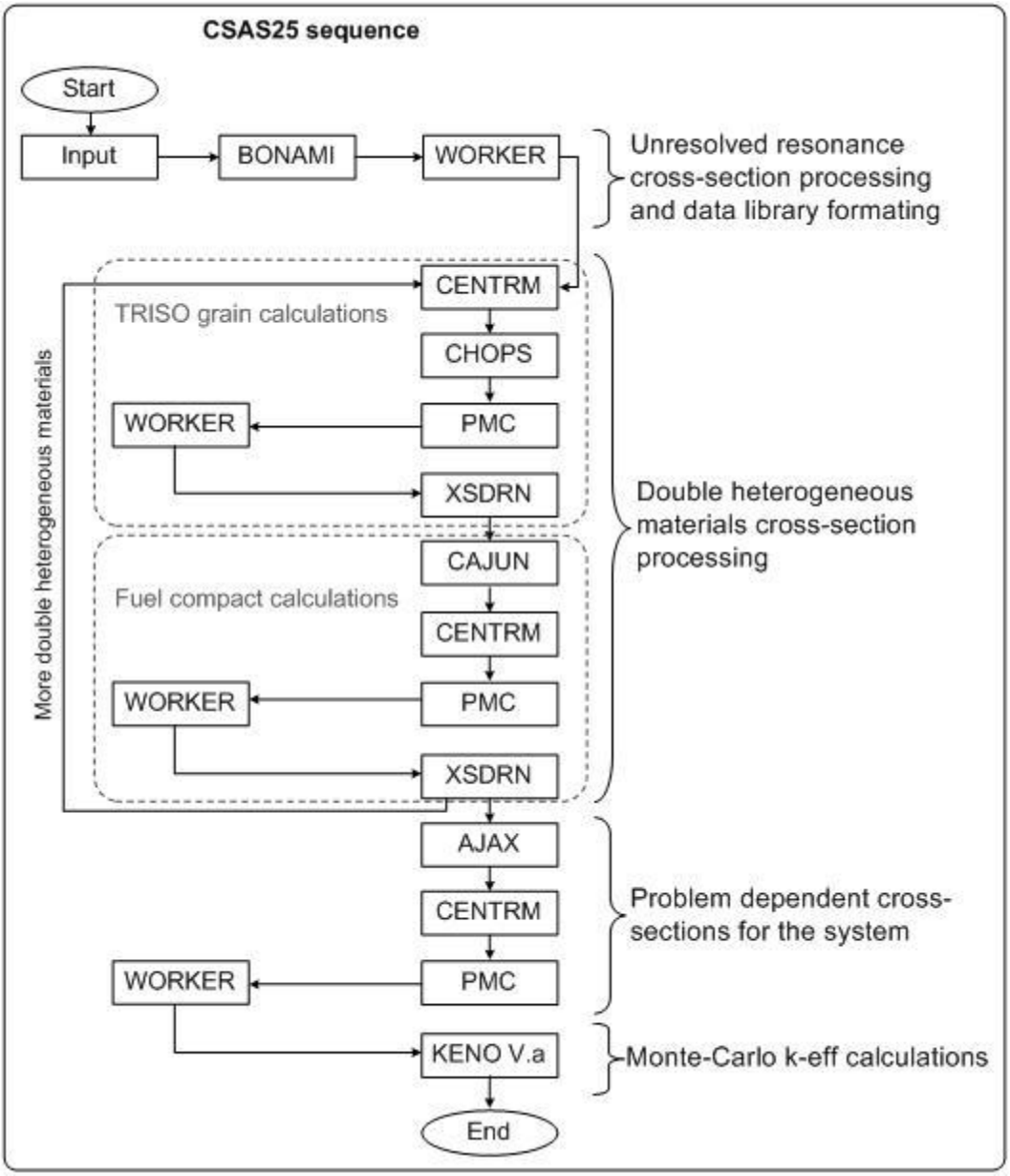

Figure 26. Flow chart of the CSAS25 sequence.

The control module reads the VHTR model data. It then creates multi-group cross-section library and point cross-section library for the functional modules. BONAMI (BONdarenko AMPX Interpolator) performs Bondarenko calculations for resonance self-

shielding using the multi-group cross-section library. The Bondarenko method is based on the assumption that collision density is constant within a narrow band of resonance. The method also assumes resonances in an infinite homogeneous medium. It accounts for the heterogeneity in the system through the use of Dancoff factors. The inputs to BONAMI are cross-sections of VHTR materials and Bondarenko factors. The output is a problem-dependent data set written as an AMPX master library, which is used in conjunction with WORKER for further cross-sections processing.

The WORKER module restructures the AMPX master library to a format readily usable by particle transport modules such as XSDRN and KENO V.a in SCALE. The input requirement is a problem-dependent AMPX master library or AMPX working libraries. The output is a new AMPX working library that is compatible with the input requirements of SCALE particle transport modules.

The first CENTRM (Continuous ENergy TRansport Module) run computes problem-dependent continuous-energy neutron flux spectrum in the lattice of TRISO particles. The CENTRM input requirements are multi-group working library from WORKER and pointwise data library. CHOPS is employed in double heterogeneity treatment of the fuel. The TRISO grains are smeared into a homogenized absorber region appearing in the fuel compact. CHOPS generates pointwise disadvantage factors from the pointwise zone fluxes from CENTRM output file. Flux weighting of the pointwise cross-section data are provided for, using the disadvantage factors in order to correctly treat spatial self-shielding in the homogenized geometry. The disadvantage factors are multiplied by the pointwise cross-section data from CENTRM to generate a new cell-homogenized pointwise library.

The PMC (Produce Multi-group Cross-sections) module is executed to create problem-dependent multi-group cross-section library for the lattice of TRISO particles. The inputs are continuous-energy flux spectrum from CENTRM and cell-homogenized pointwise data library from CHOPS. A second WORKER module is executed next, to convert libraries created to working libraries. CAJUN is executed to combine the TRISO homogenized pointwise data libraries from CHOPS with existing pointwise data libraries to create a new pointwise library.

A second CENTRM pointwise calculation is performed for the lattice of fuel compacts using multi-group library from the second WORKER run and pointwise data library from CAJUN. The CENTRM execution accounts for additional self-shielding in the fuel compact. The output is the fuel compact flux spectrum. A second PMC run modifies the TRISO particle PMC-produced multi-group library to fuel compact multi-group library using fluxes from the second CENTRM run.

The third WORKER run converts the fuel compact multi-group library to a working multi-group library. AJAX (Automatic Joining of AMPX X-Sections) removes cross-sections of mixtures and nuclides used in the TRISO lattice calculations from the latest multi-group library. This is a library cleanup step. The cross-sections are not required in further calculations since the removed data had been homogenized into the fuel compact.

CENTRM computes problem-dependent continuous-energy neutron flux spectrum using the cleaned multi-group library from AJAX and post-CAJUN modified pointwise data library. PMC creates multi-group cross-sections using continuous-energy flux spectrum and the pointwise data library. PMC generates a new problem-dependent

master library. A fourth WORKER converts the master multi-group library into a working multi-group library.

KENO V.a utilizes the multi-group working library to compute effective multiplication factor in the system. KENO V.a is a Monte Carlo code that is capable of modeling 3-D systems. KENO V.a input requirements also include geometry and lattice-cell structure. In addition, KENO V.a generates energy-dependent flux profiles, provides system mean free path and average energy of neutron causing fission.

IV.B.2 THE TRITON DEPLETION SEQUENCE

The TRITON depletion sequence (T5-DEPL) was developed to perform 3-D multi-material depletion using burnup-dependent cross-sections and KENO V.a for criticality calculations. The T5-DEPL consisted of the following modules: BONAMI, WORKER, CENTRM, PMC, CHOPS, CAJUN, AJAX, KENO V.a, KMART, COUPLE, ORIGEN-S and OPUS [24-29]. A flow chart of the TRITON sequence is shown in Figure 27 as it was applied in the present analysis. The sequences and purpose of the functional modules common to both T5-DEPL and CSAS25 are identical. The additional modules in T5-DEPL are required to execute 3-D depletion calculations.

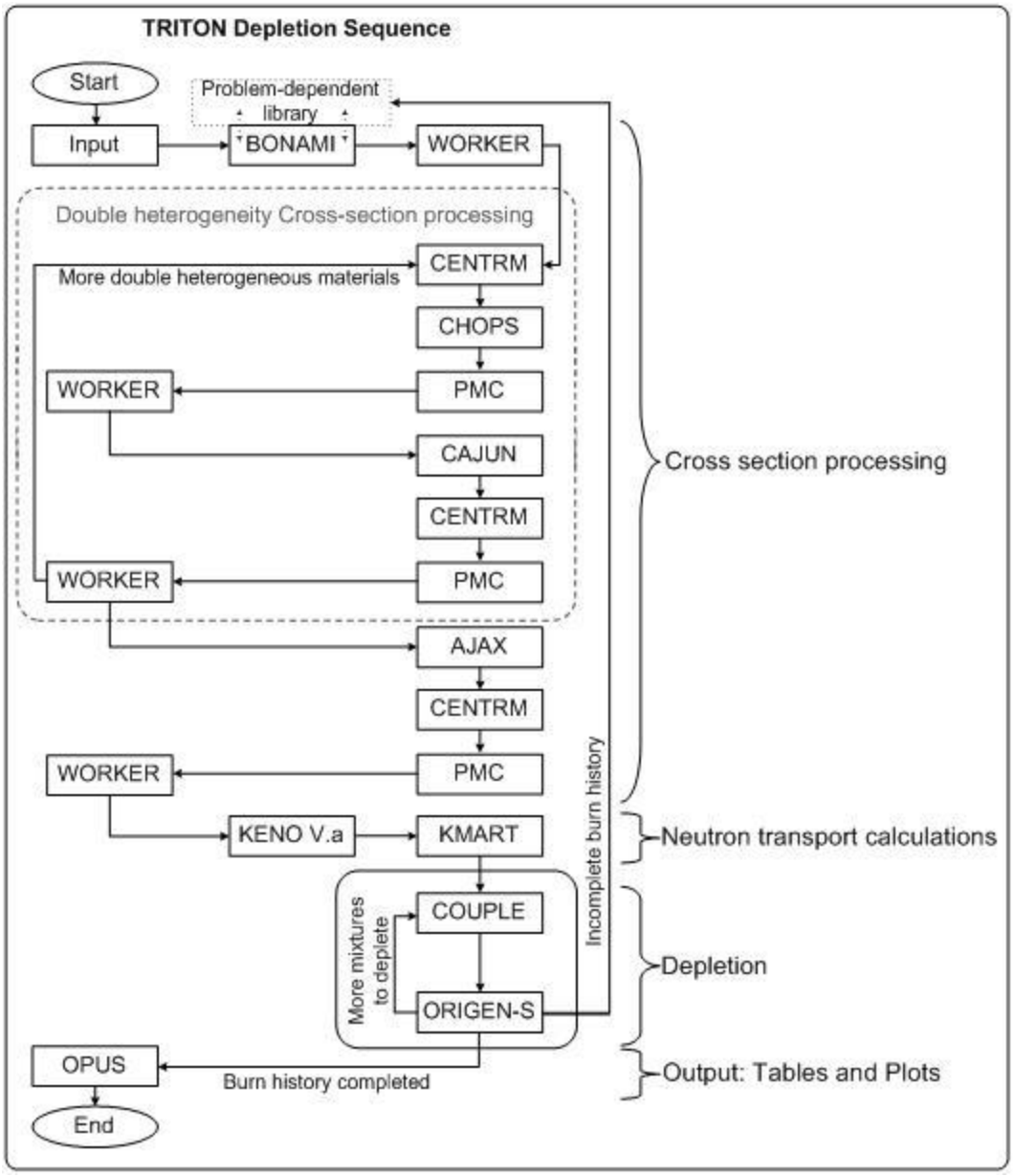

Figure 27. Flow chart of the TRITON sequence.

KMART (Keno Module for Activity-Reaction Rate Tabulation) post-processes KENO V.a computations together with the associated multi-group cross-section libraries. The output is a collapsed 3-group nuclear data library. The collapsed data is required by COUPLE and ORIGEN-S for depletion calculation. COUPLE is a library management module developed to couple problem-dependent cross-sections and flux weighting factors

into libraries used by ORIGEN-S, a SCALE depletion module. COUPLE produces binary libraries, which are the input to ORIGEN-S.

ORIGEN-S performs depletion calculations for the TRU nuclides and burnable poisons in the VHTR model. The module applies neutron cross-sections from libraries managed by COUPLE for its calculations. ORIGEN-S computes time-dependent concentrations for the nuclides. OPUS module processes output for ORIGEN-S. OPUS produces compositions of depleted fuel with time from ORIGEN-S calculations. The output file is formatted such that it can be easily read into graphic/data-plotting packages.

IV.B.3 LIMITATIONS OF SCALE

The following are limitations inherent in SCALE control modules employed [18,30]:

1. Two-dimensional (2-D) effects such as fuel rods in assemblies where some positions are filled with control rod guide tubes, burnable poison rods and/or fuel rods of different enrichments. The cross sections are processed as if the rods are in an infinite lattice of identical rods
2. The assumption of a spatially flat flux in BONAMI may not be good, especially at the peak of a large resonance.
3. The effect of CENTRM's 1-D approximation of the Boltzmann transport equation to the solution of a 3-D problem. The simple 1-D model used in the formulation may not be very accurate where strong 2-D effects occur. The 1-D approximation becomes less rigorous for short fuel pins and/or

small arrays where multidimensional spatial dependence can become important.

IV.C METRICS EMPLOYED IN ANALYSIS

The metrics employed in the VHTR analysis were in two categories:

- Metrics for the in-core fuel cycle studies.
- Metrics for the out-of-core fuel cycle studies.

Table XXV provides the complete list of metrics used in the present analysis for parametric studies.

Table XXV. Quantitative metrics for the TRU-fueled VHTR analysis.

	Metric	Category
1	Initial fuel loading	In-core analysis
2	Moderator-to-fuel (M/F) atom ratio	In-core analysis
3	Energy dependent flux spectra	In-core analysis
4	Multiplication factor changes over time	In-core analysis
5	Fuel Cycle length	In-core analysis
6	Temperature coefficient of reactivity	In-core analysis
7	Helium worth	In-core analysis
8	Boron worth	In-core analysis
9	Neutron balance	In-core analysis
10	Fraction total fissile material fissioned	In-core analysis
11	Net fissile-fuel production and consumption	In-core analysis
12	Fraction of TRU going to waste stream	Out-of-core analysis
13	P&T efficiency	Out-of-core analysis
14	TRU destruction rate	Out-of-core analysis
15	MA destruction rate	Out-of-core analysis
16	Plutonium destruction rate	Out-of-core analysis
17	Total TRU material to disposal	Out-of-core analysis
18	Total MA material to disposal	Out-of-core analysis

IV.C.1 FUEL UTILIZATION METRICS

The metrics provided in-core performance characteristics of the TRU-fueled VHTR. The analyses included LEU fuel compositions for reference purposes. The applied metrics include:

1. The initial fuel loading.
2. Moderator-to-fuel (M/F) atom ratio for the core: This metric was calculated as the atom density ratio of carbon to heavy metal in the fuel compact.
3. Flux spectra in the core: included radial zone-average fluxes, local fluxes in fuel blocks, fuel compact fluxes and TRISO particle fluxes..
4. Multiplication factor as a function of irradiation time.
5. Fuel cycle length was determined as the earlier of:
    - Time when acceptable fluence is reached.
    - Time when core becomes subcritical.
6. Temperature coefficient of reactivity: The multiplications factors from both 1223K and 1323K calculations were used to derive the coefficients of reactivity:

$$\alpha_T = \frac{d\rho}{dT} = \frac{1}{k^2}\frac{\partial k}{\partial T} \cong \frac{1}{k_i k_f}\frac{k_i - k_f}{T_i - T_f} \qquad (12)$$

Where: α_T = temperature coefficient of reactivity

T_i = core temperature at initial calculations (1223K)

T_f = core temperature at later calculations (1323K)

k_i = k-effective at 1223K

k_f = k-effective at 1323K

7. Helium reactivity worth was estimated in calculations with the helium density of 1E-20g/cc. The multiplications factors from both coolant-filled core and near-zero coolant calculations were used to derive the helium reactivity worth of the system:

$$\Delta\rho_x = \rho_x - \rho_0 = \frac{k_x - 1}{k_x} - \frac{k_0 - 1}{k_0} \quad (13)$$

Where: $\Delta\rho_x$ = reactivity worth of mixture x.

k_x = k-effective with complete insertion of mixture x.

k_0 = k-effective mixture x completely withdrawn.

A positive value of helium worth indicates negative reactivity insertion in Loss-of-Coolant-Accident (LOCA) scenario.

8. Boron worth: For each fuel composition, core calculations were performed for cases with burnable poison and cases without. The burnable poison was carbon-boron carbide. The multiplications factors from both cases were used to derive the boron worth of the system using equation (13). A negative value of boron worth indicates negative reactivity insertion due to the presence of burnable poison.
9. Core neutron balance: This was computed for TRU vectors 1 – 5 as a function of flux.
10. Fraction of the total fissile material fissioned, f_{fiss}

- $$f_{fiss} = \frac{N_{fiss,i} - N_{fiss,o}}{N_{fiss,i}} \quad (14)$$
- $N_{fiss,\,i}$ = Total fissile material loaded
- $N_{fiss,\,o}$ = Total fissile material discharged

11. Net fissile-fuel production and consumption, N_{fiss}

- $$N_{fiss} = N_{fiss,i} - N_{fiss,o} \quad (15)$$
- $N_{fiss,\,i}$ = Total fissile loaded
- $N_{fiss,\,o}$ = Total fissile discharged
- Positive N_{fiss} implies fissile consumption
- Negative N_{fiss} implies fissile production

IV.C.2 NUCLEAR WASTE GENERATION METRICS

The metrics provided out-of-core performance characteristics of the TRU-fueled VHTR:

1. Fraction of TRU going to waste stream, f_{TRU}

- $$f_{TRU} = \frac{N_o}{N_i} \quad (16)$$
- N_i = Total TRU loaded
- N_o = Total TRU discharged

2. P&T efficiency, ε_T

- $$\varepsilon_T = \left(\frac{N_i - N_o}{N_i} \right) \times 100 \quad (17)$$
- N_i = Total TRU loaded
- N_o = Total TRU discharged

3. TRU destruction rate, R_{TRU}

- $$R_{TRU} = \frac{N_{TRU,i} - N_{TRU,o}}{t} \quad (18)$$
- $N_{TRU,\,i}$ = Total TRU loaded

- $N_{TRU, o}$ = Total TRU discharged
- t = irradiation time
- Negative R_{TRU} implies TRU buildup rate

4. MA destruction rate, R_{MA}

- $$R_{MA} = \frac{N_{MA,i} - N_{MA,o}}{t} \quad (19)$$
- $N_{MA, i}$ = Total MA loaded
- $N_{MA, o}$ = Total MA discharged
- t = irradiation time
- Negative R_{MA} implies MA buildup rate

5. Pu destruction rate, R_{Pu}

- $$R_{Pu} = \frac{N_{Pu,i} - N_{Pu,o}}{t} \quad (20)$$
- $N_{Pu, i}$ = Total plutonium loaded
- $N_{Pu, o}$ = Total plutonium discharged
- t = irradiation time
- Negative R_{Pu} implies plutonium buildup rate

6. Total TRU material to disposal, $N_{TRU, o}$

- $N_{TRU, o}$ = Total TRU discharged

7. Total MA material to disposal, $N_{MA, o}$

- $N_{MA, o}$ = Total MA discharged

IV.D PERFORMANCE CHARACTERISTICS OF VHTRs WITH TRU

The analyses covered 11 different fuel kernel compositions. Uranium oxide fuel at 15% enrichment was the reference fuel for in-core performance analysis. The other fuel kernel compositions were based on the TRU vectors identified in chapter III (see Table XVI). Each TRU vector represented a fuel composition, which gave 5 fuel compositions. TRU-Carbon fuel compositions were developed with each TRU vector, giving another 5 fuel compositions. The TRU content represented 20% of the TRU-Carbon fuel kernel weight. All fuel kernel densities were fixed at 10.41g/cc. The fuel compacts in the core weighed a total of 14.37MT.

The number of histories run in CSAS25 is different from T5-DEPL sequences. A total of 1,375,000 histories were run for beginning-of-life (BOL) calculations in CSAS25. The total number is the product of the number of histories per generation (2,500) and number of generations run (550). The T5-DEPL ran a total of 200,000 histories over core life of 10 years. The total histories were derived from 1,000 histories per generation and 200 total generations. The average CSAS25 and T5-DEPL run time was about 4 hours and 7.5 hours respectively. The models were run on 2005 Dell Precision 670 Elite and 2006 Dell Precision 490 Workstations with 4GB of RAM and 3.80GHz processor speed. The results are independent of the workstation employed in calculations.

The VHTR model resulted in supercritical systems with all fuel compositions. The BOL multiplication factors from CSAS25 and T5-DEPL sequences are provided in Table XXVI. The variance in T5-DEPL BOL multiplication factors relative to CSAS25 calculations is within 3% for all TRU fuel cases. All BOL analyses utilized results from

100%TRU CSAS25. The T5-DEPL results were employed in depletion and other fuel cycle studies.

Table XXVI. Beginning-of-life (BOL) multiplication factors.

Case	100%TRU			20%TRU		
	BOL k_{eff}		Variance	BOL k_{eff}		Variance
	CSAS25	T5-DEPL	(%)	(%)	T5-DEPL	(%)
TRU1	1.0692	1.0785	-0.87	1.0535	1.0309	2.15
TRU2	1.2189	1.2461	-2.23	1.1690	1.1427	2.25
TRU3	1.2199	1.2482	-2.32	1.1685	1.1404	2.41
TRU4	1.2035	1.2331	-2.46	1.1565	1.1337	1.97
TRU5	1.1737	1.1982	-2.09	1.1368	1.1080	2.54
LEU	1.3018	1.1546	11.31	1.3018	1.1546	11.31
TRU1 w/BP	1.1058	1.1127	-0.62	1.1203	1.1124	0.71
TRU2 w/BP	1.2605	1.2879	-2.18	1.2430	1.2281	1.20
TRU3 w/BP	1.2603	1.2866	-2.09	1.2415	1.2279	1.09
TRU4 w/BP	1.2453	1.2714	-2.10	1.2313	1.2209	0.84
TRU5 w/BP	1.2121	1.2363	-2.00	1.2116	1.2039	0.64
LEU w/BP	1.4815	1.3886	6.27	1.4815	1.3886	6.27

IV.D.1 NEUTRON DISTRIBUTIONS IN VHTR CORES WITH LEU AND TRU

The active core map is provided in Figure 28. The fuel block assemblies are arranged in 3 rings: inner zone (15 fuel columns), middle zone (33 fuel columns) and outer zone (18 fuel columns). There are 36 control rod columns with 15 columns in the inner zone, 3 columns in the middle zone and 18 columns in the outer zone. The neutron flux distribution in each zone is provided in Figure 29.

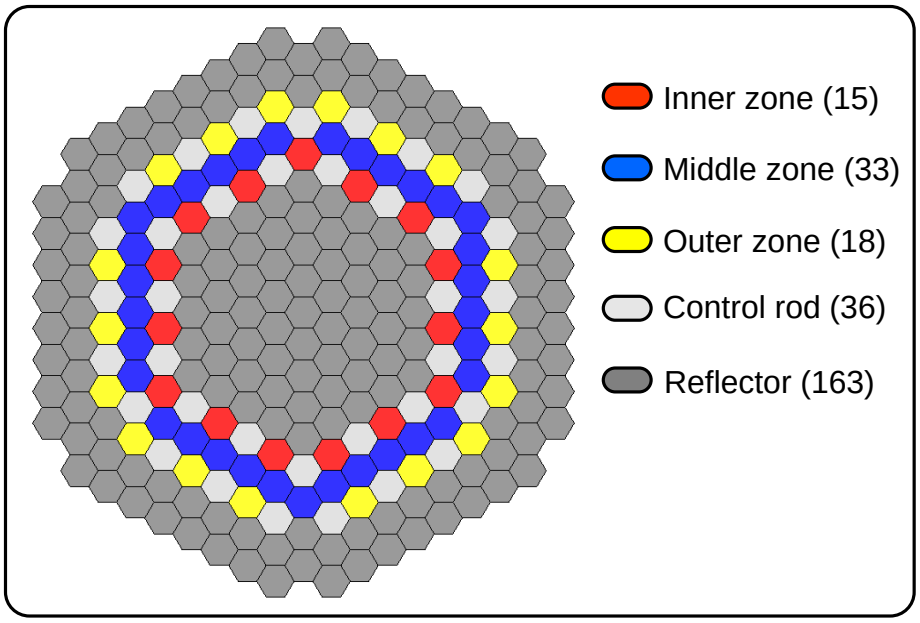

Figure 28. Active core map

As indicated, the flux profiles in the TRU-fuel configurations are similar. The inner and outer zones represented regions of higher thermal neutron peaks. The middle zone consists mostly of fuel assembly blocks, which give less moderating medium compared with the inner and outer rings. Hence, the thermal peaks in the middle zones are lower.

The fast neutron peaks in the TRU-fuel cases are more dominant than the thermal peaks. The 15% LEU flux distribution is provided as reference spectrum (see Figure 29). The peaks of the fast neutron spectrum in TRU-fueled cases are equivalent to the LEU fast neutron peak.

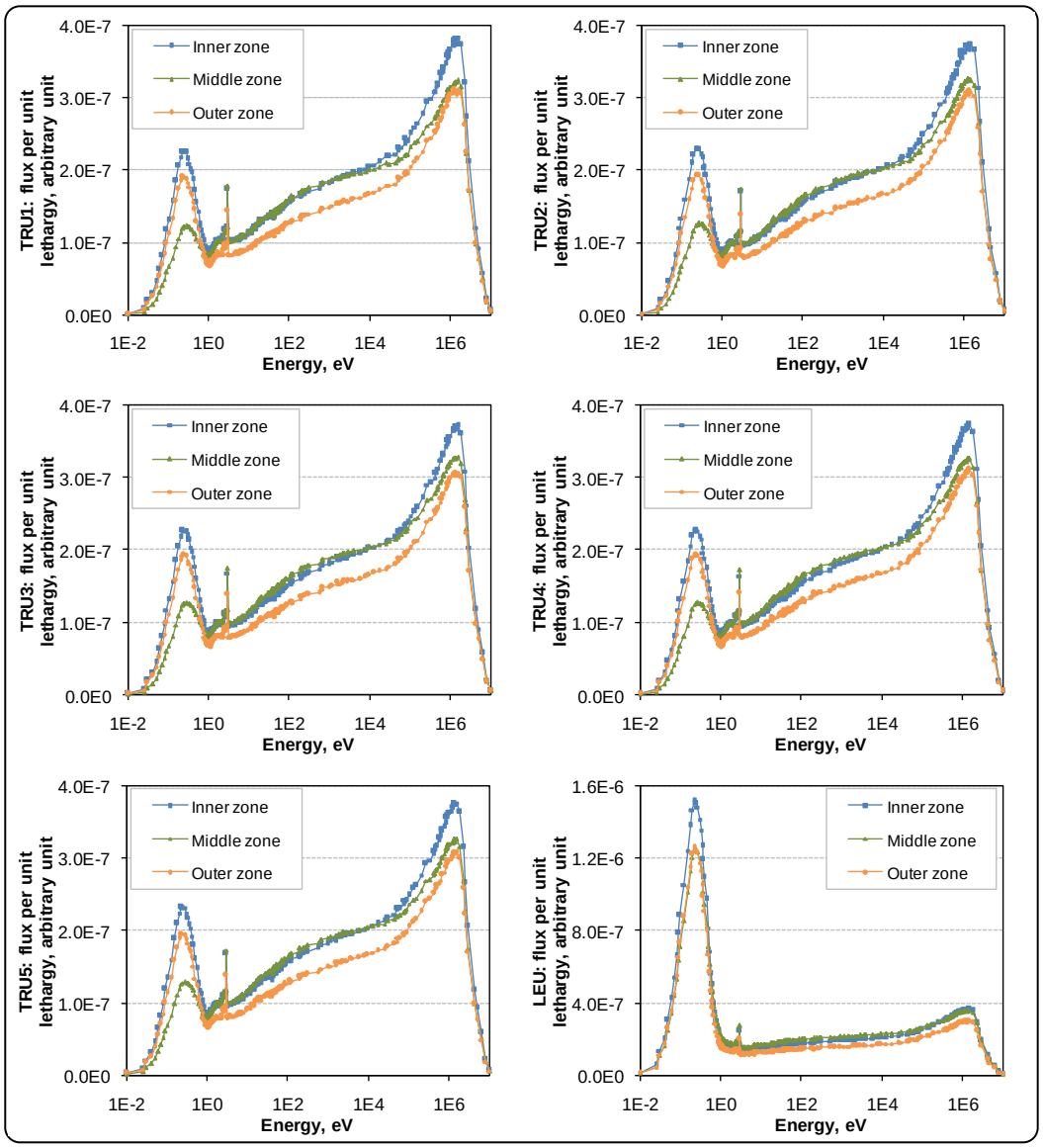

Figure 29. Neutron distributions in compacts as a function of their location in the core.

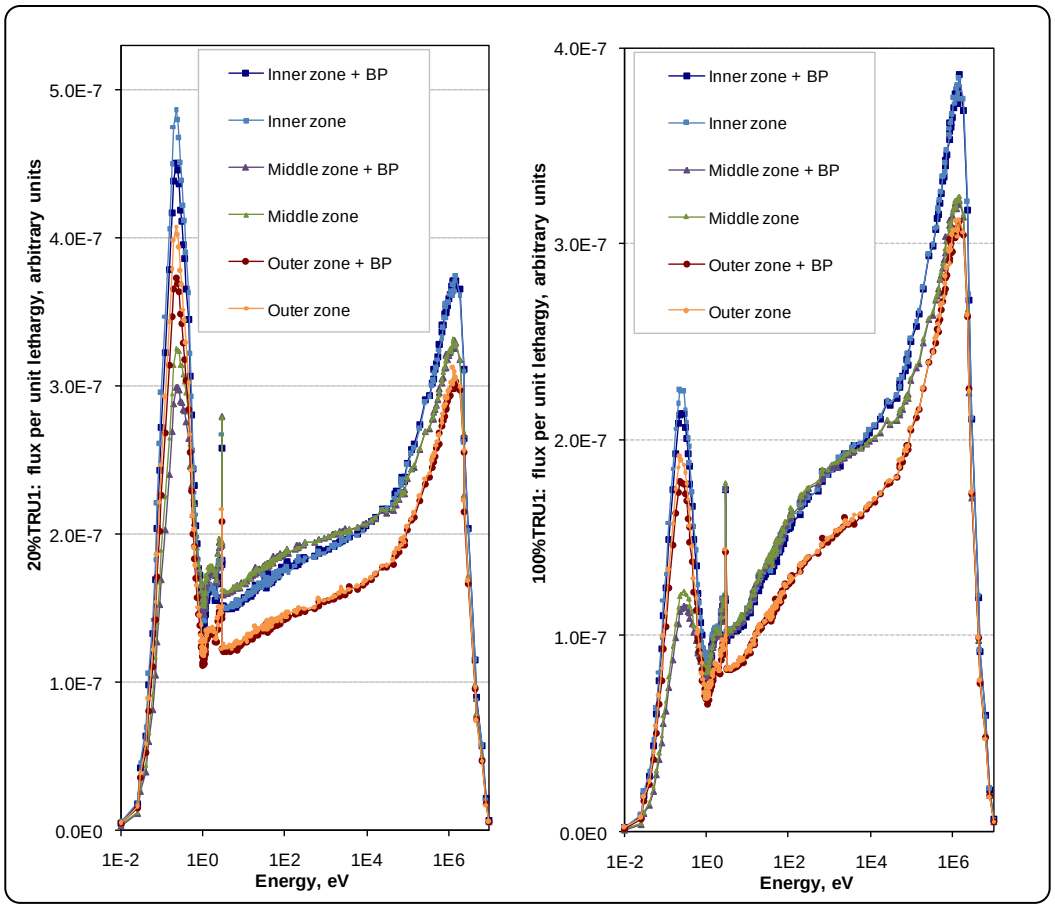

Figure 30. Neutron distribution in the fuel zones.

Figure 30 shows the neutron distribution in the fuels zones for TRU1 case with and without burnable poison. The thermal peaks in the case without burnable poison are slightly greater than the case with burnable poison. The drop in thermal peak resulted from thermal absorption in the burnable poison. The neutron distributions at other energies in cases with burnable poison are similar to the cases without. Similar trends were noted for other TRU-fuel cases.

The neutron distributions in TRU-fueled configurations are different from the distributions observed in the LEU-fueled configurations. As indicated by the flux profiles in Figure 30, the neutron distribution in the 100%TRU-fuel case tends towards fast spectrum. Figure 31 shows the flux profile in TRU1-fuel (fuel composed of legacy fuel TRU vector) and LEU. Moderation in LEU fuel compact is sufficient to achieve thermal spectrum. The 100%TRU case exhibits a fast spectrum in the fuel compact (see Figure 31(a)). As indicated in Figure 31(b), increasing C-to-HM ratio improves moderation in TRU1-fueled configuration. However, the neutron distribution in the TRU1-fueled case is less thermal compared with LEU case (Figure 31(c)). Similar trend was noted with all TRU-fuel compositions.

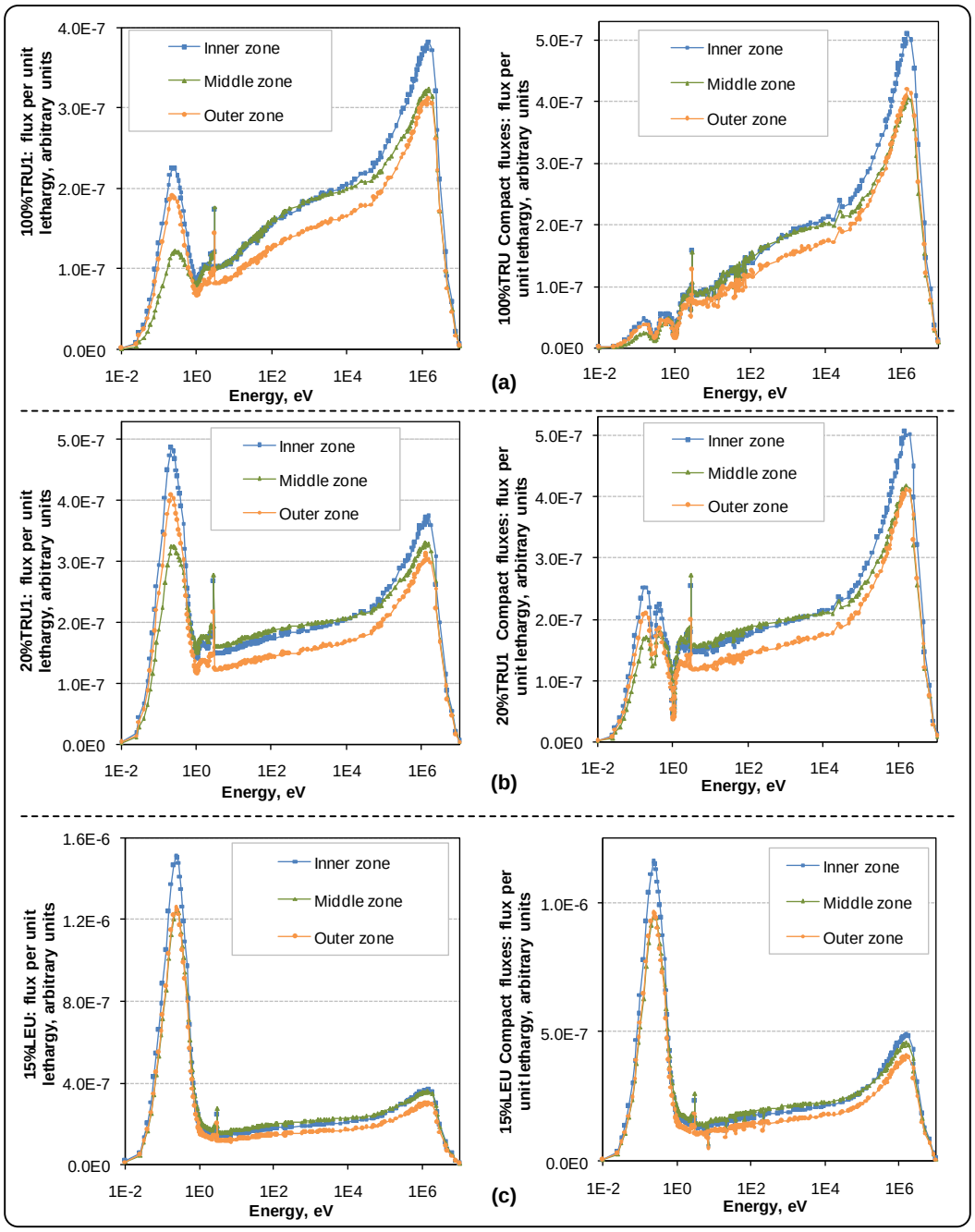

Figure 31. Neutron distributions in VHTRs with LEU and TRUs:
(a) 100%TRU (C-to-HM ratio = 57); (b) 20%TRU-80%Carbon (C-to-HM ratio = 363);
(c) 15% enriched LEU (C-to-HM ratio = 64).

IV.D.1.1 EQUILIBRIUM NEUTRON BALANCE

Figure 32 provides the equilibrium neutron balance as a function of scalar flux in the core. The neutron balance calculations for systems with thermal and fast energy neutrons indicated excess neutrons for all TRU-based fuel compositions. The thermal neutron balance shows increasing values with increasing scalar flux. This would result in improved neutron economy in the core.

In the fast spectrum, the TRU cases showed a small variation in neutron balance as scalar flux increases. There are at least 2 excess neutrons per fast neutron interaction.

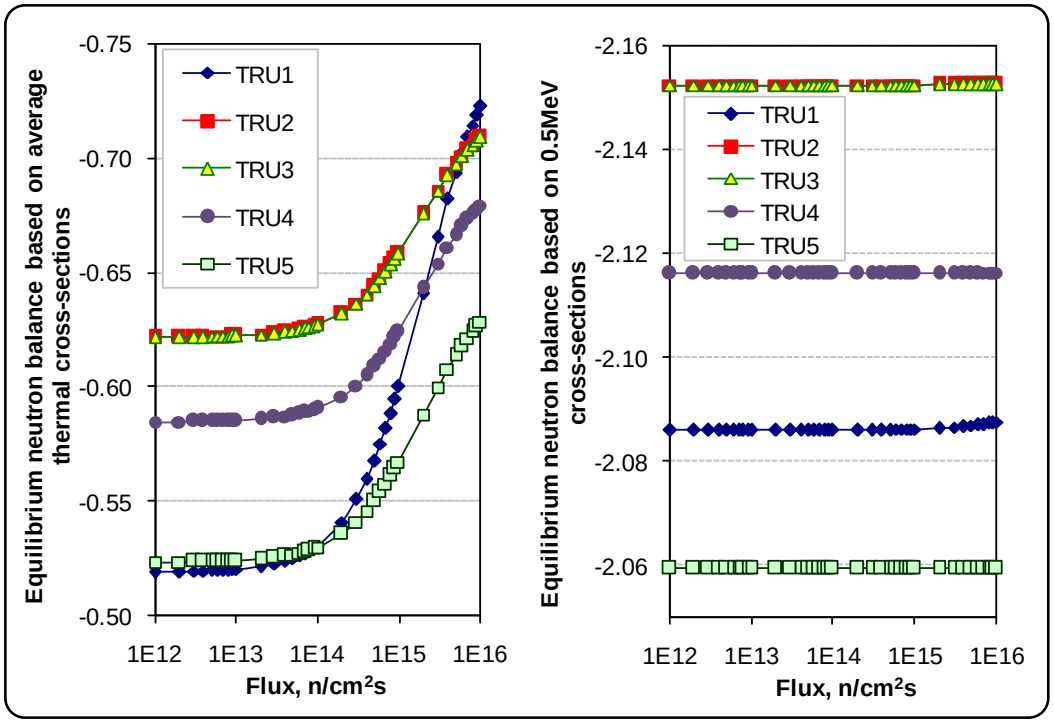

Figure 32. Flux dependent equilibrium neutron balance at thermal and fast energies.

IV.D.1.2 BEGINNING-OF-LIFE (BOL) ANALYSIS

Table XXVII provides the moderator-to-fuel atom ratio in the fuel compact. The effect of moderator-to-fuel (carbon-to-heavy metal) ratio on multiplication factor is shown in Figure 33. Increase in carbon-to-heavy metal (C-to-HM) ratio initially decreased multiplication factor. Subsequent increase in C-to-HM ratio resulted in increased multiplication factor.

The 5 TRU vectors exhibited decreasing multiplication factor with C-to-HM ratio below 135, which corresponds to 50%TRU-50%C fuel composition. Fuel depletion increases C-to-HM ratio in the compact. Hence it is expected that after system start-up, the multiplication factor will reduce with initial TRU content greater than 50%.

At C-to-HM ratios above 135, increasing multiplication factor prevailed. The increase in multiplication factor with C-to-HM ratio is less dominant in TRU fuels with burnable poison. Operating the system with higher C-to-HM ratio allows utilization of less TRU materials in the core. However, the increasing multiplication factor as fuel depletion progresses makes the system more dependent on control systems.

Table XXVII. Moderator-to-fuel ratio in fuel compact.

Fuel	**LEU-15%**	**TRU- w%; (1-w)% Carbon**								
		w=20	**w=30**	**w=40**	**w=50**	**w=60**	**w=70**	**w=80**	**w=90**	**w=100**
C-to-HM ratio	64	363	235	171	133	108	89	76	65	57

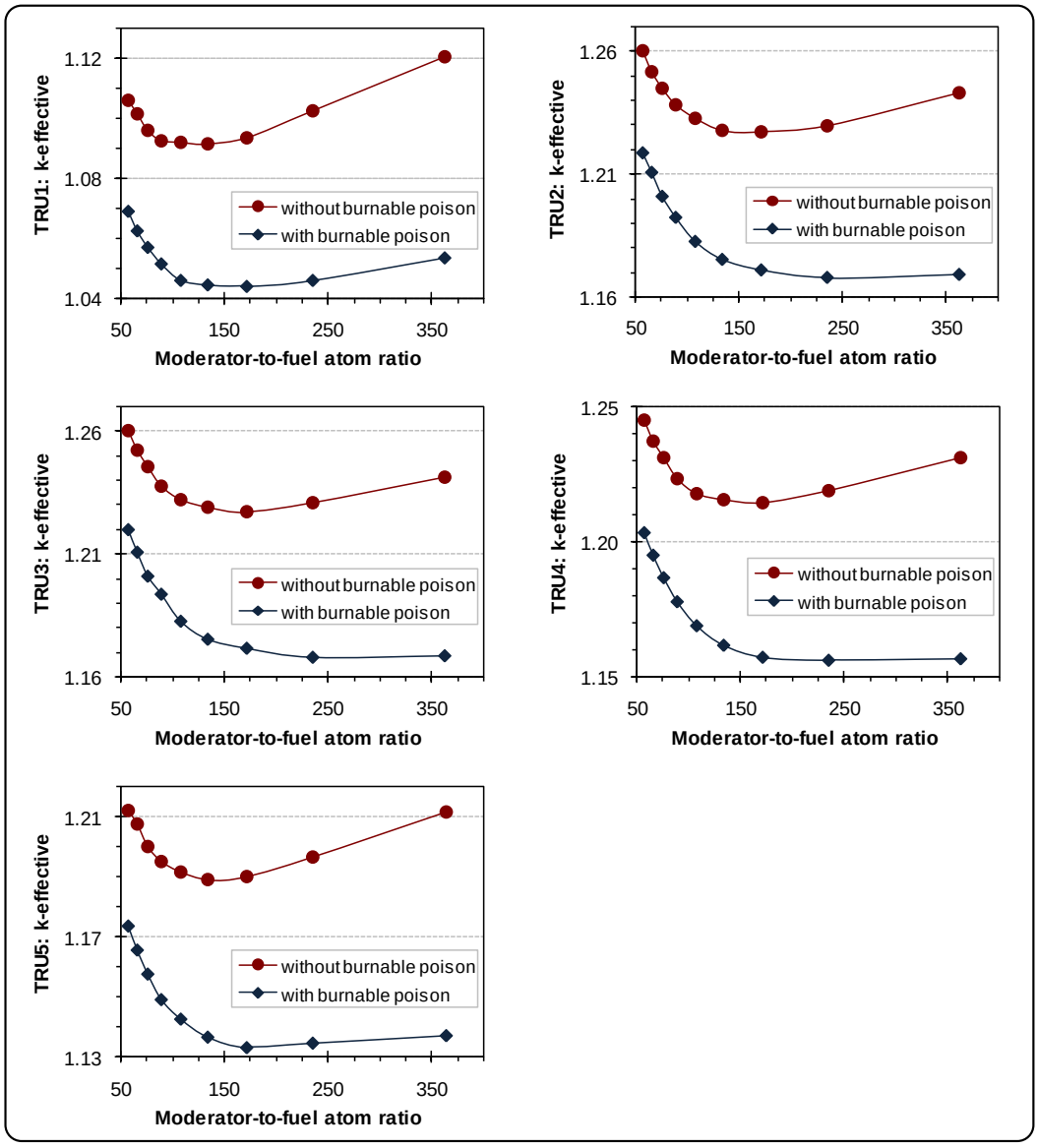

Figure 33. Multiplication factor as a function of moderator-to-fuel ratio.

The BOL temperature coefficients of reactivity are provided in Figure 34. The isothermal temperature coefficients of reactivity ($\alpha_{T,iso}$) are negative for all considered configuration. Table XXVIII summarizes the coefficients of reactivity.

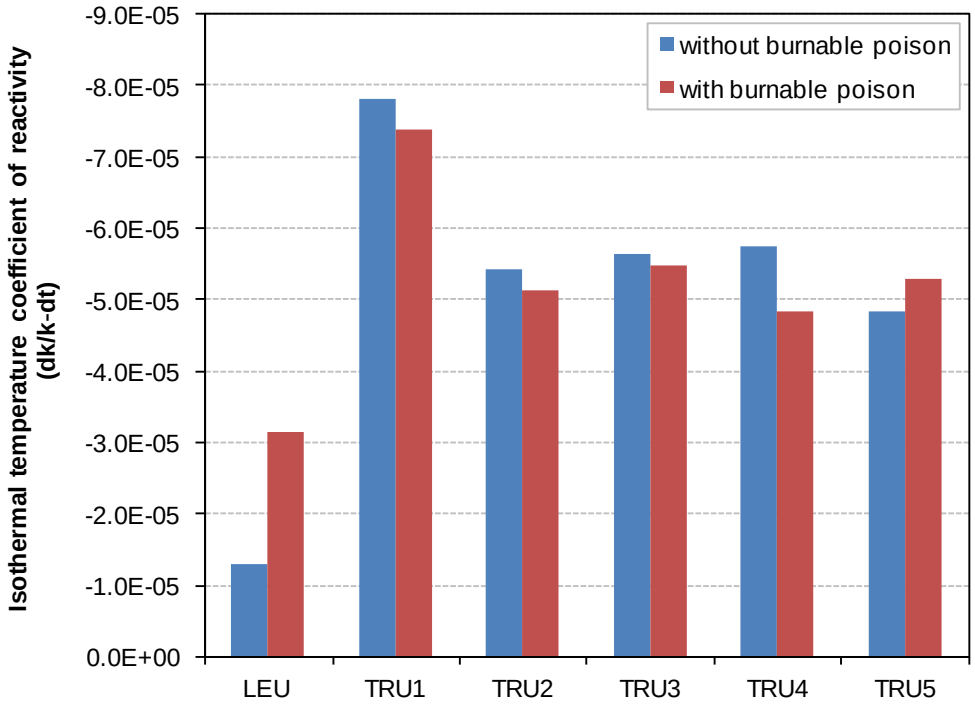

Figure 34. Temperature coefficients of reactivity.

Table XXVIII. Temperature coefficients of reactivity.

Fuel	$\alpha_{T,iso}$		$\alpha_{T,He}$		$\alpha_{T,fuel}$		$\alpha_{T,graphite}$	
	No BP	With BP	No BP	With BP	No BP	With BP	No BP	With BP
LEU	-1.30E-5	-3.15E-5	-6.38E-7	2.77E-6	-9.72E-6	-1.95E-5	2.28E-7	-7.03E-6
TRU1	-7.82E-5	-7.38E-5	-7.78E-6	-3.68E-6	-1.23E-5	-1.16E-5	-6.17E-5	-6.33E-5
TRU2	-5.44E-5	-5.14E-5	2.77E-6	7.13E-6	-1.76E-6	7.93E-6	-3.93E-5	-3.85E-5
TRU3	-5.64E-5	-5.49E-5	6.30E-7	-4.03E-7	-6.55E-6	-4.50E-6	-3.73E-5	-3.69E-5
TRU4	-5.75E-5	-4.83E-5	-7.74E-7	-3.04E-6	-1.41E-5	-1.38E-7	-4.83E-5	-3.75E-5
TRU5	-4.84E-5	-5.30E-5	4.01E-6	-5.38E-6	-1.97E-6	-1.11E-5	-3.76E-5	-4.98E-5

Table XXIX. Helium reactivity worth – Positive $\Delta\rho_{He}$ implies negative reactivity insertion.

Cases	Helium worth, $\Delta\rho_{He}$	
	Without BP	With BP
TRU1	1.032E-3	1.261E-3
TRU2	2.078E-4	-4.238E-4
TRU3	-3.839E-4	1.043E-3
TRU4	1.344E-3	-9.999E-4
TRU5	-1.244E-3	5.521E-4
LEU	6.379E-5	4.074E-4

Table XXX. Boron reactivity worth – Negative $\Delta\rho_{B4C}$ implies negative reactivity insertion.

Cases	Boron worth, $\Delta\rho_{B4C}$	
	100% TRU	20% TRU
TRU1	-0.0310	-0.0566
TRU2	-0.0271	-0.0509
TRU3	-0.0262	-0.0503
TRU4	-0.0279	-0.0525
TRU5	-0.0270	-0.0543
LEU	-0.0932	

Table XXIX provides the helium reactivity worth of the system. The TRU-composition from legacy fuels (TRU1) would experience negative reactivity insertion in the event of LOCA. The reactivity insertions resulting from helium worth in models with other TRU-based fuels are less desirable. Fuels based on TRU3 and TRU5 gave positive reactivity insertion in LOCA scenario. In cases with burnable poison in the model, TRU2 and TRU4 based fuels resulted in positive reactivity insertion in LOCA scenario. The order of magnitude of helium worth in each case is 10^{-3} or less. The effect of the positive reactivity can be mitigated with control rod insertion, following a LOCA event.

The Boron worth in each TRU fuel the model is provided in Table XXX. The burnable poison (BP) is more effective in reducing BOL multiplication factor in models with 20% TRU-based fuel kernel compared with the 100%TRU fuels. Phenomena such as better neutron moderation and reduced thermal utilization in the 20% TRU-based fuel are responsible for the BP effectiveness.

It should be noted that the observations from reactivity worth calculations are for the given VHTR geometry. The configurations have not been optimized to achieve better coefficients of reactivity.

IV.D.1.3 CORE LIFETIME

The multiplication factors from T5-DEPL calculations were used to determine fuel cycle length for each fuel composition. Fast fluence was calculated from the flux output in T5-DEPL. The primary limiting factor for the fuel cycle length is the fast fluence limit of 5E+21 n/cm^2 [32]. Cycle lengths were determined as the year before the core becomes subcritical.

Table XXXI summarizes the cycle lengths and the corresponding fast fluence. All cases with 100% TRU fuel exceeded the fast fluence limit before attaining subcriticality. The 20% TRU cases were within the fast fluence limit except for TRU2 and TRU3 fuels without burnable poison. The fast fluence for both cases was slightly above the allowed fluence limit. The multiplication factor variation over time is provided in Figure 35.

Table XXXI. Cycle lengths (T_{cyc}) and fast fluence (Φ_{fast}) with various fuels.

Case	20% TRU				100% TRU			
	Without BP		With BP		Without BP		With BP	
	T_{cyc} (yrs)	Φ_{fast} (n/cm^2)	T_{cyc} (yrs)	Φ_{fast} (n/cm^2)	T_{cyc} (yrs)	Φ_{fast} (n/cm^2)	T_{cyc} (yrs)	Φ_{fast} (n/cm^2)
TRU1	6	3.920E21	4	2.721E21	5	1.349E22	5	1.369E22
TRU2	8	5.011E21	7	4.531E21	7	1.781E22	7	1.799E22
TRU3	8	5.017E21	7	4.535E21	7	1.780E22	7	1.802E22
TRU4	7	4.371E21	6	3.895E21	6	1.519E22	6	1.539E22
TRU5	6	3.777E21	5	3.286E21	5	1.275E22	5	1.296E22
LEU	3	7.301E21	3	7.755E21	3	7.301E21	3	7.755E21

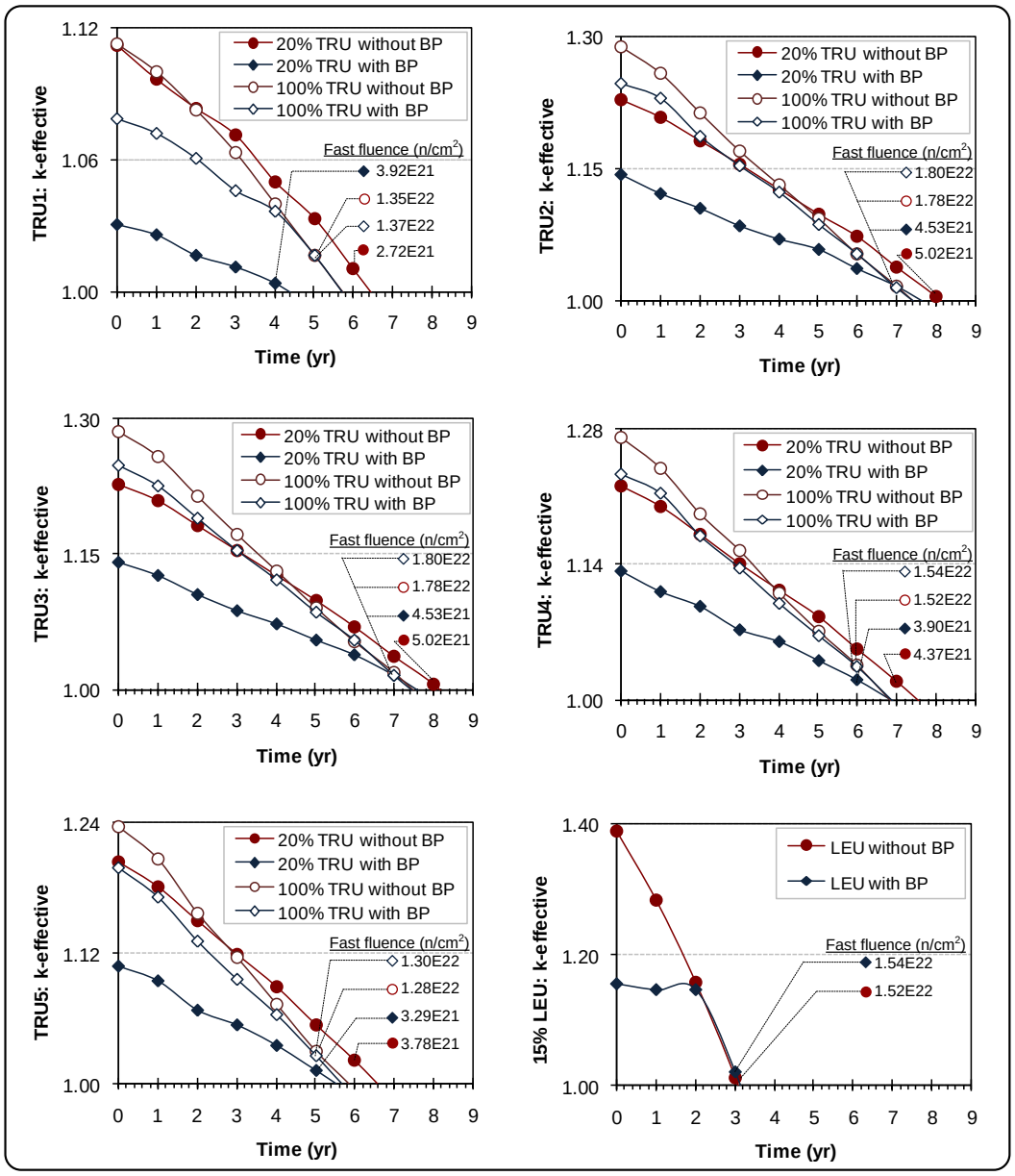

Figure 35. Time dependent multiplication factor.

IV.D.1.4 FUEL UTILIZATION

The fraction of total fissile material fissioned (f_{fiss}) is summarized in Table XXXII. The legacy fuels vector (TRU1) experienced the least f_{fiss} value. Generally, the f_{fiss} value is improved with longer fuel cycle length. The LEU fuel utilizes about 75% of

fissile fuel over 3 year cycle. All TRU based fuels utilize less fissile fuel over a longer cycle length. This confirms the effectiveness of TRU as fuel component.

Fissile fuel utilization in all fuel types reduced with insertion of burnable poison. As indicated in Figure 36, the reduction in fissile utilization was significant in cases with 20%TRU-based fuel. Burnable poison had negligible effect on cases with 100% TRU-based fuel.

Table XXXII. Cycle lengths (T_{cyc}) and fraction of fissile fuel utilized (f_{fiss}).

Case	20% TRU				100% TRU			
	Without BP		With BP		Without BP		With BP	
	T_{cyc} (yrs)	f_{fiss}	T_{cyc} (yrs)	f_{fiss}	T_{cyc} (yrs)	f_{fiss}	T_{cyc} (yrs)	f_{fiss}
TRU1	6	0.4727	4	0.3179	5	0.3860	5	0.3855
TRU2	8	0.6186	7	0.5469	7	0.5343	7	0.5331
TRU3	8	0.6179	7	0.5469	7	0.5342	7	0.5328
TRU4	7	0.5701	6	0.4923	6	0.4814	6	0.4804
TRU5	6	0.5296	5	0.4450	5	0.4325	5	0.4310
LEU	3	0.7469	3	0.7383	3	0.7469	3	0.7383

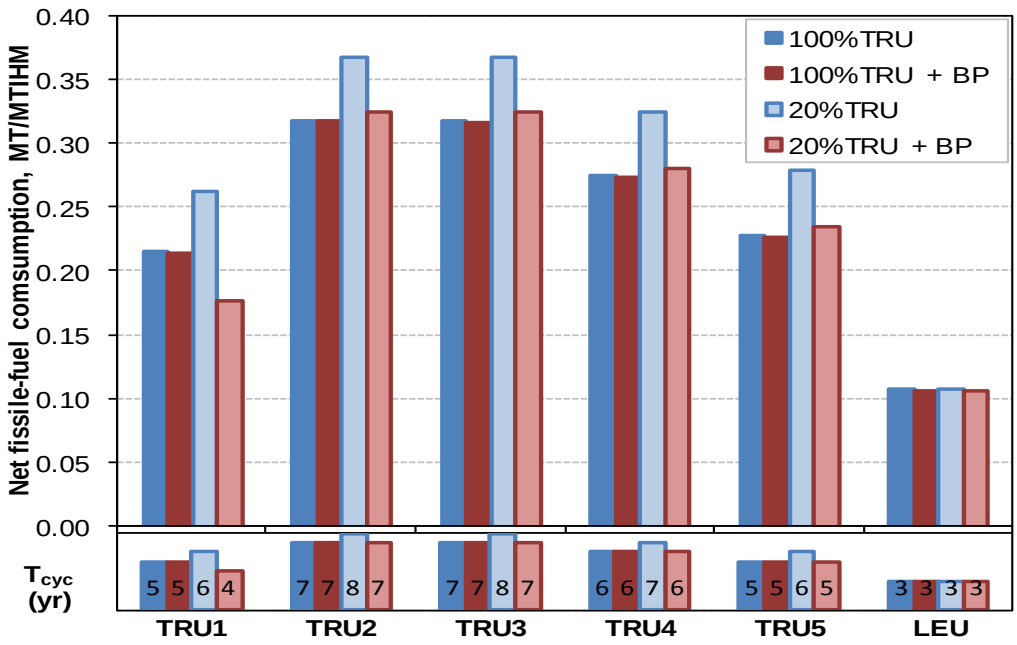

Figure 36. Fissile fuel utilization. The numbers on the lower bars are fuel cycle lengths.

IV.D.2 OUT-OF-CORE FUEL CYCLE ANALYSIS

The fractions of initial TRU content going to waste stream are provided in Table XXXIII. The reference LEU discharged about 87% of initial heavy metal loading. All TRU fuels discharged less quantity of heavy metal, which further confirms the effectiveness of TRU as fuel component. In a similar trend to fuel utilization, addition of burnable poison to the 100% TRU fuels had negligible effect on discharged quantities. In the cases with 20% TRU fuel, addition of burnable poison resulted in increased discharge quantities, which are higher than the discharge from corresponding 100% TRU case. Figure 37 provides the resulting transmutation efficiencies. As indicated in the Figure, the 20% TRU cases without burnable poison are more efficient than other cases.

Table XXXIII. Fraction of initial TRU material going to waste stream.

Case	20% TRU				100% TRU			
	Without BP		With BP		Without BP		With BP	
	T_{cyc} (yrs)	f_{TRU}	T_{cyc} (yrs)	f_{TRU}	T_{cyc} (yrs)	f_{TRU}	T_{cyc} (yrs)	f_{TRU}
TRU1	6	0.7705	4	0.8472	5	0.8084	5	0.8085
TRU2	8	0.6936	7	0.7322	7	0.7302	7	0.7303
TRU3	8	0.6936	7	0.7322	7	0.7301	7	0.7302
TRU4	7	0.7315	6	0.7701	6	0.7683	6	0.7684
TRU5	6	0.7694	5	0.8080	5	0.8064	5	0.8065
LEU	3	0.8677	3	0.8685	3	0.8677	3	0.8685

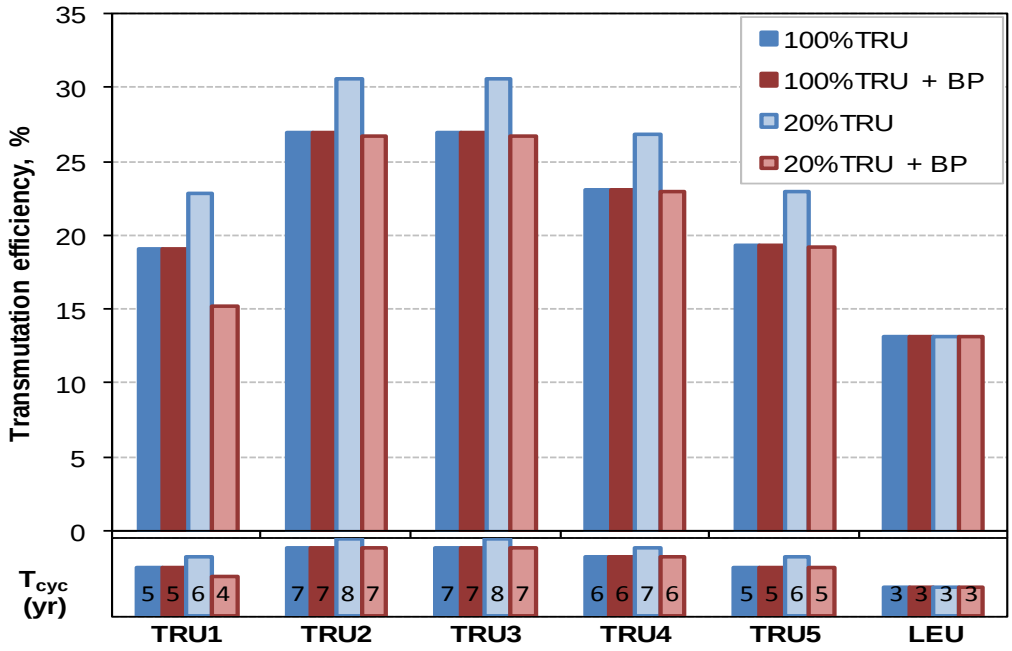

Figure 37. Transmutation efficiency. The numbers on the lower bars are fuel cycle lengths.

Figure 38 shows the destruction (+)/production (-) rate. Plutonium destruction rates are lower in TRU1. This can be attributed to the high concentration of plutonium (^{239}Pu & ^{241}Pu) in TRU2, TRU3 and TRU4. The TRU5 vector contains less plutonium than TRU1. However, TRU5 contains more fertile (^{238}Pu, ^{240}Pu, ^{242}Cm and ^{244}Cm) than other compositions.

Net MA production was observed for all TRU fuels except TRU1. The net MA production is attributable to higher ^{242}Pu content in the 4 TRU vectors. Parasitic absorption in ^{242}Pu leads to creation of minor actinides. The MA buildup is more significant in cases with 20% TRU fuels.

The net TRU destruction rate is a net of plutonium production/consumption and MA consumption/production. Net TRU destruction rates improved in cases with 100%

TRU fuel. In all heavy metal destruction analysis, there was negligible effect of burnable poison addition to the 100% TRU cases.

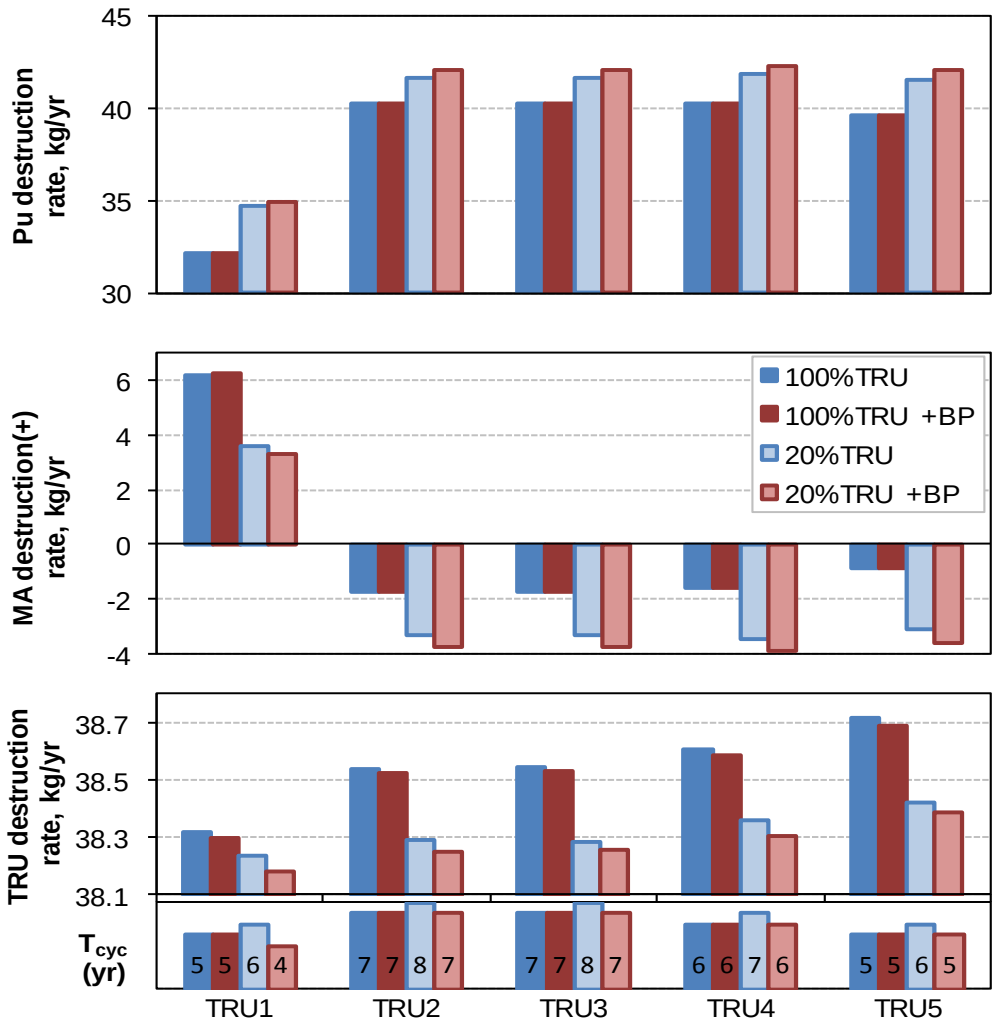

Figure 38. TRU, MA and Plutonium destruction rates. The numbers on the lower bars are fuel cycle lengths.

Figure 39 provides the TRU and MA materials to disposal. Compositions based on TRU1 and TRU5 resulted in the highest quantity of annual waste materials per metric ton of initial heavy metal loading. It should be noted that analyses involving material disposal considered magnitude of discharge fuel. The radiotoxicity of the discharge fuel was not analyzed in this thesis.

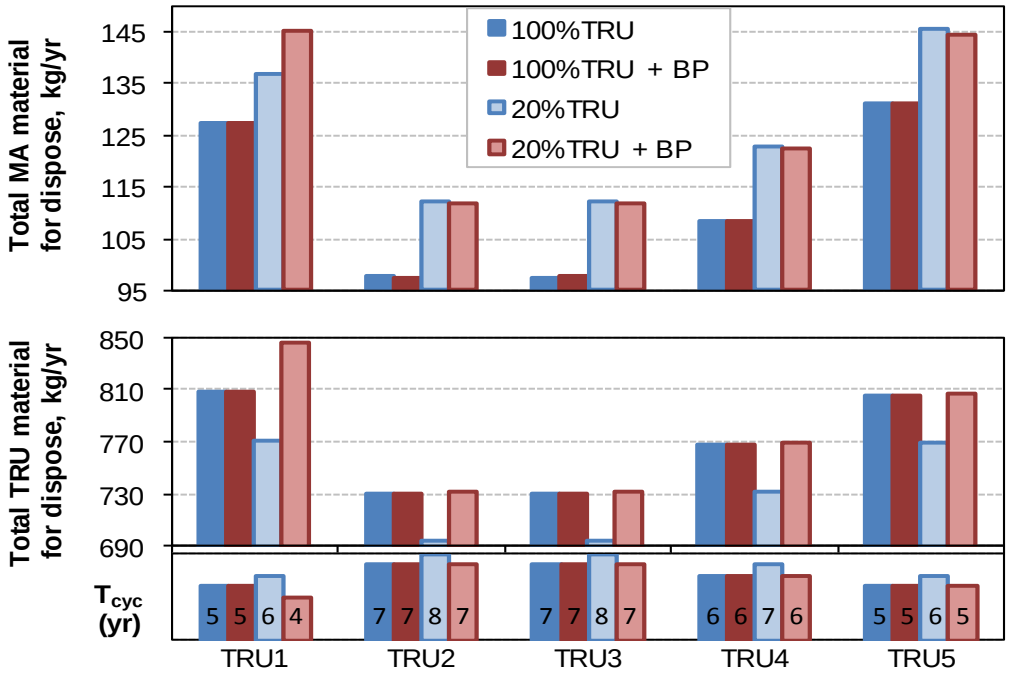

Figure 39. TRU and MA materials to be disposed. The numbers on the lower bars are fuel cycle lengths.

CHAPTER V

CONCLUSIONS

The objective of this thesis was to analyze the impact of conventional PWR spent fuel variations on TRU-fueled Very High Temperature Reactor (VHTR) systems.

Five TRU vectors were selected as fuel components for VHTRs:

1. TRU1: Legacy spent nuclear fuel: average burnup of 41.2 GWd/MTHM.
2. TRU2: PWR spent fuel at 45 GWd/tHM burnup and 100% load factor.
3. TRU3: PWR spent fuel at 45 GWd/tHM burnup and 85% load factor.
4. TRU4: PWR spent fuel at 50 GWd/tHM burnup and 85% load factor.
5. TRU5: PWR spent fuel at 60 GWd/tHM burnup and 85% load factor.

The vectors included TRU composition from legacy PWR fuels and 4 compositions from PWR spent fuel simulations using VISTA code system. Ten different fuel compositions were developed from the TRU vectors for the VHTR performance analyses. Uranium oxide fuel at 15% enrichment was the reference fuel.

The 3D whole-core VHTR model has been developed for calculations with the SCALE5.1 code system. In-core and out-of-core fuel cycle analyses were performed. All studies were performed for cases with and without burnable poison.

The results indicated strong potential of TRU-based fuel in VHTRs. The preliminary safety assessment of the TRU-fueled systems showed promising performance characteristics. Neutron balances calculations indicated excess neutron from TRU fuel transmutation. The isothermal temperature coefficients of reactivity are negative in all TRU-fueled cases.

Startup multiplication factors in TRU-fueled cased were lower than the corresponding LEU case. Addition of burnable poison to 20% TRU-fueled cases lowered BOL multiplication factors but also affected transmutation efficiency. Burnable poison was less effective with 100% TRU fuel cases.

The neutron distributions in TRU-fueled systems were indicative of harder spectra in cases with 100% TRU compositions. Improved moderation in the cases with 20%TRU-80%Carbon fuel compositions resulted in softer spectra.

The variation in PWR spent fuel vectors propagated to both fuel utilization (in-core) and waste generation (out-of-core) characteristics. The single-batch core lifetimes ranged between 5 and 8 years for all TRU-based fuels whereas the reference LEU core sustained 3 years. The fast fluence limitations reduce the achievable core lifetime. Observed transmutation efficiencies are ranged between 15% and 31% for TRU-based fuels. Net TRU destruction rates are ranged between 38.2 and 38.7 kg/yr per metric ton of initial heavy metal loading. Total TRU material contents for disposal are ranged between 693 and 847 kg/yr per metric ton of initial heavy metal loading.

Utilization of TRUs as fuel components should facilitate development of new fuel cycles and support fuel supply sustainability. The development of TRU-fueled VHTRs is expected to provide the following benefits:

- Prolonged operation on a single fuel loading
- Reduction of the long-term radiotoxicity and heat load of high-level waste sent to a geologic repository.
- Reduction of technical need for additional repositories per year of reactor operation.

- Recovery of the energy contained in spent fuel.
- Increased sustainability of nuclear energy.

The follow-on studies may include further optimization of VHTRs with TRUs covering:

- Configuration adjustments to reduce start-up reactivity.
- Achievability of lower fast fluence and longer core lifetime.
- Detailed safety studies.
- Identification of performance requirements that would lead to the actinide-free high-level waste.
- Impact of discharged fuel's radiotoxicity on repository and storage facilities.

These efforts contribute to the analysis of the VHTR role in advanced fuel cycles. The success of future research plans would enhance capabilities of the Generation IV VHTR in spent fuel management and environmental friendliness.

REFERENCES

1. L. H. BAETSLE, "Application of Partitioning/Transmutation of Radioactive Materials in Radioactive Waste Management," LNS0212001, Nuclear Research Centre of Belgium Sck/Cen, Mol, Belgium (2001).

2. "Report to Congress on Advanced Fuel Cycle Initiative: The Future Path for Advanced Spent Fuel Treatment and Transmutation Research," 03-GA50439-06, Office of Nuclear Energy, Science, and Technology, USDOE (January 2003).

3. "Global Nuclear Energy Partnership Strategic Plan," GNEP-167312, Rev. 0, Office of Nuclear Energy - Office of Fuel Cycle Management, USDOE (January 2007).

4. "The US Generation IV Implementation Strategy," 03-GA50439-06, Office of Nuclear Energy, Science, and Technology, USDOE (September 2003).

5. C. RODRIGUEZ, A. BAXTER, D. MCEACHERN, M. FIKANI and F. VENNERI, "Deep-Burn: Making Nuclear Waste Transmutation Practical," *Nuclear Engineering and Design*, **222**, 299-317 (2003).

6. T.K. KIM, T.A. TAIWO, R.N. HILL, and W.S. YANG and F. VENNERI, "A Feasibility Study of Reactor-Based Deep-Burn Concepts," ANL-AFCI-155, Nuclear Engineering Division, Argonne National Laboratory, USDOE (August 2005).

7. "Current Status and Future Development of Modular High Temperature Gas-cooled Reactor Technology," IAEA-TECDOC-1198, International Atomic Energy Agency, Vienna, Austria (February 2001).

8. P. E. MCDONALD, "Next Generation Nuclear Plant (NGNP): A Very High Temperature Gas-cooled Reactor (VHTR)," *USDOE Advanced Reactor, Fuel Cycle, and Energy Products Workshop for Universities*, Gaithersburg, MD, March 4–5, 2004, U.S. DOE (2004).

9. "Evaluation of High Temperature Gas-cooled Reactor Performance: Benchmark Analysis Related to Initial Testing of the HTTR and HTR-10," IAEA-TECDOC-1382, International Atomic Energy Agency, Vienna, Austria (2003).

10. "JANIS user guide," Nuclear Energy Agency - Organization for Economic Co-Operation and Development (May 2005).

11. N. SOPPERA, M. BOSSANT, H. HENRIKSSON, P. NAGEL and Y. RUGAMA, "Recent upgrades to the nuclear data tool Janis," *International Conference on Nuclear Data for Science and Technology*, Nice, France, 22 – 27 April 2007, Nuclear Energy Agency - Organization for Economic Co-Operation and Development (2007).

12. M. SALVATORES, R. HILL, I. SLESSAREV and G. YOUINOU, "The Physics of TRU Transmutation – A Systematic Approach to the Intercomparison of Systems," *Proc. PHYSOR 2004 -The Physics of Fuel Cycles and Advanced*

Nuclear Systems: Global Developments, Chicago, Illinois, April 25-29, 2004, American Nuclear Society, Lagrange Park, IL. (2004).

13. "Fuels and Materials for Transmutation: A Status Report," NEA No. 5419, Organization for Economic Co-operation and Development - Nuclear Energy Agency, ISBN 92-64-01066-1 (2005).

14. Final Environmental Impact Statement for a Geologic Repository for the Disposal of Spent Nuclear Fuel and High-Level Radioactive Waste at Yucca Mountain, Nye County, Nevada, Vol. 2, Appendix A, "Inventory and Characteristics of Spent Nuclear Fuel, High-Level Radioactive Waste, and Other Materials," DOE/EIS-0250, U.S. DOE (2002).

15. "Nuclear Fuel Cycle Simulation System (VISTA)," IAEA-TECDOC-1535, International Atomic Energy Agency, Vienna, Austria (2007).

16. N.E. TODREAS and M.S. KASIMI, "Nuclear Systems I: Thermal Hydraulic Fundamentals," 1st ed., Levittown, PA.,Taylor & Francis, 1993 (ISBN: 1-56032-079-6).

17. "SCALE: A Modular Code System for Performing Standardized Computer Analyses for Licensing Evaluation," ORNL/TM-2005/39, 3 Volumes (November 2006).

18. S. GOLUOGLU, N. F. LANDERS, L. M. PETRIE and D. F. HOLLENBACH, "CSAS: Control Module for Enhanced Criticality Safety Analysis Sequences,"

Vol. I, Book 1, Sect. C4 of *SCALE: A Modular Code System for Performing Standardized Computer Analyses for Licensing Evaluation*, ORNL/TM-2005/39, 3 Volumes (November 2006).

19. N. M. GREENE "BONAMI: Resonance Self-shielding by the Bondarenko Method," Vol. II, Book 1, Sect. F1 of *SCALE: A Modular Code System for Performing Standardized Computer Analyses for Licensing Evaluation*, ORNL/TM-2005/39, 3 Volumes (November 2006).

20. D. F. HOLLENBACH and L. M. PETRIE, "WORKER: SCALE System Module for Creating and Modifying Working Format Libraries," Vol. II, Book 4, Sect. F20 of *SCALE: A Modular Code System for Performing Standardized Computer Analyses for Licensing Evaluation*, ORNL/TM-2005/39, 3 Volumes (November 2006).

21. M. L. WILLIAMS, M. ASGARIA and D. F. HOLLENBACH, "CENTRM: A One-Dimensional Neutron Transport Code for Computing Pointwise Energy Spectra," Vol. II, Book 4, Sect. F18 of *SCALE: A Modular Code System for Performing Standardized Computer Analyses for Licensing Evaluation*, ORNL/TM-2005/39, 3 Volumes (November 2006).

22. M. L. WILLIAMS and D. F. HOLLENBACH, "PMC: A Program to Produce Multi-group Cross Sections Using Pointwise Energy Spectra from Centrm," Vol. II, Book 4, Sect. F19 of *SCALE: A Modular Code System for Performing*

Standardized Computer Analyses for Licensing Evaluation, ORNL/TM-2005/39, 3 Volumes (November 2006).

23. N. M. GREENE and L. M. PETRIE, "XSDRNPM: A One-Dimensional Discrete-Ordinates Code for Transport Analysis," Vol. II, Book 1, Sect. F3 of *SCALE: A Modular Code System for Performing Standardized Computer Analyses for Licensing Evaluation*, ORNL/TM-2005/39, 3 Volumes (November 2006).

24. L. M. PETRIE D. F. HOLLENBACH and M. L. WILLIAMS, "Miscellaneous Scale Utility Modules," Vol. III, Sect. M17 of *SCALE: A Modular Code System for Performing Standardized Computer Analyses for Licensing Evaluation*, ORNL/TM-2005/39, 3 Volumes (November 2006).

25. M. D. DEHART, "TRITON: A Two-Dimensional Transport and Depletion Module for Characterization of Spent Nuclear Fuel," Vol. I, Book 3, Sect. T1 of *SCALE: A Modular Code System for Performing Standardized Computer Analyses for Licensing Evaluation*, ORNL/TM-2005/39, 3 Volumes (November 2006).

26. L. M. PETRIE, N. F. LANDERS, D. F. HOLLENBACH and B. T. REARDEN, "KENO V.a: An Improved Monte Carlo Criticality Program," Vol. II, Book 2, Sect. F11 of *SCALE: A Modular Code System for Performing Standardized Computer Analyses for Licensing Evaluation*, ORNL/TM-2005/39, 3 Volumes (November 2006).

27. I. C. GAULD and O. W. HERMANN, "COUPLE: SCALE System Module to Process Problem-Dependent Cross Sections and Neutron Spectral Data for Origen-S Analyses," Vol. II, Book 1, Sect. F6 of *SCALE: A Modular Code System for Performing Standardized Computer Analyses for Licensing Evaluation*, ORNL/TM-2005/39, 3 Volumes (November 2006).

28. I. C. GAULD, O. W. HERMANN and R. M. WESTFALL, "ORIGEN-S: SCALE System Module to Calculate Fuel Depletion, Actinide Transmutation, Fission Product Buildup and Decay, and Associated Radiation Source Terms," Vol. II, Book 1, Sect. F7 of *SCALE: A Modular Code System for Performing Standardized Computer Analyses for Licensing Evaluation*, ORNL/TM-2005/39, 3 Volumes (November 2006).

29. I. C. GAULD and J. E. HORWEDEL, "OPUS/PLOTOPUS: An ORIGEN-S Post-Processing Utility and Plotting Program for SCALE," Vol. II, Book 3, Sect. F15 of *SCALE: A Modular Code System for Performing Standardized Computer Analyses for Licensing Evaluation*, ORNL/TM-2005/39, 3 Volumes (November 2006).

30. S. GOLUOGLU, D. F. HOLLENBACH, N. F. LANDERS, L. M. PETRIE, J. A. BUCHOLZ, C. F. WEBER and C. M. HOPPER, "The Material Information Processor for SCALE," Vol. III, Sect. M7 of *SCALE: A Modular Code System for Performing Standardized Computer Analyses for Licensing Evaluation*, ORNL/TM-2005/39, 3 Volumes (November 2006).

31. T. IYOKU, S. UETA, J. SUMITA, M. UMEDA and M. ISHIHARA, "Design of core components," *Nuclear Engineering and Design*, **233**, 71–79 (2004).

32. "Screening Tests for Selection of VHTR Advanced Fuel" issued by General Atomics for the Department of Energy Contract No. DE-AC03-01SF22343, (2003).

APPENDIX A

SCALE 5.1 INPUT FILES

A.1 EXAMPLE CSAS25 INPUT FILE

```
'SCALE 5.1 KENO Va. Jan. 2007
=csas25 parm=centrm
VHTR Prismatic Powercore 3zone 3tgt 100perc-TRUvector1 VF20 BP-B4C
1223k
v6-238
read comp
' uo2          21 den=10.41 1 1223 92235 15 92238 85 end
'Legacy fuel TRU vector for UO2 fuel:
 wtptTRU    21  10.41  14 93237 6.056132 94238 1.973126 94239 51.605541
94240 21.943351
            94241 4.129537 94242 4.497216 95241 8.301571 95601 0.020373
95243 1.247513
            96242 0.000049 96243 0.003342 96244 0.197768 96245 0.021760
96246 0.002721 1 1223 end
 b-10         31 0 7.221155e-09 1223 end
 b-11         31 0 2.924932e-08 1223 end
 c-graphite   31 0 0.07291468 1223 end
 si           31 0 0.01017942 1223 end
 b            41 den=1.69 8.2e-07 1223 5010 19.9 5011 80.1 end
 c-graphite   41 den=1.69 0.9999992 1223 end
 c-graphite   51 den=1.77 0.9999996 1223 end
 b            51 den=1.77 3.7e-07 1223 5010 19.9 5011 80.1 end
'Graphite fuel block:
 c-graphite   61 den=1.77 0.9999996 1223 end
 b            61 den=1.77 4.0e-07 1223 5010 19.9 5011 80.1 end
'Graphite Sleeve (Fuel rod):
 c-graphite   71 den=1.77 0.9999996 1223 end
 b            71 den=1.77 3.7e-07 1223 5010 19.9 5011 80.1 end
'Helium:
 he           81 den=0.001569 1 1223 end
' uo2          22 den=10.41 1 1223 92235 15 92238 85 end
'Legacy fuel TRU vector for UO2 fuel:
 wtptTRU    22  10.41  14 93237 6.056132 94238 1.973126 94239 51.605541
94240 21.943351
            94241 4.129537 94242 4.497216 95241 8.301571 95601 0.020373
95243 1.247513
            96242 0.000049 96243 0.003342 96244 0.197768 96245 0.021760
96246 0.002721 1 1223 end
 b-10         32 0 7.221155e-09 1223 end
 b-11         32 0 2.924932e-08 1223 end
 c-graphite   32 0 0.07291468 1223 end
 si           32 0 0.01017942 1223 end
 b            42 den=1.69 8.2e-07 1223 5010 19.9 5011 80.1 end
 c-graphite   42 den=1.69 0.9999992 1223 end
 c-graphite   52 den=1.77 0.9999996 1223 end
 b            52 den=1.77 3.7e-07 1223 5010 19.9 5011 80.1 end
'Graphite fuel block:
 c-graphite   62 den=1.77 0.9999996 1223 end
 b            62 den=1.77 4.0e-07 1223 5010 19.9 5011 80.1 end
'Graphite Sleeve (Fuel rod):
 c-graphite   72 den=1.77 0.9999996 1223 end
 b            72 den=1.77 3.7e-07 1223 5010 19.9 5011 80.1 end
'Helium:
 he           82 den=0.001569 1 1223 end
```

```
' uo2         23 den=10.41 1 1223 92235 15 92238 85 end
'Legacy fuel TRU vector for UO2 fuel:
 wtptTRU    23  10.41  14 93237 6.056132 94238 1.973126 94239 51.605541
94240 21.943351
            94241 4.129537 94242 4.497216 95241 8.301571 95601 0.020373
95243 1.247513
            96242 0.000049 96243 0.003342 96244 0.197768 96245 0.021760
96246 0.002721 1 1223 end
 b-10        33 0 7.221155e-09 1223 end
 b-11        33 0 2.924932e-08 1223 end
 c-graphite  33 0 0.07291468 1223 end
 si          33 0 0.01017942 1223 end
 b           43 den=1.69 8.2e-07 1223 5010 19.9 5011 80.1 end
 c-graphite  43 den=1.69 0.9999992 1223 end
 c-graphite  53 den=1.77 0.9999996 1223 end
 b           53 den=1.77 3.7e-07 1223 5010 19.9 5011 80.1 end
'Graphite fuel block:
 c-graphite  63 den=1.77 0.9999996 1223 end
 b           63 den=1.77 4.0e-07 1223 5010 19.9 5011 80.1 end
'Graphite Sleeve (Fuel rod):
 c-graphite  73 den=1.77 0.9999996 1223 end
 b           73 den=1.77 3.7e-07 1223 5010 19.9 5011 80.1 end
'Helium:
 he          83 den=0.001569 1 1223 end
' uo2         24 den=10.41 1 1223 92235 15 92238 85 end
'Legacy fuel TRU vector for UO2 fuel:
 wtptTRU    24  10.41  14 93237 6.056132 94238 1.973126 94239 51.605541
94240 21.943351
            94241 4.129537 94242 4.497216 95241 8.301571 95601 0.020373
95243 1.247513
            96242 0.000049 96243 0.003342 96244 0.197768 96245 0.021760
96246 0.002721 1 1223 end
 b-10        34 0 7.221155e-09 1223 end
 b-11        34 0 2.924932e-08 1223 end
 c-graphite  34 0 0.07291468 1223 end
 si          34 0 0.01017942 1223 end
 b           44 den=1.69 8.2e-07 1223 5010 19.9 5011 80.1 end
 c-graphite  44 den=1.69 0.9999992 1223 end
 c-graphite  54 den=1.77 0.9999996 1223 end
 b           54 den=1.77 3.7e-07 1223 5010 19.9 5011 80.1 end
'Graphite fuel block:
 c-graphite  64 den=1.77 0.9999996 1223 end
 b           64 den=1.77 4.0e-07 1223 5010 19.9 5011 80.1 end
'Graphite Sleeve (Fuel rod):
 c-graphite  74 den=1.77 0.9999996 1223 end
 b           74 den=1.77 3.7e-07 1223 5010 19.9 5011 80.1 end
'Helium:
 he          84 den=0.001569 1 1223 end
' uo2         25 den=10.41 1 1223 92235 15 92238 85 end
'Legacy fuel TRU vector for UO2 fuel:
 wtptTRU    25  10.41  14 93237 6.056132 94238 1.973126 94239 51.605541
94240 21.943351
            94241 4.129537 94242 4.497216 95241 8.301571 95601 0.020373
95243 1.247513
            96242 0.000049 96243 0.003342 96244 0.197768 96245 0.021760
96246 0.002721 1 1223 end
 b-10        35 0 7.221155e-09 1223 end
```

```
 b-11         35 0 2.924932e-08 1223 end
 c-graphite   35 0 0.07291468 1223 end
 si           35 0 0.01017942 1223 end
 b            45 den=1.69 8.2e-07 1223 5010 19.9 5011 80.1 end
 c-graphite   45 den=1.69 0.9999992 1223 end
 c-graphite   55 den=1.77 0.9999996 1223 end
 b            55 den=1.77 3.7e-07 1223 5010 19.9 5011 80.1 end
'Graphite fuel block:
 c-graphite   65 den=1.77 0.9999996 1223 end
 b            65 den=1.77 4.0e-07 1223 5010 19.9 5011 80.1 end
'Graphite Sleeve (Fuel rod):
 c-graphite   75 den=1.77 0.9999996 1223 end
 b            75 den=1.77 3.7e-07 1223 5010 19.9 5011 80.1 end
'Helium:
 he           85 den=0.001569 1 1223 end
' uo2          26 den=10.41 1 1223 92235 15 92238 85 end
'Legacy fuel TRU vector for UO2 fuel:
 wtptTRU    26  10.41  14 93237 6.056132 94238 1.973126 94239 51.605541
94240 21.943351
            94241 4.129537 94242 4.497216 95241 8.301571 95601 0.020373
95243 1.247513
            96242 0.000049 96243 0.003342 96244 0.197768 96245 0.021760
96246 0.002721 1 1223 end
 b-10         36 0 7.221155e-09 1223 end
 b-11         36 0 2.924932e-08 1223 end
 c-graphite   36 0 0.07291468 1223 end
 si           36 0 0.01017942 1223 end
 b            46 den=1.69 8.2e-07 1223 5010 19.9 5011 80.1 end
 c-graphite   46 den=1.69 0.9999992 1223 end
 c-graphite   56 den=1.77 0.9999996 1223 end
 b            56 den=1.77 3.7e-07 1223 5010 19.9 5011 80.1 end
'Graphite fuel block:
 c-graphite   66 den=1.77 0.9999996 1223 end
 b            66 den=1.77 4.0e-07 1223 5010 19.9 5011 80.1 end
'Graphite Sleeve (Fuel rod):
 c-graphite   76 den=1.77 0.9999996 1223 end
 b            76 den=1.77 3.7e-07 1223 5010 19.9 5011 80.1 end
'Helium:
 he           86 den=0.001569 1 1223 end
 c-graphite   1 den=1.77 0.9999996 1223 end
 b            1 den=1.77 4e-07 1223 5010 19.9 5011 80.1 end
 b4c          3 den=1.82 0.0274 1223 5010 19.9 5011 80.1 end
 carbon       3 den=1.82 0.9726 1223 end
 he           5 den=0.001569 1 1223 end
 c-graphite   9 den=1.76 0.9999996 1223 end
 b            9 den=1.76 3.7e-07 1223 5010 19.9 5011 80.1 end
 c-graphite   10 den=1.732 0.999998 1223 end
 b            10 den=1.732 1.91e-06 1223 5010 19.9 5011 80.1 end
end comp
read celldata
doublehet  right_bdy=white fuelmix=121 end
  gfr=0.02985 21  coatr=0.04645 31 VF=0.2 matrix=41  end grain
  rod triangpitch right_bdy=white hpitch=2.575 61 fuelr=1.2 gapr=1.6 71
cladr=2.05 81 fuelh=54.6 end
doublehet  right_bdy=white fuelmix=122 end
  gfr=0.02985 22  coatr=0.04645 32 VF=0.2 matrix=42  end grain
```

```
  rod triangpitch right_bdy=white hpitch=2.575 62 fuelr=1.2 gapr=1.6 72
cladr=2.05 82 fuelh=54.6 end
doublehet  right_bdy=white fuelmix=123 end
  gfr=0.02985 23  coatr=0.04645 33 VF=0.2 matrix=43  end grain
  rod triangpitch right_bdy=white hpitch=2.575 63 fuelr=1.2 gapr=1.6 73
cladr=2.05 83 fuelh=54.6 end
doublehet  right_bdy=white fuelmix=124 end
  gfr=0.02985 24  coatr=0.04645 34 VF=0.2 matrix=44  end grain
  rod triangpitch right_bdy=white hpitch=2.575 64 fuelr=1.2 gapr=1.6 74
cladr=2.05 84 fuelh=54.6 end
doublehet  right_bdy=white fuelmix=125 end
  gfr=0.02985 25  coatr=0.04645 35 VF=0.2 matrix=45  end grain
  rod triangpitch right_bdy=white hpitch=2.575 65 fuelr=1.2 gapr=1.6 75
cladr=2.05 85 fuelh=54.6 end
doublehet  right_bdy=white fuelmix=126 end
  gfr=0.02985 26  coatr=0.04645 36 VF=0.2 matrix=46  end grain
  rod triangpitch right_bdy=white hpitch=2.575 66 fuelr=1.2 gapr=1.6 76
cladr=2.05 86 fuelh=54.6 end
end celldata
read parameter
           gen=550
           npg=2500
           nsk=50
           FLX=yes
end parameter
read geometry
unit 1
com='inner fuel block'
 zcylinder 1 1 17.9  58  0
  hole 12 -7.875  13.64  4.2
  hole 4 -7.875  -13.6399  4.2
  hole 4 -7.875  -13.6399  34.2
  hole 4 15.75  0  4.2
  hole 4 15.75  0  34.2
  hole 8 0  8.92  0
  hole 8 0  -8.92  0
  hole 8 2.575  4.46  0
  hole 8 2.575  -4.46  0
  hole 8 2.575  13.38  0
  hole 8 2.575  -13.38  0
  hole 8 -2.575  4.46  0
  hole 8 -2.575  -4.46  0
  hole 8 -2.575  13.38  0
  hole 8 -2.575  -13.38  0
  hole 8 5.15  0  0
  hole 8 5.15  8.92  0
  hole 8 5.15  -8.92  0
  hole 8 -5.15  0  0
  hole 8 -5.15  8.92  0
  hole 8 -5.15  -8.92  0
  hole 8 7.725  4.46  0
  hole 8 7.725  -4.46  0
  hole 8 -7.725  4.46  0
  hole 8 -7.725  -4.46  0
  hole 8 10.3  0  0
  hole 8 10.3  8.92  0
  hole 8 10.3  -8.92  0
```

```
hole 8 -10.3  0  0
hole 8 -10.3  8.92  0
hole 8 -10.3  -8.92  0
hole 8 12.875  4.46  0
hole 8 12.875  -4.46  0
hole 8 -12.875  4.46  0
hole 8 -12.875  -4.46  0
hole 8 -15.45  0  0
hole 8 0  8.92  56.3
hole 8 0  -8.92  56.3
hole 8 2.575  4.46  56.3
hole 8 2.575  -4.46  56.3
hole 8 2.575  13.38  56.3
hole 8 2.575  -13.38  56.3
hole 8 -2.575  4.46  56.3
hole 8 -2.575  -4.46  56.3
hole 8 -2.575  13.38  56.3
hole 8 -2.575  -13.38  56.3
hole 8 5.15  0  56.3
hole 8 5.15  8.92  56.3
hole 8 5.15  -8.92  56.3
hole 8 -5.15  0  56.3
hole 8 -5.15  8.92  56.3
hole 8 -5.15  -8.92  56.3
hole 8 7.725  4.46  56.3
hole 8 7.725  -4.46  56.3
hole 8 -7.725  4.46  56.3
hole 8 -7.725  -4.46  56.3
hole 8 10.3  0  56.3
hole 8 10.3  8.92  56.3
hole 8 10.3  -8.92  56.3
hole 8 -10.3  0  56.3
hole 8 -10.3  8.92  56.3
hole 8 -10.3  -8.92  56.3
hole 8 12.875  4.46  56.3
hole 8 12.875  -4.46  56.3
hole 8 -12.875  4.46  56.3
hole 8 -12.875  -4.46  56.3
hole 8 -15.45  0  56.3
hole 7 0  0  33
hole 6 0  0  43
hole 5 0  0  49
hole 2 0  8.92  1.7
hole 2 0  -8.92  1.7
hole 2 2.575  4.46  1.7
hole 2 2.575  -4.46  1.7
hole 2 2.575  13.38  1.7
hole 2 2.575  -13.38  1.7
hole 2 -2.575  4.46  1.7
hole 2 -2.575  -4.46  1.7
hole 2 -2.575  13.38  1.7
hole 2 -2.575  -13.38  1.7
hole 2 5.15  0  1.7
hole 2 5.15  8.92  1.7
hole 2 5.15  -8.92  1.7
hole 2 -5.15  0  1.7
hole 2 -5.15  8.92  1.7
```

```
  hole 2 -5.15  -8.92  1.7
  hole 2 7.725  4.46  1.7
  hole 2 7.725  -4.46  1.7
  hole 2 -7.725  4.46  1.7
  hole 2 -7.725  -4.46  1.7
  hole 2 10.3  0  1.7
  hole 2 10.3  8.92  1.7
  hole 2 10.3  -8.92  1.7
  hole 2 -10.3  0  1.7
  hole 2 -10.3  8.92  1.7
  hole 2 -10.3  -8.92  1.7
  hole 2 12.875  4.46  1.7
  hole 2 12.875  -4.46  1.7
  hole 2 -12.875  4.46  1.7
  hole 2 -12.875  -4.46  1.7
  hole 2 -15.45  0  1.7
unit 2
com='inner fuel (pin) hole'
 zcylinder 5 1 0.5  54.6  0
 zcylinder 121 1 1.3  54.6  0
 zcylinder 51 1 1.7  54.6  0
 zcylinder 5 1 2.05  54.6  0
unit 21
com='middle fuel block'
 zcylinder 1 1 17.9  58  0
  hole 12 -7.875  13.64  4.2
  hole 4 -7.875  -13.6399  4.2
  hole 4 -7.875  -13.6399  34.2
  hole 4 15.75  0  4.2
  hole 4 15.75  0  34.2
  hole 8 0  8.92  0
  hole 8 0  -8.92  0
  hole 8 2.575  4.46  0
  hole 8 2.575  -4.46  0
  hole 8 2.575  13.38  0
  hole 8 2.575  -13.38  0
  hole 8 -2.575  4.46  0
  hole 8 -2.575  -4.46  0
  hole 8 -2.575  13.38  0
  hole 8 -2.575  -13.38  0
  hole 8 5.15  0  0
  hole 8 5.15  8.92  0
  hole 8 5.15  -8.92  0
  hole 8 -5.15  0  0
  hole 8 -5.15  8.92  0
  hole 8 -5.15  -8.92  0
  hole 8 7.725  4.46  0
  hole 8 7.725  -4.46  0
  hole 8 -7.725  4.46  0
  hole 8 -7.725  -4.46  0
  hole 8 10.3  0  0
  hole 8 10.3  8.92  0
  hole 8 10.3  -8.92  0
  hole 8 -10.3  0  0
  hole 8 -10.3  8.92  0
  hole 8 -10.3  -8.92  0
  hole 8 12.875  4.46  0
```

```
hole 8 12.875  -4.46  0
hole 8 -12.875  4.46  0
hole 8 -12.875  -4.46  0
hole 8 -15.45  0  0
hole 8 0  8.92  56.3
hole 8 0  -8.92  56.3
hole 8 2.575  4.46  56.3
hole 8 2.575  -4.46  56.3
hole 8 2.575  13.38  56.3
hole 8 2.575  -13.38  56.3
hole 8 -2.575  4.46  56.3
hole 8 -2.575  -4.46  56.3
hole 8 -2.575  13.38  56.3
hole 8 -2.575  -13.38  56.3
hole 8 5.15  0  56.3
hole 8 5.15  8.92  56.3
hole 8 5.15  -8.92  56.3
hole 8 -5.15  0  56.3
hole 8 -5.15  8.92  56.3
hole 8 -5.15  -8.92  56.3
hole 8 7.725  4.46  56.3
hole 8 7.725  -4.46  56.3
hole 8 -7.725  4.46  56.3
hole 8 -7.725  -4.46  56.3
hole 8 10.3  0  56.3
hole 8 10.3  8.92  56.3
hole 8 10.3  -8.92  56.3
hole 8 -10.3  0  56.3
hole 8 -10.3  8.92  56.3
hole 8 -10.3  -8.92  56.3
hole 8 12.875  4.46  56.3
hole 8 12.875  -4.46  56.3
hole 8 -12.875  4.46  56.3
hole 8 -12.875  -4.46  56.3
hole 8 -15.45  0  56.3
hole 7 0  0  33
hole 6 0  0  43
hole 5 0  0  49
hole 22 0  8.92  1.7
hole 22 0  -8.92  1.7
hole 22 2.575  4.46  1.7
hole 22 2.575  -4.46  1.7
hole 22 2.575  13.38  1.7
hole 22 2.575  -13.38  1.7
hole 22 -2.575  4.46  1.7
hole 22 -2.575  -4.46  1.7
hole 22 -2.575  13.38  1.7
hole 22 -2.575  -13.38  1.7
hole 22 5.15  0  1.7
hole 22 5.15  8.92  1.7
hole 22 5.15  -8.92  1.7
hole 22 -5.15  0  1.7
hole 22 -5.15  8.92  1.7
hole 22 -5.15  -8.92  1.7
hole 22 7.725  4.46  1.7
hole 22 7.725  -4.46  1.7
hole 22 -7.725  4.46  1.7
```

```
  hole 22 -7.725  -4.46  1.7
  hole 22 10.3  0  1.7
  hole 22 10.3  8.92  1.7
  hole 22 10.3  -8.92  1.7
  hole 22 -10.3  0  1.7
  hole 22 -10.3  8.92  1.7
  hole 22 -10.3  -8.92  1.7
  hole 22 12.875  4.46  1.7
  hole 22 12.875  -4.46  1.7
  hole 22 -12.875  4.46  1.7
  hole 22 -12.875  -4.46  1.7
  hole 22 -15.45  0  1.7
unit 22
com='middle fuel (pin) hole'
 zcylinder 5 1 0.5  54.6  0
 zcylinder 122 1 1.3  54.6  0
 zcylinder 52 1 1.7  54.6  0
 zcylinder 5 1 2.05  54.6  0
unit 31
com='outer fuel block'
 zcylinder 1 1 17.9  58  0
  hole 12 -7.875  13.64  4.2
  hole 4 -7.875  -13.6399  4.2
  hole 4 -7.875  -13.6399  34.2
  hole 4 15.75  0  4.2
  hole 4 15.75  0  34.2
  hole 8 0  8.92  0
  hole 8 0  -8.92  0
  hole 8 2.575  4.46  0
  hole 8 2.575  -4.46  0
  hole 8 2.575  13.38  0
  hole 8 2.575  -13.38  0
  hole 8 -2.575  4.46  0
  hole 8 -2.575  -4.46  0
  hole 8 -2.575  13.38  0
  hole 8 -2.575  -13.38  0
  hole 8 5.15  0  0
  hole 8 5.15  8.92  0
  hole 8 5.15  -8.92  0
  hole 8 -5.15  0  0
  hole 8 -5.15  8.92  0
  hole 8 -5.15  -8.92  0
  hole 8 7.725  4.46  0
  hole 8 7.725  -4.46  0
  hole 8 -7.725  4.46  0
  hole 8 -7.725  -4.46  0
  hole 8 10.3  0  0
  hole 8 10.3  8.92  0
  hole 8 10.3  -8.92  0
  hole 8 -10.3  0  0
  hole 8 -10.3  8.92  0
  hole 8 -10.3  -8.92  0
  hole 8 12.875  4.46  0
  hole 8 12.875  -4.46  0
  hole 8 -12.875  4.46  0
  hole 8 -12.875  -4.46  0
  hole 8 -15.45  0  0
```

```
hole 8 0  8.92  56.3
hole 8 0  -8.92  56.3
hole 8 2.575  4.46  56.3
hole 8 2.575  -4.46  56.3
hole 8 2.575  13.38  56.3
hole 8 2.575  -13.38  56.3
hole 8 -2.575  4.46  56.3
hole 8 -2.575  -4.46  56.3
hole 8 -2.575  13.38  56.3
hole 8 -2.575  -13.38  56.3
hole 8 5.15  0  56.3
hole 8 5.15  8.92  56.3
hole 8 5.15  -8.92  56.3
hole 8 -5.15  0  56.3
hole 8 -5.15  8.92  56.3
hole 8 -5.15  -8.92  56.3
hole 8 7.725  4.46  56.3
hole 8 7.725  -4.46  56.3
hole 8 -7.725  4.46  56.3
hole 8 -7.725  -4.46  56.3
hole 8 10.3  0  56.3
hole 8 10.3  8.92  56.3
hole 8 10.3  -8.92  56.3
hole 8 -10.3  0  56.3
hole 8 -10.3  8.92  56.3
hole 8 -10.3  -8.92  56.3
hole 8 12.875  4.46  56.3
hole 8 12.875  -4.46  56.3
hole 8 -12.875  4.46  56.3
hole 8 -12.875  -4.46  56.3
hole 8 -15.45  0  56.3
hole 7 0  0  33
hole 6 0  0  43
hole 5 0  0  49
hole 23 0  8.92  1.7
hole 23 0  -8.92  1.7
hole 23 2.575  4.46  1.7
hole 23 2.575  -4.46  1.7
hole 23 2.575  13.38  1.7
hole 23 2.575  -13.38  1.7
hole 23 -2.575  4.46  1.7
hole 23 -2.575  -4.46  1.7
hole 23 -2.575  13.38  1.7
hole 23 -2.575  -13.38  1.7
hole 23 5.15  0  1.7
hole 23 5.15  8.92  1.7
hole 23 5.15  -8.92  1.7
hole 23 -5.15  0  1.7
hole 23 -5.15  8.92  1.7
hole 23 -5.15  -8.92  1.7
hole 23 7.725  4.46  1.7
hole 23 7.725  -4.46  1.7
hole 23 -7.725  4.46  1.7
hole 23 -7.725  -4.46  1.7
hole 23 10.3  0  1.7
hole 23 10.3  8.92  1.7
hole 23 10.3  -8.92  1.7
```

```
  hole 23 -10.3  0  1.7
  hole 23 -10.3  8.92  1.7
  hole 23 -10.3  -8.92  1.7
  hole 23 12.875  4.46  1.7
  hole 23 12.875  -4.46  1.7
  hole 23 -12.875  4.46  1.7
  hole 23 -12.875  -4.46  1.7
  hole 23 -15.45  0  1.7
unit 23
com='outer fuel (pin) hole'
 zcylinder 5 1 0.5  54.6  0
 zcylinder 123 1 1.3  54.6  0
 zcylinder 53 1 1.7  54.6  0
 zcylinder 5 1 2.05  54.6  0
unit 41
com='target block'
 zcylinder 1 1 17.9  58  0
  hole 12 -7.875  13.64  4.2
  hole 12 -7.875  -13.6399  4.2
  hole 12 15.75  0  4.2
  hole 8 0  8.92  0
  hole 8 0  -8.92  0
  hole 8 2.575  4.46  0
  hole 8 2.575  -4.46  0
  hole 8 2.575  13.38  0
  hole 8 2.575  -13.38  0
  hole 8 -2.575  4.46  0
  hole 8 -2.575  -4.46  0
  hole 8 -2.575  13.38  0
  hole 8 -2.575  -13.38  0
  hole 8 5.15  0  0
  hole 8 5.15  8.92  0
  hole 8 5.15  -8.92  0
  hole 8 -5.15  0  0
  hole 8 -5.15  8.92  0
  hole 8 -5.15  -8.92  0
  hole 8 7.725  4.46  0
  hole 8 7.725  -4.46  0
  hole 8 -7.725  4.46  0
  hole 8 -7.725  -4.46  0
  hole 8 10.3  0  0
  hole 8 10.3  8.92  0
  hole 8 10.3  -8.92  0
  hole 8 -10.3  0  0
  hole 8 -10.3  8.92  0
  hole 8 -10.3  -8.92  0
  hole 8 12.875  4.46  0
  hole 8 12.875  -4.46  0
  hole 8 -12.875  4.46  0
  hole 8 -12.875  -4.46  0
  hole 8 -15.45  0  0
  hole 8 0  8.92  56.3
  hole 8 0  -8.92  56.3
  hole 8 2.575  4.46  56.3
  hole 8 2.575  -4.46  56.3
  hole 8 2.575  13.38  56.3
  hole 8 2.575  -13.38  56.3
```

```
hole 8 -2.575  4.46  56.3
hole 8 -2.575  -4.46  56.3
hole 8 -2.575  13.38  56.3
hole 8 -2.575  -13.38  56.3
hole 8 5.15  0  56.3
hole 8 5.15  8.92  56.3
hole 8 5.15  -8.92  56.3
hole 8 -5.15  0  56.3
hole 8 -5.15  8.92  56.3
hole 8 -5.15  -8.92  56.3
hole 8 7.725  4.46  56.3
hole 8 7.725  -4.46  56.3
hole 8 -7.725  4.46  56.3
hole 8 -7.725  -4.46  56.3
hole 8 10.3  0  56.3
hole 8 10.3  8.92  56.3
hole 8 10.3  -8.92  56.3
hole 8 -10.3  0  56.3
hole 8 -10.3  8.92  56.3
hole 8 -10.3  -8.92  56.3
hole 8 12.875  4.46  56.3
hole 8 12.875  -4.46  56.3
hole 8 -12.875  4.46  56.3
hole 8 -12.875  -4.46  56.3
hole 8 -15.45  0  56.3
hole 7 0  0  33
hole 6 0  0  43
hole 5 0  0  49
hole 24 0  8.92  1.7
hole 24 0  -8.92  1.7
hole 24 2.575  4.46  1.7
hole 24 2.575  -4.46  1.7
hole 24 2.575  13.38  1.7
hole 24 2.575  -13.38  1.7
hole 24 -2.575  4.46  1.7
hole 24 -2.575  -4.46  1.7
hole 24 -2.575  13.38  1.7
hole 24 -2.575  -13.38  1.7
hole 24 5.15  0  1.7
hole 24 5.15  8.92  1.7
hole 24 5.15  -8.92  1.7
hole 24 -5.15  0  1.7
hole 24 -5.15  8.92  1.7
hole 24 -5.15  -8.92  1.7
hole 24 7.725  4.46  1.7
hole 24 7.725  -4.46  1.7
hole 24 -7.725  4.46  1.7
hole 24 -7.725  -4.46  1.7
hole 24 10.3  0  1.7
hole 24 10.3  8.92  1.7
hole 24 10.3  -8.92  1.7
hole 24 -10.3  0  1.7
hole 24 -10.3  8.92  1.7
hole 24 -10.3  -8.92  1.7
hole 24 12.875  4.46  1.7
hole 24 12.875  -4.46  1.7
hole 24 -12.875  4.46  1.7
```

```
  hole 24 -12.875  -4.46  1.7
  hole 24 -15.45  0  1.7
unit 24
com='outer fuel (pin) hole'
 zcylinder 5 1 0.5  54.6  0
 zcylinder 124 1 1.3  54.6  0
 zcylinder 54 1 1.7  54.6  0
 zcylinder 5 1 2.05  54.6  0
unit 51
com='target block'
 zcylinder 1 1 17.9  58  0
  hole 12 -7.875  13.64  4.2
  hole 12 -7.875  -13.6399  4.2
  hole 12 15.75  0  4.2
  hole 8 0  8.92  0
  hole 8 0  -8.92  0
  hole 8 2.575  4.46  0
  hole 8 2.575  -4.46  0
  hole 8 2.575  13.38  0
  hole 8 2.575  -13.38  0
  hole 8 -2.575  4.46  0
  hole 8 -2.575  -4.46  0
  hole 8 -2.575  13.38  0
  hole 8 -2.575  -13.38  0
  hole 8 5.15  0  0
  hole 8 5.15  8.92  0
  hole 8 5.15  -8.92  0
  hole 8 -5.15  0  0
  hole 8 -5.15  8.92  0
  hole 8 -5.15  -8.92  0
  hole 8 7.725  4.46  0
  hole 8 7.725  -4.46  0
  hole 8 -7.725  4.46  0
  hole 8 -7.725  -4.46  0
  hole 8 10.3  0  0
  hole 8 10.3  8.92  0
  hole 8 10.3  -8.92  0
  hole 8 -10.3  0  0
  hole 8 -10.3  8.92  0
  hole 8 -10.3  -8.92  0
  hole 8 12.875  4.46  0
  hole 8 12.875  -4.46  0
  hole 8 -12.875  4.46  0
  hole 8 -12.875  -4.46  0
  hole 8 -15.45  0  0
  hole 8 0  8.92  56.3
  hole 8 0  -8.92  56.3
  hole 8 2.575  4.46  56.3
  hole 8 2.575  -4.46  56.3
  hole 8 2.575  13.38  56.3
  hole 8 2.575  -13.38  56.3
  hole 8 -2.575  4.46  56.3
  hole 8 -2.575  -4.46  56.3
  hole 8 -2.575  13.38  56.3
  hole 8 -2.575  -13.38  56.3
  hole 8 5.15  0  56.3
  hole 8 5.15  8.92  56.3
```

```
  hole 8 5.15  -8.92  56.3
  hole 8 -5.15  0  56.3
  hole 8 -5.15  8.92  56.3
  hole 8 -5.15  -8.92  56.3
  hole 8 7.725  4.46  56.3
  hole 8 7.725  -4.46  56.3
  hole 8 -7.725  4.46  56.3
  hole 8 -7.725  -4.46  56.3
  hole 8 10.3  0  56.3
  hole 8 10.3  8.92  56.3
  hole 8 10.3  -8.92  56.3
  hole 8 -10.3  0  56.3
  hole 8 -10.3  8.92  56.3
  hole 8 -10.3  -8.92  56.3
  hole 8 12.875  4.46  56.3
  hole 8 12.875  -4.46  56.3
  hole 8 -12.875  4.46  56.3
  hole 8 -12.875  -4.46  56.3
  hole 8 -15.45  0  56.3
  hole 7 0  0  33
  hole 6 0  0  43
  hole 5 0  0  49
  hole 25 0  8.92  1.7
  hole 25 0  -8.92  1.7
  hole 25 2.575  4.46  1.7
  hole 25 2.575  -4.46  1.7
  hole 25 2.575  13.38  1.7
  hole 25 2.575  -13.38  1.7
  hole 25 -2.575  4.46  1.7
  hole 25 -2.575  -4.46  1.7
  hole 25 -2.575  13.38  1.7
  hole 25 -2.575  -13.38  1.7
  hole 25 5.15  0  1.7
  hole 25 5.15  8.92  1.7
  hole 25 5.15  -8.92  1.7
  hole 25 -5.15  0  1.7
  hole 25 -5.15  8.92  1.7
  hole 25 -5.15  -8.92  1.7
  hole 25 7.725  4.46  1.7
  hole 25 7.725  -4.46  1.7
  hole 25 -7.725  4.46  1.7
  hole 25 -7.725  -4.46  1.7
  hole 25 10.3  0  1.7
  hole 25 10.3  8.92  1.7
  hole 25 10.3  -8.92  1.7
  hole 25 -10.3  0  1.7
  hole 25 -10.3  8.92  1.7
  hole 25 -10.3  -8.92  1.7
  hole 25 12.875  4.46  1.7
  hole 25 12.875  -4.46  1.7
  hole 25 -12.875  4.46  1.7
  hole 25 -12.875  -4.46  1.7
  hole 25 -15.45  0  1.7
unit 25
com='outer fuel (pin) hole'
 zcylinder 5 1 0.5  54.6  0
 zcylinder 125 1 1.3  54.6  0
```

```
 zcylinder 55 1 1.7  54.6  0
 zcylinder 5 1 2.05  54.6  0
unit 61
com='target block'
 zcylinder 1 1 17.9  58  0
  hole 12 -7.875  13.64  4.2
  hole 12 -7.875  -13.6399  4.2
  hole 12 15.75  0  4.2
  hole 8 0  8.92  0
  hole 8 0  -8.92  0
  hole 8 2.575  4.46  0
  hole 8 2.575  -4.46  0
  hole 8 2.575  13.38  0
  hole 8 2.575  -13.38  0
  hole 8 -2.575  4.46  0
  hole 8 -2.575  -4.46  0
  hole 8 -2.575  13.38  0
  hole 8 -2.575  -13.38  0
  hole 8 5.15  0  0
  hole 8 5.15  8.92  0
  hole 8 5.15  -8.92  0
  hole 8 -5.15  0  0
  hole 8 -5.15  8.92  0
  hole 8 -5.15  -8.92  0
  hole 8 7.725  4.46  0
  hole 8 7.725  -4.46  0
  hole 8 -7.725  4.46  0
  hole 8 -7.725  -4.46  0
  hole 8 10.3  0  0
  hole 8 10.3  8.92  0
  hole 8 10.3  -8.92  0
  hole 8 -10.3  0  0
  hole 8 -10.3  8.92  0
  hole 8 -10.3  -8.92  0
  hole 8 12.875  4.46  0
  hole 8 12.875  -4.46  0
  hole 8 -12.875  4.46  0
  hole 8 -12.875  -4.46  0
  hole 8 -15.45  0  0
  hole 8 0  8.92  56.3
  hole 8 0  -8.92  56.3
  hole 8 2.575  4.46  56.3
  hole 8 2.575  -4.46  56.3
  hole 8 2.575  13.38  56.3
  hole 8 2.575  -13.38  56.3
  hole 8 -2.575  4.46  56.3
  hole 8 -2.575  -4.46  56.3
  hole 8 -2.575  13.38  56.3
  hole 8 -2.575  -13.38  56.3
  hole 8 5.15  0  56.3
  hole 8 5.15  8.92  56.3
  hole 8 5.15  -8.92  56.3
  hole 8 -5.15  0  56.3
  hole 8 -5.15  8.92  56.3
  hole 8 -5.15  -8.92  56.3
  hole 8 7.725  4.46  56.3
  hole 8 7.725  -4.46  56.3
```

```
  hole 8 -7.725  4.46  56.3
  hole 8 -7.725  -4.46  56.3
  hole 8 10.3  0  56.3
  hole 8 10.3  8.92  56.3
  hole 8 10.3  -8.92  56.3
  hole 8 -10.3  0  56.3
  hole 8 -10.3  8.92  56.3
  hole 8 -10.3  -8.92  56.3
  hole 8 12.875  4.46  56.3
  hole 8 12.875  -4.46  56.3
  hole 8 -12.875  4.46  56.3
  hole 8 -12.875  -4.46  56.3
  hole 8 -15.45  0  56.3
  hole 7 0  0  33
  hole 6 0  0  43
  hole 5 0  0  49
  hole 26 0  8.92  1.7
  hole 26 0  -8.92  1.7
  hole 26 2.575  4.46  1.7
  hole 26 2.575  -4.46  1.7
  hole 26 2.575  13.38  1.7
  hole 26 2.575  -13.38  1.7
  hole 26 -2.575  4.46  1.7
  hole 26 -2.575  -4.46  1.7
  hole 26 -2.575  13.38  1.7
  hole 26 -2.575  -13.38  1.7
  hole 26 5.15  0  1.7
  hole 26 5.15  8.92  1.7
  hole 26 5.15  -8.92  1.7
  hole 26 -5.15  0  1.7
  hole 26 -5.15  8.92  1.7
  hole 26 -5.15  -8.92  1.7
  hole 26 7.725  4.46  1.7
  hole 26 7.725  -4.46  1.7
  hole 26 -7.725  4.46  1.7
  hole 26 -7.725  -4.46  1.7
  hole 26 10.3  0  1.7
  hole 26 10.3  8.92  1.7
  hole 26 10.3  -8.92  1.7
  hole 26 -10.3  0  1.7
  hole 26 -10.3  8.92  1.7
  hole 26 -10.3  -8.92  1.7
  hole 26 12.875  4.46  1.7
  hole 26 12.875  -4.46  1.7
  hole 26 -12.875  4.46  1.7
  hole 26 -12.875  -4.46  1.7
  hole 26 -15.45  0  1.7
unit 26
com='outer fuel (pin) hole'
 zcylinder 5 1 0.5  54.6  0
 zcylinder 126 1 1.3  54.6  0
 zcylinder 56 1 1.7  54.6  0
 zcylinder 5 1 2.05  54.6  0
unit 13
com='coolant channel'
 zcylinder 5 1 2.05  58  0
unit 4
```

```
com='bp ii'
 zcylinder 3 1 0.75  20  0
unit 5
com='handling hole i'
 zcylinder 5 1 2  9  0
unit 6
com='handling hole ii'
 zcylinder 5 1 1.5  6  0
unit 7
com='handling hole iii'
 zcylinder 5 1 2.25  10  0
unit 8
com='coolant above/below fuel rod'
 zcylinder 5 1 2.05  1.7  0
unit 12
com='bp hole'
 zcylinder 5 1 0.75  50  0
unit 9
com='coolant block 1: (empty bp 120 degree)'
 zcylinder 9 1 17.9  58  0
  hole 7 0  0  33
  hole 6 0  0  43
  hole 5 0  0  49
  hole 13 0  8.92  0
  hole 13 0  -8.92  0
  hole 13 2.575  4.46  0
  hole 13 2.575  -4.46  0
  hole 13 2.575  13.38  0
  hole 13 2.575  -13.38  0
  hole 13 -2.575  4.46  0
  hole 13 -2.575  -4.46  0
  hole 13 -2.575  13.38  0
  hole 13 -2.575  -13.38  0
  hole 13 5.15  0  0
  hole 13 5.15  8.92  0
  hole 13 5.15  -8.92  0
  hole 13 -5.15  0  0
  hole 13 -5.15  8.92  0
  hole 13 -5.15  -8.92  0
  hole 13 7.725  4.46  0
  hole 13 7.725  -4.46  0
  hole 13 -7.725  4.46  0
  hole 13 -7.725  -4.46  0
  hole 13 10.3  0  0
  hole 13 10.3  8.92  0
  hole 13 10.3  -8.92  0
  hole 13 -10.3  0  0
  hole 13 -10.3  8.92  0
  hole 13 -10.3  -8.92  0
  hole 13 12.875  4.46  0
  hole 13 12.875  -4.46  0
  hole 13 -12.875  4.46  0
  hole 13 -12.875  -4.46  0
  hole 13 -15.45  0  0
unit 10
com='cr block'
 zcylinder 1 1 17.8  58  0
```

```
  hole 11 -5.4  9.353  0
  hole 11 -5.4  -9.353  0
  hole 11 10.8  0  0
  hole 7 0  0  33
  hole 6 0  0  43
  hole 5 0  0  49
unit 11
com='cr hole'
 zcylinder 5 1 6.15  58  0
unit 101
com='slice above/below fuel'
 zcylinder 9 1 310  58  0
  hole 10 0  216  0
  hole 10 0  -180  0
  hole 10 31.1769  162  0
  hole 10 31.1769  -234  0
  hole 10 -31.1769  162  0
  hole 10 -31.1769  -234  0
  hole 10 62.3538  216  0
  hole 10 62.3538  -144  0
  hole 10 -62.3538  216  0
  hole 10 -62.3538  -144  0
  hole 10 93.5307  126  0
  hole 10 93.5307  -198  0
  hole 10 -93.5307  126  0
  hole 10 -93.5307  -198  0
  hole 10 124.7076  180  0
  hole 10 124.7076  -108  0
  hole 10 -124.7076  180  0
  hole 10 -124.7076  -108  0
  hole 10 155.8845  18  0
  hole 10 155.8845  90  0
  hole 10 155.8845  -54  0
  hole 10 155.8845  -162  0
  hole 10 -155.8845  18  0
  hole 10 -155.8845  90  0
  hole 10 -155.8845  -54  0
  hole 10 -155.8845  -162  0
  hole 10 187.0614  144  0
  hole 10 187.0614  -108  0
  hole 10 -187.0614  144  0
  hole 10 -187.0614  -108  0
  hole 10 218.2383  18  0
  hole 10 218.2383  90  0
  hole 10 218.2383  -54  0
  hole 10 -218.2383  18  0
  hole 10 -218.2383  90  0
  hole 10 -218.2383  -54  0
  hole 9 0  180  0
  hole 9 0  -216  0
  hole 9 31.1769  198  0
  hole 9 31.1769  234  0
  hole 9 31.1769  -162  0
  hole 9 31.1769  -198  0
  hole 9 -31.1769  198  0
  hole 9 -31.1769  234  0
  hole 9 -31.1769  -162  0
```

```
hole 9 -31.1769  -198  0
hole 9 62.3538  144  0
hole 9 62.3538  180  0
hole 9 62.3538  -180  0
hole 9 62.3538  -216  0
hole 9 -62.3538  144  0
hole 9 -62.36  180  0
hole 9 -62.3538  -180  0
hole 9 -62.3538  -216  0
hole 9 93.5307  162  0
hole 9 93.5307  198  0
hole 9 93.5307  -126  0
hole 9 93.5307  -162  0
hole 9 -93.5307  162  0
hole 9 -93.5307  198  0
hole 9 -93.5307  -126  0
hole 9 -93.5307  -162  0
hole 9 124.7076  108  0
hole 9 124.7076  144  0
hole 9 124.7076  -144  0
hole 9 124.7076  -180  0
hole 9 -124.7076  108  0
hole 9 -124.7076  144  0
hole 9 -124.7076  -144  0
hole 9 -124.7076  -180  0
hole 9 155.8845  54  0
hole 9 155.8845  126  0
hole 9 155.8845  162  0
hole 9 155.8845  -18  0
hole 9 155.8845  -90  0
hole 9 155.8845  -126  0
hole 9 -155.8845  54  0
hole 9 -155.8845  126  0
hole 9 -155.8845  162  0
hole 9 -155.8845  -18  0
hole 9 -155.8845  -90  0
hole 9 -155.8845  -126  0
hole 9 187.0614  0  0
hole 9 187.0614  36  0
hole 9 187.0614  72  0
hole 9 187.0614  108  0
hole 9 187.0614  -36  0
hole 9 187.0614  -72  0
hole 9 187.0614  -144  0
hole 9 -187.0614  0  0
hole 9 -187.0614  36  0
hole 9 -187.0614  72  0
hole 9 -187.0614  108  0
hole 9 -187.0614  -36  0
hole 9 -187.0614  -72  0
hole 9 -187.0614  -144  0
hole 9 218.2383  54  0
hole 9 218.2383  -18  0
hole 9 218.2383  -90  0
hole 9 -218.2383  54  0
hole 9 -218.2383  -18  0
hole 9 -218.2383  -90  0
```

```
 zcylinder 10 1 340  58  0
 cuboid 0 1  400  -400  400  -400  58  0
unit 102
com='slice with fuel and tgt'
 zcylinder 9 1 310  58  0
  hole 10 0  216  0
  hole 10 0  -180  0
  hole 10 31.1769  162  0
  hole 10 31.1769  -234  0
  hole 10 -31.1769  162  0
  hole 10 -31.1769  -234  0
  hole 10 62.3538  216  0
  hole 10 62.3538  -144  0
  hole 10 -62.3538  216  0
  hole 10 -62.3538  -144  0
  hole 10 93.5307  126  0
  hole 10 93.5307  -198  0
  hole 10 -93.5307  126  0
  hole 10 -93.5307  -198  0
  hole 10 124.7076  180  0
  hole 10 124.7076  -108  0
  hole 10 -124.7076  180  0
  hole 10 -124.7076  -108  0
  hole 10 155.8845  18  0
  hole 10 155.8845  90  0
  hole 10 155.8845  -54  0
  hole 10 155.8845  -162  0
  hole 10 -155.8845  18  0
  hole 10 -155.8845  90  0
  hole 10 -155.8845  -54  0
  hole 10 -155.8845  -162  0
  hole 10 187.0614  144  0
  hole 10 187.0614  -108  0
  hole 10 -187.0614  144  0
  hole 10 -187.0614  -108  0
  hole 10 218.2383  18  0
  hole 10 218.2383  90  0
  hole 10 218.2383  -54  0
  hole 10 -218.2383  18  0
  hole 10 -218.2383  90  0
  hole 10 -218.2383  -54  0
  hole 1 0  180  0
  hole 21 0  -216  0
  hole 21 31.1769  198  0
  hole 31 31.1769  234  0
  hole 1 31.1769  -162  0
  hole 21 31.1769  -198  0
  hole 21 -31.1769  198  0
  hole 31 -31.1769  234  0
  hole 1 -31.1769  -162  0
  hole 21 -31.1769  -198  0
  hole 1 62.3538  144  0
  hole 21 62.3538  180  0
  hole 21 62.3538  -180  0
  hole 31 62.3538  -216  0
  hole 1 -62.3538  144  0
  hole 21 -62.36  180  0
```

```
  hole 21 -62.3538  -180  0
  hole 31 -62.3538  -216  0
  hole 51 93.5307  162  0
  hole 31 93.5307  198  0
  hole 1 93.5307  -126  0
  hole 21 93.5307  -162  0
  hole 21 -93.5307  162  0
  hole 31 -93.5307  198  0
  hole 1 -93.5307  -126  0
  hole 21 -93.5307  -162  0
  hole 1 124.7076  108  0
  hole 21 124.7076  144  0
  hole 21 124.7076  -144  0
  hole 61 124.7076  -180  0
  hole 1 -124.7076  108  0
  hole 21 -124.7076  144  0
  hole 21 -124.7076  -144  0
  hole 31 -124.7076  -180  0
  hole 1 155.8845  54  0
  hole 21 155.8845  126  0
  hole 31 155.8845  162  0
  hole 1 155.8845  -18  0
  hole 1 155.8845  -90  0
  hole 21 155.8845  -126  0
  hole 1 -155.8845  54  0
  hole 21 -155.8845  126  0
  hole 31 -155.8845  162  0
  hole 41 -155.8845  -18  0
  hole 1 -155.8845  -90  0
  hole 21 -155.8845  -126  0
  hole 21 187.0614  0  0
  hole 21 187.0614  36  0
  hole 21 187.0614  72  0
  hole 21 187.0614  108  0
  hole 21 187.0614  -36  0
  hole 21 187.0614  -72  0
  hole 31 187.0614  -144  0
  hole 21 -187.0614  0  0
  hole 21 -187.0614  36  0
  hole 21 -187.0614  72  0
  hole 21 -187.0614  108  0
  hole 21 -187.0614  -36  0
  hole 21 -187.0614  -72  0
  hole 31 -187.0614  -144  0
  hole 31 218.2383  54  0
  hole 31 218.2383  -18  0
  hole 31 218.2383  -90  0
  hole 31 -218.2383  54  0
  hole 31 -218.2383  -18  0
  hole 31 -218.2383  -90  0
 zcylinder 10 1 340  58  0
 cuboid 0 1  400  -400  400  -400  58  0
end geometry
read array
ara=1 nux=1 nuy=1 nuz=18  gbl=1
com=''
fill 3*101 13*102 2*101
```

```
end fill
end array
end data
end
```

A.2 EXAMPLE TRITON T5-DEPL INPUT FILE

```
'SCALE 5.1 KENO Va. Jan. 2007
=t5-depl parm=(orgnflux)
VHTR Prismatic Power-core 1cyc 3650d 10libs 1zone b4c 100perc-
TRUvector1
v6-238
read comp
' uo2          21 den=10.41 1 1223 92235 15 92238 85 end
'Legacy fuel TRU vector for UO2 fuel:
 wtptTRU    21  10.41  14 93237 6.056132 94238 1.973126 94239 51.605541
94240 21.943351
            94241 4.129537 94242 4.497216 95241 8.301571 95601 0.020373
95243 1.247513
            96242 0.000049 96243 0.003342 96244 0.197768 96245 0.021760
96246 0.002721 1 1223 end
 b-10        31 0 7.221155e-09 1223 end
 b-11        31 0 2.924932e-08 1223 end
 c-graphite  31 0 0.07291468 1223 end
 si          31 0 0.01017942 1223 end
 b           41 den=1.69 8.2e-07 1223 5010 19.9 5011 80.1 end
 c-graphite  41 den=1.69 0.9999992 1223 end
 c-graphite  51 den=1.77 0.9999996 1223 end
 b           51 den=1.77 3.7e-07 1223 5010 19.9 5011 80.1 end
'Graphite fuel block:
 c-graphite  61 den=1.77 0.9999996 1223 end
 b           61 den=1.77 4.0e-07 1223 5010 19.9 5011 80.1 end
'Graphite Sleeve (Fuel rod):
 c-graphite  71 den=1.77 0.9999996 1223 end
 b           71 den=1.77 3.7e-07 1223 5010 19.9 5011 80.1 end
'Helium:
 he          81 den=0.001569 1 1223 end
 c-graphite  1 den=1.77 0.9999996 1223 end
 b           1 den=1.77 4e-07 1223 5010 19.9 5011 80.1 end
 b4c         3 den=1.82 0.0274 1223 5010 19.9 5011 80.1 end
 carbon      3 den=1.82 0.9726 1223 end
 he          5 den=0.001569 1 1223 end
 c-graphite  9 den=1.76 0.9999996 1223 end
 b           9 den=1.76 3.7e-07 1223 5010 19.9 5011 80.1 end
 c-graphite  10 den=1.732 0.999998 1223 end
 b           10 den=1.732 1.91e-06 1223 5010 19.9 5011 80.1 end
end comp
read celldata
doublehet  right_bdy=white fuelmix=121 end
  gfr=0.02985 21  coatr=0.04645 31 VF=0.2 matrix=41  end grain
  rod triangpitch right_bdy=white hpitch=2.575 61 fuelr=1.2 gapr=1.6 71
cladr=2.05 81 fuelh=54.6 end
end celldata
read depletion
 21 3
end depletion
read history
 power=103 burn=3650 nlib=10 end
end history
read opus
  symnuc=u-235 u-238 pu-238 pu-239 pu-240 pu-241
```

```
pu-242 np-237 am-241 am-243 cm-242 cm-243
cm-244 cm-245 cm-246 cm-247 am-242m cs-133 end
  units=grams
  time=years
  matl=0 21 3 end
end opus
read model
read parameter
           gen=200
           npg=1000
           nsk=10
           FLX=yes
end parameter
read geometry
unit 1
com='fuel block'
 zcylinder 1 1 17.9  58  0
  hole 12 -7.875  13.64  4.2
  hole 4 -7.875  -13.6399  4.2
  hole 4 -7.875  -13.6399  34.2
  hole 4 15.75  0  4.2
  hole 4 15.75  0  34.2
  hole 8 0  8.92  0
  hole 8 0  -8.92  0
  hole 8 2.575  4.46  0
  hole 8 2.575  -4.46  0
  hole 8 2.575  13.38  0
  hole 8 2.575  -13.38  0
  hole 8 -2.575  4.46  0
  hole 8 -2.575  -4.46  0
  hole 8 -2.575  13.38  0
  hole 8 -2.575  -13.38  0
  hole 8 5.15  0  0
  hole 8 5.15  8.92  0
  hole 8 5.15  -8.92  0
  hole 8 -5.15  0  0
  hole 8 -5.15  8.92  0
  hole 8 -5.15  -8.92  0
  hole 8 7.725  4.46  0
  hole 8 7.725  -4.46  0
  hole 8 -7.725  4.46  0
  hole 8 -7.725  -4.46  0
  hole 8 10.3  0  0
  hole 8 10.3  8.92  0
  hole 8 10.3  -8.92  0
  hole 8 -10.3  0  0
  hole 8 -10.3  8.92  0
  hole 8 -10.3  -8.92  0
  hole 8 12.875  4.46  0
  hole 8 12.875  -4.46  0
  hole 8 -12.875  4.46  0
  hole 8 -12.875  -4.46  0
  hole 8 -15.45  0  0
  hole 8 0  8.92  56.3
  hole 8 0  -8.92  56.3
  hole 8 2.575  4.46  56.3
  hole 8 2.575  -4.46  56.3
```

```
hole 8 2.575  13.38  56.3
hole 8 2.575  -13.38  56.3
hole 8 -2.575  4.46  56.3
hole 8 -2.575  -4.46  56.3
hole 8 -2.575  13.38  56.3
hole 8 -2.575  -13.38  56.3
hole 8 5.15  0  56.3
hole 8 5.15  8.92  56.3
hole 8 5.15  -8.92  56.3
hole 8 -5.15  0  56.3
hole 8 -5.15  8.92  56.3
hole 8 -5.15  -8.92  56.3
hole 8 7.725  4.46  56.3
hole 8 7.725  -4.46  56.3
hole 8 -7.725  4.46  56.3
hole 8 -7.725  -4.46  56.3
hole 8 10.3  0  56.3
hole 8 10.3  8.92  56.3
hole 8 10.3  -8.92  56.3
hole 8 -10.3  0  56.3
hole 8 -10.3  8.92  56.3
hole 8 -10.3  -8.92  56.3
hole 8 12.875  4.46  56.3
hole 8 12.875  -4.46  56.3
hole 8 -12.875  4.46  56.3
hole 8 -12.875  -4.46  56.3
hole 8 -15.45  0  56.3
hole 7 0  0  33
hole 6 0  0  43
hole 5 0  0  49
hole 2 0  8.92  1.7
hole 2 0  -8.92  1.7
hole 2 2.575  4.46  1.7
hole 2 2.575  -4.46  1.7
hole 2 2.575  13.38  1.7
hole 2 2.575  -13.38  1.7
hole 2 -2.575  4.46  1.7
hole 2 -2.575  -4.46  1.7
hole 2 -2.575  13.38  1.7
hole 2 -2.575  -13.38  1.7
hole 2 5.15  0  1.7
hole 2 5.15  8.92  1.7
hole 2 5.15  -8.92  1.7
hole 2 -5.15  0  1.7
hole 2 -5.15  8.92  1.7
hole 2 -5.15  -8.92  1.7
hole 2 7.725  4.46  1.7
hole 2 7.725  -4.46  1.7
hole 2 -7.725  4.46  1.7
hole 2 -7.725  -4.46  1.7
hole 2 10.3  0  1.7
hole 2 10.3  8.92  1.7
hole 2 10.3  -8.92  1.7
hole 2 -10.3  0  1.7
hole 2 -10.3  8.92  1.7
hole 2 -10.3  -8.92  1.7
hole 2 12.875  4.46  1.7
```

```
  hole 2 12.875  -4.46  1.7
  hole 2 -12.875  4.46  1.7
  hole 2 -12.875  -4.46  1.7
  hole 2 -15.45  0  1.7
unit 2
com='fuel (pin) hole'
 zcylinder 5 1 0.5  54.6  0
 zcylinder 121 1 1.3  54.6  0
 zcylinder 51 1 1.7  54.6  0
 zcylinder 5 1 2.05  54.6  0
unit 13
com='coolant channel'
 zcylinder 5 1 2.05  58  0
unit 4
com='bp ii'
 zcylinder 3 1 0.75  20  0
unit 5
com='handling hole i'
 zcylinder 5 1 2  9  0
unit 6
com='handling hole ii'
 zcylinder 5 1 1.5  6  0
unit 7
com='handling hole iii'
 zcylinder 5 1 2.25  10  0
unit 8
com='coolant above/below fuel rod'
 zcylinder 5 1 2.05  1.7  0
unit 12
com='bp hole'
 zcylinder 5 1 0.75  50  0
unit 9
com='coolant block 1: (empty bp 120 degree)'
 zcylinder 9 1 17.9  58  0
  hole 7 0  0  33
  hole 6 0  0  43
  hole 5 0  0  49
  hole 13 0  8.92  0
  hole 13 0  -8.92  0
  hole 13 2.575  4.46  0
  hole 13 2.575  -4.46  0
  hole 13 2.575  13.38  0
  hole 13 2.575  -13.38  0
  hole 13 -2.575  4.46  0
  hole 13 -2.575  -4.46  0
  hole 13 -2.575  13.38  0
  hole 13 -2.575  -13.38  0
  hole 13 5.15  0  0
  hole 13 5.15  8.92  0
  hole 13 5.15  -8.92  0
  hole 13 -5.15  0  0
  hole 13 -5.15  8.92  0
  hole 13 -5.15  -8.92  0
  hole 13 7.725  4.46  0
  hole 13 7.725  -4.46  0
  hole 13 -7.725  4.46  0
  hole 13 -7.725  -4.46  0
```

```
  hole 13 10.3  0  0
  hole 13 10.3  8.92  0
  hole 13 10.3  -8.92  0
  hole 13 -10.3  0  0
  hole 13 -10.3  8.92  0
  hole 13 -10.3  -8.92  0
  hole 13 12.875  4.46  0
  hole 13 12.875  -4.46  0
  hole 13 -12.875  4.46  0
  hole 13 -12.875  -4.46  0
  hole 13 -15.45  0  0
unit 10
com='cr block'
 zcylinder 1 1 17.8  58  0
  hole 11 -5.4  9.353  0
  hole 11 -5.4  -9.353  0
  hole 11 10.8  0  0
  hole 7 0  0  33
  hole 6 0  0  43
  hole 5 0  0  49
unit 11
com='cr hole'
 zcylinder 5 1 6.15  58  0
unit 101
com='slice above/below fuel'
 zcylinder 9 1 310  58  0
  hole 10 0  216  0
  hole 10 0  -180  0
  hole 10 31.1769  162  0
  hole 10 31.1769  -234  0
  hole 10 -31.1769  162  0
  hole 10 -31.1769  -234  0
  hole 10 62.3538  216  0
  hole 10 62.3538  -144  0
  hole 10 -62.3538  216  0
  hole 10 -62.3538  -144  0
  hole 10 93.5307  126  0
  hole 10 93.5307  -198  0
  hole 10 -93.5307  126  0
  hole 10 -93.5307  -198  0
  hole 10 124.7076  180  0
  hole 10 124.7076  -108  0
  hole 10 -124.7076  180  0
  hole 10 -124.7076  -108  0
  hole 10 155.8845  18  0
  hole 10 155.8845  90  0
  hole 10 155.8845  -54  0
  hole 10 155.8845  -162  0
  hole 10 -155.8845  18  0
  hole 10 -155.8845  90  0
  hole 10 -155.8845  -54  0
  hole 10 -155.8845  -162  0
  hole 10 187.0614  144  0
  hole 10 187.0614  -108  0
  hole 10 -187.0614  144  0
  hole 10 -187.0614  -108  0
  hole 10 218.2383  18  0
```

```
hole 10 218.2383  90  0
hole 10 218.2383  -54  0
hole 10 -218.2383  18  0
hole 10 -218.2383  90  0
hole 10 -218.2383  -54  0
hole 9 0  180  0
hole 9 0  -216  0
hole 9 31.1769  198  0
hole 9 31.1769  234  0
hole 9 31.1769  -162  0
hole 9 31.1769  -198  0
hole 9 -31.1769  198  0
hole 9 -31.1769  234  0
hole 9 -31.1769  -162  0
hole 9 -31.1769  -198  0
hole 9 62.3538  144  0
hole 9 62.3538  180  0
hole 9 62.3538  -180  0
hole 9 62.3538  -216  0
hole 9 -62.3538  144  0
hole 9 -62.36  180  0
hole 9 -62.3538  -180  0
hole 9 -62.3538  -216  0
hole 9 93.5307  162  0
hole 9 93.5307  198  0
hole 9 93.5307  -126  0
hole 9 93.5307  -162  0
hole 9 -93.5307  162  0
hole 9 -93.5307  198  0
hole 9 -93.5307  -126  0
hole 9 -93.5307  -162  0
hole 9 124.7076  108  0
hole 9 124.7076  144  0
hole 9 124.7076  -144  0
hole 9 124.7076  -180  0
hole 9 -124.7076  108  0
hole 9 -124.7076  144  0
hole 9 -124.7076  -144  0
hole 9 -124.7076  -180  0
hole 9 155.8845  54  0
hole 9 155.8845  126  0
hole 9 155.8845  162  0
hole 9 155.8845  -18  0
hole 9 155.8845  -90  0
hole 9 155.8845  -126  0
hole 9 -155.8845  54  0
hole 9 -155.8845  126  0
hole 9 -155.8845  162  0
hole 9 -155.8845  -18  0
hole 9 -155.8845  -90  0
hole 9 -155.8845  -126  0
hole 9 187.0614  0  0
hole 9 187.0614  36  0
hole 9 187.0614  72  0
hole 9 187.0614  108  0
hole 9 187.0614  -36  0
hole 9 187.0614  -72  0
```

```
  hole 9 187.0614  -144  0
  hole 9 -187.0614  0  0
  hole 9 -187.0614  36  0
  hole 9 -187.0614  72  0
  hole 9 -187.0614  108  0
  hole 9 -187.0614  -36  0
  hole 9 -187.0614  -72  0
  hole 9 -187.0614  -144  0
  hole 9 218.2383  54  0
  hole 9 218.2383  -18  0
  hole 9 218.2383  -90  0
  hole 9 -218.2383  54  0
  hole 9 -218.2383  -18  0
  hole 9 -218.2383  -90  0
 zcylinder 10 1 340  58  0
 cuboid 0 1  400  -400  400  -400  58  0
unit 100
com='slice with fuel'
 zcylinder 9 1 310  58  0
  hole 10 0  216  0
  hole 10 0  -180  0
  hole 10 31.1769  162  0
  hole 10 31.1769  -234  0
  hole 10 -31.1769  162  0
  hole 10 -31.1769  -234  0
  hole 10 62.3538  216  0
  hole 10 62.3538  -144  0
  hole 10 -62.3538  216  0
  hole 10 -62.3538  -144  0
  hole 10 93.5307  126  0
  hole 10 93.5307  -198  0
  hole 10 -93.5307  126  0
  hole 10 -93.5307  -198  0
  hole 10 124.7076  180  0
  hole 10 124.7076  -108  0
  hole 10 -124.7076  180  0
  hole 10 -124.7076  -108  0
  hole 10 155.8845  18  0
  hole 10 155.8845  90  0
  hole 10 155.8845  -54  0
  hole 10 155.8845  -162  0
  hole 10 -155.8845  18  0
  hole 10 -155.8845  90  0
  hole 10 -155.8845  -54  0
  hole 10 -155.8845  -162  0
  hole 10 187.0614  144  0
  hole 10 187.0614  -108  0
  hole 10 -187.0614  144  0
  hole 10 -187.0614  -108  0
  hole 10 218.2383  18  0
  hole 10 218.2383  90  0
  hole 10 218.2383  -54  0
  hole 10 -218.2383  18  0
  hole 10 -218.2383  90  0
  hole 10 -218.2383  -54  0
  hole 1 0  180  0
  hole 1 0  -216  0
```

```
hole 1 31.1769  198  0
hole 1 31.1769  234  0
hole 1 31.1769  -162  0
hole 1 31.1769  -198  0
hole 1 -31.1769  198  0
hole 1 -31.1769  234  0
hole 1 -31.1769  -162  0
hole 1 -31.1769  -198  0
hole 1 62.3538  144  0
hole 1 62.3538  180  0
hole 1 62.3538  -180  0
hole 1 62.3538  -216  0
hole 1 -62.3538  144  0
hole 1 -62.36  180  0
hole 1 -62.3538  -180  0
hole 1 -62.3538  -216  0
hole 1 93.5307  162  0
hole 1 93.5307  198  0
hole 1 93.5307  -126  0
hole 1 93.5307  -162  0
hole 1 -93.5307  162  0
hole 1 -93.5307  198  0
hole 1 -93.5307  -126  0
hole 1 -93.5307  -162  0
hole 1 124.7076  108  0
hole 1 124.7076  144  0
hole 1 124.7076  -144  0
hole 1 124.7076  -180  0
hole 1 -124.7076  108  0
hole 1 -124.7076  144  0
hole 1 -124.7076  -144  0
hole 1 -124.7076  -180  0
hole 1 155.8845  54  0
hole 1 155.8845  126  0
hole 1 155.8845  162  0
hole 1 155.8845  -18  0
hole 1 155.8845  -90  0
hole 1 155.8845  -126  0
hole 1 -155.8845  54  0
hole 1 -155.8845  126  0
hole 1 -155.8845  162  0
hole 1 -155.8845  -18  0
hole 1 -155.8845  -90  0
hole 1 -155.8845  -126  0
hole 1 187.0614  0  0
hole 1 187.0614  36  0
hole 1 187.0614  72  0
hole 1 187.0614  108  0
hole 1 187.0614  -36  0
hole 1 187.0614  -72  0
hole 1 187.0614  -144  0
hole 1 -187.0614  0  0
hole 1 -187.0614  36  0
hole 1 -187.0614  72  0
hole 1 -187.0614  108  0
hole 1 -187.0614  -36  0
hole 1 -187.0614  -72  0
```

```
  hole 1 -187.0614  -144  0
  hole 1 218.2383  54  0
  hole 1 218.2383  -18  0
  hole 1 218.2383  -90  0
  hole 1 -218.2383  54  0
  hole 1 -218.2383  -18  0
  hole 1 -218.2383  -90  0
 zcylinder 10 1 340  58  0
 cuboid 0 1  400  -400  400  -400  58  0
end geometry
read array
ara=1 nux=1 nuy=1 nuz=18  gbl=1
com=''
fill 3*101 13*100 2*101
end fill
end array
end data
end model
end
```

APPENDIX B

EVALUATED NUCLEAR DATA EMPLOYED IN SCALE 5.1 CALCULATIONS

S/N	Material Id	2nd Id	Source	Title
1	6312	6312-3-1	Scale	6-C-0 LANL,ORNL; EVAL-JUN96 M.B.CHADWICK, P
2	2004	2004-0	Scale	2-HE-4 LANL; EVAL-OCT73 NISLEY, HALE, Y
3	5010	5010-2	Scale	5-B-10 LANL; EVAL-NOV89 G.M.HALE, P.G.Y
4	5011	5011-1	Scale	5-B 11 LANL; EVAL-MAY89 P.G.YOUNG
5	6000	6000-3	Scale	6-C-0 LANL,ORNL; EVAL-JUN96 M.B.CHADWICK, P
6	8016	8016-2	Scale	8-O-16 LANL; EVAL-JUN96 M.B.CHADWICK AN
7	14000	14000-0	Scale	14-SI-0 ORNL; EVAL-FEB74 LARSON,PEREY,DR
8	92235	92235-6	Scale	92-U-235 ORNL,LANL+; EVAL-NOV89 WESTON, YOUNG,
9	92238	92238-4	Scale	92-U-238 ORNL,LANL+; EVAL-NOV89 L.W.WESTON,P.G.
10	93237	93237-2	Scale	93-NP-237 LANL; EVAL-APR90 P.YOUNG, E.ARTH
11	94238	94238-1	Scale	94-PU-238 HEDL,AI,+; EVAL-APR78 MANN,SCHENTER,A
12	94239	94239-3	Scale	94-Pu-239 LANL; EVAL-APR89 P.YOUNG, L.WEST
13	94240	94240-3	Scale	94-PU-240 ORNL; EVAL-AUG86 L.W. WESTON AND
14	94241	94241-3	Scale	94-PU-241 ORNL; EVAL-OCT88 L.WESTON,R.WRIG
15	94242	94242-1	Scale	94-PU-242 HEDL,SRL,+; EVAL-OCT78 MANN,BENJAMIN,M
16	95241	95241-3	Scale	95-AM-241 LANL,CNDC; EVAL-FEB94 YOUNG,MADLAND,Z
17	95601	95601-2	Scale	95-AM-242MHEDL,SRL,+; EVAL-APR78 MANN,BENJAMIN,H
18	95243	95243-2	Scale	95-Am-243 LANL,ORNL; EVAL-SEP96 P. G. YOUNG,L.
19	96242	96242-1	Scale	96-CM-242 HEDL,SRL,+; EVAL-APR78 MANN,BENJAMIN,H
20	96243	96243-1	Scale	96-Cm-243 MINSK; EVAL-JUL95 V.MASLOV,ET AL.
21	96244	96244-0	Scale	96-CM-244 HEDL,SRL,+; EVAL-APR78 MANN,BENJAMIN,H
22	96245	96245-3	Scale	96-Cm-245 MINSK; EVAL-NOV95 V.MASLOV ET AL
23	96246	96246-3	Scale	96-Cm-246 MINSK; EVAL-NOV95 V.MASLOV ET AL.

APPENDIX C

TRANSFORMATION CHAINS EMPLOYED IN EQUILIBRIUM CONCENTRATION CALCULATIONS

^{237}Np Chain

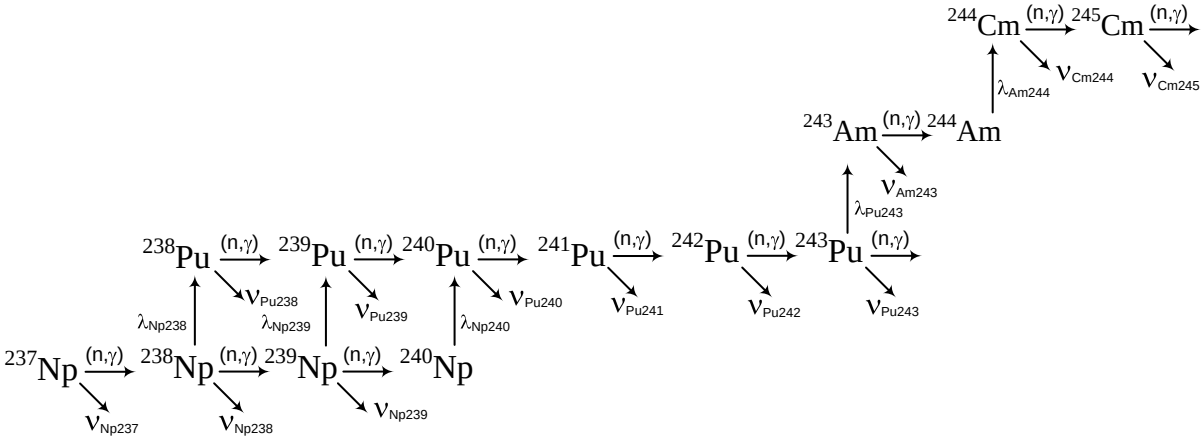

^{238}Pu Chain

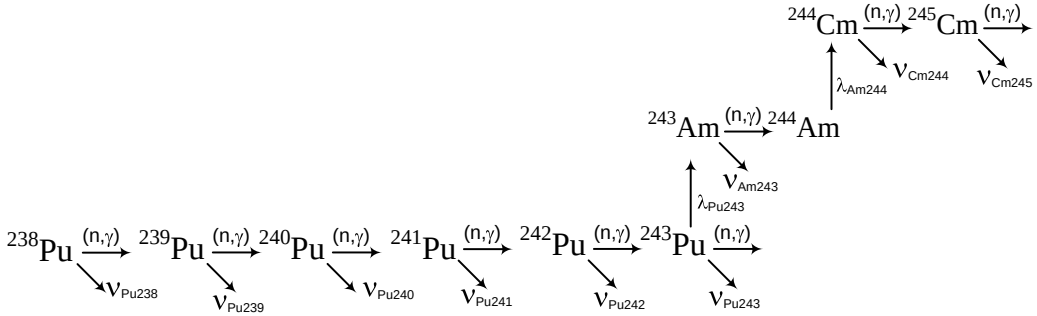

^{239}Pu Chain

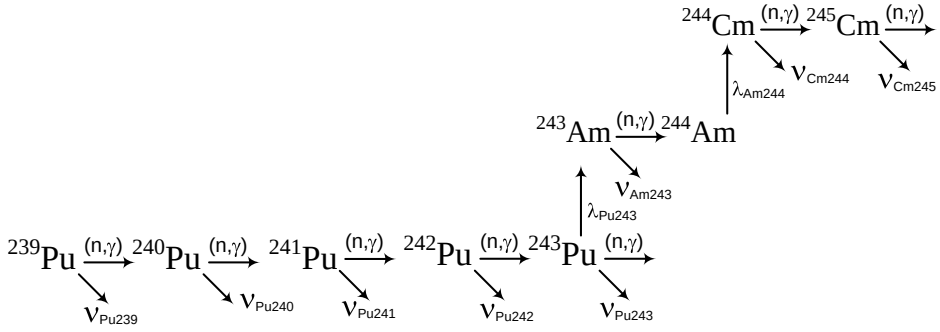

^{240}Pu Chain

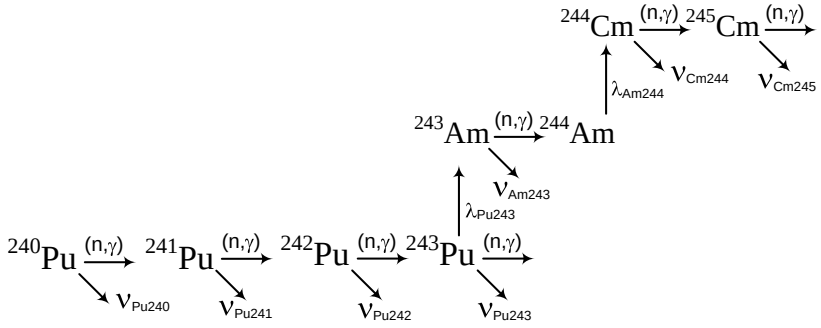

^{241}Pu Chain

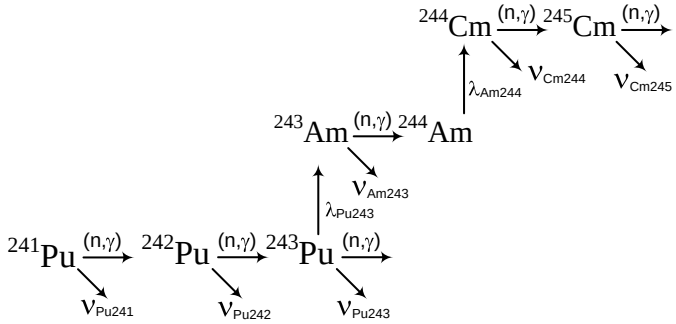

^{242}Pu Chain

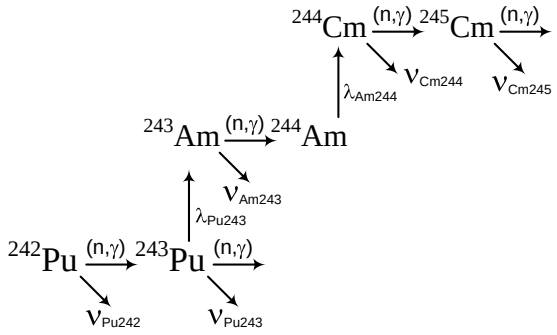

^{241}Am Chain

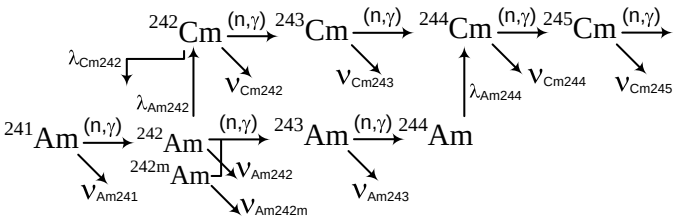

^{242m}Am Chain

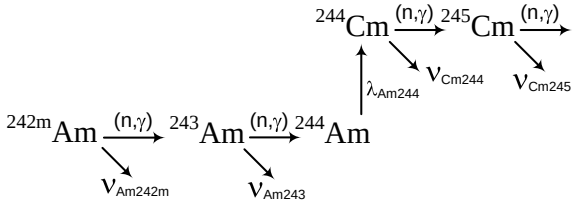

^{243}Am Chain

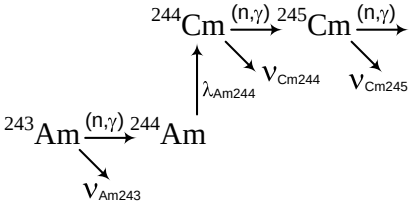

^{242}Cm Chain

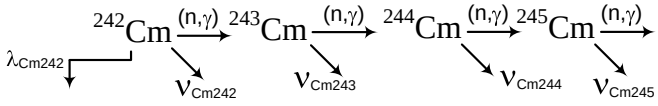

^{243}Cm Chain

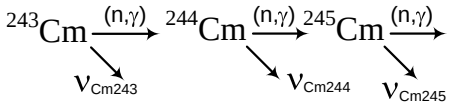

^{244}Cm Chain

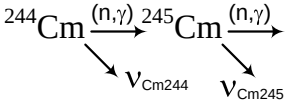

^{245}Cm Chain

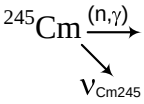

VITA

Name:	Ayodeji B. Alajo
Address:	Nuclear Engineering Department, 129 Zachary Engineering Building, 3133 TAMU, College Station TX 77843
Email Address:	dejialajo@yahoo.com
Education:	B.Sc., Mechanical Engineering, University of Ibadan, Nigeria, 2001 M.S., Nuclear Engineering, Texas A&M University, 2007